UNIVERSITY OF OKLAHOMA

GRADUATE COLLEGE

NATURALNESS IN SUPERSYMMETRY

A DISSERTATION

SUBMITTED TO THE GRADUATE FACULTY

in partial fulfillment of the requirements for the

Degree of

DOCTOR OF PHILOSOPHY

By

MAREN PADEFFKE-KIRKLAND
Norman, Oklahoma
2015

NATURALNESS IN SUPERSYMMETRY

A DISSERTATION APPROVED FOR THE
DEPARTMENT OF PHYSICS & ASTRONOMY

BY

Dr. Howard Baer, Chair

Dr. Patrick Skubic

Dr. Ronald Kantowski

Dr. Deborah Watson

Dr. Nikola Petrov

To my wonderful husband Ryan Kirkland, without whom I could have never accomplished this.

Acknowledgements

I would like to acknowledge the extraordinary help and understanding of my advisor Howard Baer, without whom this would not have been possible. Also many thanks to all my teachers and professors that have inspired me on this journey.

Table of Contents

List of Tables

List of Figures

Abstract

Weak scale supersymmetry solves the Big Hierarchy problem of the Standard Model. But recent severe sparticle mass limits from the LHC accentuate the Little Hierarchy Problem: Why are the W, Z and h masses so small (~ 100 GeV) when the supersymmetric parameters are at or above the TeV scale? This problem can be addressed quantitatively by studying the *fine-tuning* of a specific model. Fine-tuning allows for a unique way of giving upper bounds for masses of the superpartners. This dissertation studies a variety of models for their naturalness while satisfying experimental constraints. It is shown that fine-tuning puts most SUSY models under severe pressure: only the Non-Universal Higgs Mass model with two extra parameters (NUHM2) survives the naturalness criteria. Inspired by gauge coupling unification, these models assume gaugino mass unification, however, this may not be required by nature. This text examines how the phenomenology of supersymmetric models changes if non-universal gaugino masses (NUGM) are allowed without impacting naturalness. Within the NUGM model, supersymmetry could be detected from electroweak gaugino production at the LHC in multiple channels. Discovery prospects at the LHC13 vastly improve for the case of low gaugino masses due to observable signals from chargino and/or neutralino states. An International Linear Collider shows rich prospects for production of light electroweak -ino states. Also, direct and indirect searches for WIMPs could offer a means of discovery. In addition, this dissertation explores decoupled sfermions within natural supersymmetry. It is shown that low fine-tuning implies

intra-generational degeneracy for decoupled squarks and sleptons.

Chapter 1

Introduction

The Standard Model (SM) has been a highly successful framework for describing particle physics. The ultimate accomplishment occured when the Large Hadron Collider (LHC) recently discovered the long predicted Higgs boson with $m_h \simeq 125$ GeV. Despite this successful discovery, in the SM the Higgs mass is quadratically divergent. These quadratic divergences can be removed if one considers supersymmetry (SUSY), which introduces to each particle supersymmetric partners. The lack of signals for these supersymmetric particles at the LHC leads to mass limits of $m_{\tilde{g}} \gtrsim 1.8$ TeV (for $m_{\tilde{g}} \simeq m_{\tilde{q}}$) and $m_{\tilde{g}} \gtrsim 1.3$ TeV (for $m_{\tilde{g}} \ll m_{\tilde{q}}$) [1, 2]. These mass limits on gluinos and squarks are obtained within popular models such as mSUGRA/CMSSM [3, 4] and can, if one understands to only consider first generation squarks, be qualitatively valid in other models. In contrast, physicists have argued that sparticles have to be well below the TeV scale if one wants to maintain naturalness in SUSY [5, 6, 7, 8, 9, 10, 11, 12, 13]. This dilemma leads to the little hierarchy problem (LHP): Why are the W, Z and h masses so small (~ 100 GeV) when the SUSY parameters are so large? The LHP is addressed by models of *natural supersymmetry* (NS) [14], which pose a spectrum of light top- and bottom-squarks with $m_{\tilde{t}_{1,2},\tilde{b}_1} \lesssim 600$ GeV but very heavy first/second generation squarks and light higgsinos $\lesssim 200$ GeV but TeV-scale gluinos [15, 16, 17, 18]. Since no third generation squarks have been seen at LHC8, SUSY searches cause some to question whether supersymmetry is indeed the solution to the naturalness

problem in the SM.

In contrast to naive notions of naturalness, the mass of the light Higgs, m_h, requires highly mixed, TeV-scale top squarks. Previous studies find the radiatively-driven natural supersymmetry (RNS) model to be natural, while satisfying the constraints experimental data requires [19]. This dissertation explores a variety of models within the framework of the MSSM for their naturalness while satisfying all experimental constraints to test if other models can do as well as the non-universal Higgs mass model with 2 extra parameters (NUHM2) or even better. The remainder of this chapter summarizes the Standard Model which is the framework for the remaining text. Problems of the SM are pointed out which lead one to believe that the SM is incomplete. Supersymmetry as one possible theory beyond the SM is introduced and a general supersymmetric Lagrangian is derived. At the end of this chapter, the Minimal Supersymmetric Standard Model (MSSM) will be discussed along with several models within this framework. In Chapter 2, 'Naturalness' and various fine-tuning measures are defined and the SUGRA19 model is studied in depth. Chapter 3 discusses the overestimate of some fine-tuning measures and proposes a Rule of Fine-tuning. Following this rule, the three naturalness measures are shown to converge and a variety of models will be explored for their naturalness. Chapter 4 investigates non-universal gaugino mass (NUGM) models and how the phenomenology of natural SUSY differs from Radiatively-driven Natural Supersymmetry (RNS) models with gaugino mass unification. In Chapter 5, an interesting implication of naturalness on decoupled squarks and sleptons will be discussed, which hints at the existence

of intra-generational degeneracy.

1.1 The Standard Model

The Standard Model (SM) was finalized in the 1970's and is one of the most successful theories in describing the interactions of quarks and leptons. It is a non-Abelian Yang-Mills type gauge theory which uses quantum chromodynamics (QCD) to describe the strong interactions and the electroweak framework to combine the weak and electromagnetic interactions.

1.1.1 Quantum Chromodynamics

Quantum chromodynamics is the $SU(3)_C$ color theory describing the strong interactions and is assumed to be unbroken. The gauge bosons of the theory are the gluons which couple directly to quarks and anti-quarks. The QCD Lagrangian is given by

$$\mathcal{L}_{QCD} = -\frac{1}{4} G_{A\mu\nu} G_A^{\mu\nu} + \sum_{i=flavors} \overline{q}_i (i \not{D} - m_i) q_i, \tag{1.1}$$

where the G's are the $SU(3)_C$ gauge fields of the theory:

$$G_{A\mu\nu} = \partial_\mu G_{A\nu} - \partial_\nu G_{A\mu} - g_S f_{ABC} G_{B\mu} G_{C\nu}. \tag{1.2}$$

The covariant derivative is given by

$$D_\mu = \partial_\mu + i g_S \frac{\lambda_A}{2} G_{A\mu}, \tag{1.3}$$

where g_S is the strong coupling constant, and the generators of the theory are λ_A, the eight Gell-Mann matrices. For the quarks the color indices are $i = 1, 2, 3$, usually called red, blue, and green, with their anti-colors anti-red, anti-blue, and anti-green. The color indices for the gluons take values $A, B, C = 1, ..., 8$, representing the combinations of red, blue, green, and their anti-colors. The color charge, much like electric charge, must be conserved during all QCD interactions.

1.1.2 The Electroweak Theory

The electroweak (EW) theory combines the electromagnetic and weak interactions into one framework based on $SU(2)_L \times U(1)_Y$. The electroweak Lagrangian is given by

$$\mathcal{L}_{EW} = \mathcal{L}_{gauge} + \mathcal{L}_{matter} + \mathcal{L}_{Higgs} + \mathcal{L}_{Yukawa}. \tag{1.4}$$

Here,

$$\mathcal{L}_{gauge} = -\frac{1}{4} W_{A\mu\nu} W_A^{\mu\nu} - B_{\mu\nu} B^{\mu\nu}, \tag{1.5}$$

with W_A and B as the gauge fields of $SU(2)_L$ and $U(1)_Y$, respectively. The matter Lagrangian,

$$\mathcal{L}_{matter} = i\overline{\psi} \not{D} \psi, \tag{1.6}$$

where the covariant derivative is given by

$$D_\mu = \partial_\mu + igW_\mu \cdot T + \frac{1}{2} ig' B_\mu Y. \tag{1.7}$$

Here, g and g' are the coupling constants of $SU(2)_L$ and $U(1)_Y$, W_μ is the gauge isotriplet for $SU(2)_L$, B_μ is the gauge singlet of $U(1)_Y$, T is the weak isospin, and Y is the weak hypercharge.

$$\mathcal{L}_{Higgs} = (D\Phi)^\dagger(D\Phi) + \mu^2\Phi^\dagger\Phi - \lambda(\Phi^\dagger\Phi)^2, \tag{1.8}$$

where Ψ is the Higgs doublet and μ is the SM Higgs mass parameter. The Yukawa interactions of the fermions with the Higgs field is given by

$$\mathcal{L}_{Yukawa} = \sum_{\text{generations}} \Big[- \lambda_e \overline{L} \cdot \phi e_R - \lambda_d \overline{Q} \cdot \phi d_R - \lambda_u \epsilon^{ab} \overline{Q}_a \phi_b^\dagger u_R + h.c. \Big], \tag{1.9}$$

where L and e_R are the lepton fields, Q, u_R and d_R are the quark fields ϵ^{ab} is the complete antisymmetric $SU(2)_C$ tensor with $\epsilon^{12} = 1$.

1.1.3 The Higgs Mechanism

Electroweak symmetry is spontaneously broken from the $SU(2)_L \times U(1)_Y \rightarrow U(1)_{QED}$ via the Higgs Mechanism [20, 21]. This process introduces an $SU(2)_L$ doublet of complex spin zero fields

$$\Phi = \begin{pmatrix} \phi^+ \\ \\ \phi^0 \end{pmatrix}. \tag{1.10}$$

Its self-interactions give masses to the gauge fields and give rise to a new CP-even scalar particle, called the Higgs boson.

The corresponding Higgs Lagrangian is, as introduced in the previous section,

$$\mathcal{L}_{Higgs} = (D\Phi)^{\dagger}(D\Phi) - V(|\Phi|^2) \tag{1.11}$$

and the Higgs potential is given by

$$V(|\Phi|^2) = -\mu^2\Phi^{\dagger}\Phi + \lambda(\Phi^{\dagger}\Phi)^2, \tag{1.12}$$

where $\phi^0 = (\phi_R^0 + i\phi_I^0)/\sqrt{2}$. Upon minimization of this potential, the Higgs field accquires a non-zero vacuum expectation value (vev) of $v = \langle\phi_R\rangle/2 = \sqrt{-\mu^2/2\lambda}$. The physical Higgs scalar mass in the SM

$$m_h = \sqrt{-2\mu^2} \tag{1.13}$$

is a free parameter that must be measured. During the highly successful runs at the Large Hadron Collider (LHC) at CERN in Geneva, the ATLAS and CMS collaborations discovered a SM Higgs-like resonance [22, 23]. Present analysis seem to confirm that it is indeed the SM Higgs, the combined measurments found a mass of $m_h = 125.09 \pm 0.24$ GeV[24].

1.1.4 Why do we need Physics Beyond the Standard Model?

While the Standard Model is one of the most successful theories in physics, it leaves several questions unanswered suggesting that it is incomplete. Theoretically, these include:

- the strong CP fine-tuning problem that CP-symmetry is conserved in QCD interactions. (The QCD θ-vacuum requires an extra term $\mathcal{L}_\theta = -\frac{\bar{\theta}}{32\pi^2} G^A_{\mu\nu} G^{A\mu\nu}$ in Eq. 1.1 while measurments of the neutron electromagnetic dipole moment (EDM) imply it is not there.)

- the big gauge hierarchy problem: Why is there such a discrepancy between the weak scale and grand unification energy? (Quantum corrections to m_h should cause it to blow up to some high energy scale, e.g. m_{GUT}.)

- the fact that gauge coupling unification is expected at the grand unified theory (GUT) energy, but does not occur in the SM

Experimental arguments include:

- the existence of gravity.

- in the SM neutrinos are treated massless though solar and atmospheric neutrino data suggests otherwise.

- cosmological observations suggest the existence of dark matter and dark energy and requires a mechanism for baryogenesis.

To approach these and other issues, one needs to move to theories beyond the SM. Supersymmetry or the introduction of new particles or a combination of both could be the answer. But as experiments continue, one could also discover new and unexpected physics.

1.2 Supersymmetry

1.2.1 The Wess-Zumino Toy Model

In 1974 Julius Wess and Bruno Zumino wrote a simple four-dimensional quantum field theory with supersymmetry. Though it is only a toy framework, it illustrates many of the characteristics of supersymmetry. Let us consider the following Lagrangian

$$\mathcal{L} = \mathcal{L}_{kin} + \mathcal{L}_{mass}, \tag{1.14}$$

where,

$$\mathcal{L}_{kin} = \frac{1}{2}(\partial_\mu A)^2 + \frac{1}{2}(\partial_\mu B)^2 + \frac{i}{2}\overline{\psi}\partial\!\!\!/\psi + \frac{1}{2}(F^2 + G^2), \tag{1.15}$$

and

$$\mathcal{L}_{mass} = -m[\frac{1}{2}\overline{\psi}\psi - GA - FB]. \tag{1.16}$$

Here, A, B, F, and G are real scalar fields and ψ is a Majorana spinor field. Since F and G do not have kinetic terms, they are called *auxiliary* fields

Wess and Zumino observed that this Lagrangian density only changes by a

total derivative if we consider the following transformations:

$$\begin{aligned}
\partial A &= i\overline{\alpha}\gamma_5\psi, \\
\partial B &= -i\overline{\alpha}\psi, \\
\partial \psi &= -F\alpha + iG\gamma_5\alpha + \not{\partial}\gamma_5 A\alpha + i\not{\partial}B\alpha, \\
\partial F &= i\overline{\alpha}\not{\partial}\psi, \\
\partial G &= \overline{\alpha}\gamma_5\not{\partial}\psi.
\end{aligned} \tag{1.17}$$

As the result of a supersymmetry transformation, the action is invariant so that the same equations of motion are derived. This supersymmetry mixes boson and fermion fields as can be seen from Eq.(1.17). The generators of the supersymmetric transformation follow a Graded Lie Algebra, typified by $\{Q_a, \overline{Q}_b\} = 2(\gamma^\mu)_{ab}P_\mu$ and commute with all internal symmetry generators. Thus, any particle and its superpartner have the same internal quantum numbers.

One motivation for supersummetric models as extentions to the SM is that they remove the quadratic divergences that destabilize the scalar sector of a generic field theory. To demonstrate this, one could add an interaction term to the Lagrangian given by

$$\mathcal{L}_{int} = -\frac{g}{\sqrt{2}}A\overline{\psi}\psi + \frac{ig}{\sqrt{2}}B\overline{\psi}\gamma_5\psi + \frac{g}{\sqrt{2}}(A^2 - B^2)G + g\sqrt{2}ABF. \tag{1.18}$$

Since the fields F and G do not have kinectic terms and therefore do not propagate, they can be eliminated via their Euler-Lagrange equations. Thus, one obtains a

Lagrangian only in terms of dynamical fields,

$$\begin{aligned}\mathcal{L} =&\frac{1}{2}(\partial_\mu A)^2 + \frac{1}{2}(\partial_\mu B)^2 + \frac{i}{2}\overline{\psi}\partial\!\!\!/\psi + \frac{1}{2}m^2(A^2+B^2) - m[\frac{1}{2}\overline{\psi}\psi \\ &- \frac{g}{\sqrt{2}}A\overline{\psi}\psi + \frac{ig}{\sqrt{2}}B\overline{\psi}\gamma_5\psi - gm\sqrt{2}AB^2 - \frac{gm}{\sqrt{2}}A(A^2-B^2) \\ &- g^2A^2B^2 - \frac{1}{4}g^2(A^2-B^2)^2.\end{aligned} \tag{1.19}$$

Now as an example, the corrections to the "one point function" of the scalar field A to first order in the coupling constant g are given by

$$\begin{aligned}\langle 0|\mathcal{L}_{int}|0\rangle &\sim \frac{g}{\sqrt{2}}\Big\{Tr\int\frac{d^4p}{p\!\!\!/ - m_\psi} - m\int\frac{d^4p}{p^2-m_B} - 3m\int\frac{d^4p}{p^2-m_A}\Big\} \\ &= \frac{g}{\sqrt{2}}\Big\{\int\frac{d^4p}{p^2-m}4m - m\int\frac{d^4p}{p^2-m} - 3m\int\frac{d^4p}{p^2-m}\Big\}.\end{aligned} \tag{1.20}$$

One sees that though each of the terms are quadratically divergent, the contribution from the fermion loop exactly cancels the contributions from the boson loops. This cancelation occurs for *all* particle masses and to *all* orders in perturbation theory.

1.2.2 The supersymmetric Lagrangian

In the SM, the proton and neutron form a doublet isospin. In the Wess-Zumino model, the fields can be re-written in terms of a complex scalar field $\mathcal{S}$, auxiliary field $\mathcal{F}$ and the left chiral component of the Majorana spinor field ψ_L. With

$\mathcal{S} = \frac{1}{\sqrt{2}}(A + iB)$ and $\mathcal{F} = \frac{1}{\sqrt{2}}(F + iG)$ the transformations are given by

$$\begin{aligned} \delta\mathcal{S} &= -i\sqrt{2}\overline{\alpha}\psi_L, \\ \delta\psi_L &= -\sqrt{2}\mathcal{F}\alpha_L + \sqrt{2}\partial\!\!\!/\mathcal{S}\alpha_R, \\ \delta\mathcal{F} &= i\sqrt{2}\overline{\alpha}\partial\!\!\!/\psi_L. \end{aligned} \tag{1.21}$$

The three fields form an irreducible supermultiplet and can be combined into a single *superfield*

$$\hat{\mathcal{S}}(\hat{x}) = \mathcal{S}(\hat{x}) + i\sqrt{2}\overline{\theta}\psi_L(\hat{x}) + i\theta\overline{\theta}\mathcal{F}(\hat{x}), \tag{1.22}$$

where $\hat{x}_\mu = x_\mu + \frac{i}{2}\overline{\theta}\gamma_5\gamma_\mu\theta$ and θ are the anti-commuting Grassman numbers. These Grassman numbers make up an extension to spacetime called *superspace*: $x_\mu \to (x_\mu, \theta)$, where the spinor θ contains four anti-commuting elements θ_a.

Re-writing the Wess-Zumino Lagrangian in terms of the supermultiplet gives

$$\mathcal{L}_D = \partial_\mu\mathcal{S}^\dagger\partial^\mu\mathcal{S} + \frac{i}{2}\overline{\psi}\partial\!\!\!/\psi + \mathcal{F}^\dagger\mathcal{F}, \tag{1.23}$$

often called the D-term of the Lagrangian density.

The interactions of the scalars with the fermions may be included by introducing a function $\hat{f}$ which can be chosen by the model builder and is often refered to as

the *superpotential*. The Lagrangian resulting from the superpotential is given by

$$\begin{aligned}\mathcal{L}_{chiral} = &-i\sum_i \frac{\partial \hat{f}}{\partial \hat{\mathcal{S}}}\bigg|_{\hat{\mathcal{S}}=\mathcal{S}} \mathcal{F}_i - \frac{1}{2}\sum_{i,j} \frac{\partial^2 \hat{f}}{\partial \hat{\mathcal{S}}_i \partial \hat{\mathcal{S}}_i}\bigg|_{\hat{\mathcal{S}}=\mathcal{S}} \overline{\psi}_i P_L \psi_j \\ &+ i\sum_i \left(\frac{\partial \hat{f}}{\partial \hat{\mathcal{S}}}\right)^\dagger\bigg|_{\hat{\mathcal{S}}=\mathcal{S}} \mathcal{F}_i^\dagger - \frac{1}{2}\sum_{i,j} \left(\frac{\partial^2 \hat{f}}{\partial \hat{\mathcal{S}}_i \partial \hat{\mathcal{S}}_i}\right)^\dagger\bigg|_{\hat{\mathcal{S}}=\mathcal{S}} \overline{\psi}_i P_R \psi_j.\end{aligned} \tag{1.24}$$

Here, P_L and P_R are projecting operators into left and right chiral superfields.

The curl supermultiplet consists of the gauge potential V_μ, a Majorana spinor field λ and the auxiliar field $\mathcal{D}$. It is neither a right nor left chiral superfield and is sometimes called the gauge supermultiplet. The Majorana field λ is the *gaugino* and will be the superpartner of the SM gauge bosons. Defining the field strength tensor field $F^{\mu\nu} \equiv \partial^\mu V^\nu - \partial^\nu V^\mu$, the supersymmetric transformations of these fields are given by:

$$\begin{aligned}\delta F^{\mu\nu} &= -i\overline{\alpha}[\gamma^\mu \partial^\nu - \gamma^\nu \partial^\mu], \\ \delta\lambda &= -i\gamma_5 \alpha \mathcal{D} + \frac{1}{4}[\gamma_\nu, \gamma_\mu] F^{\mu\nu}\alpha, \\ \delta\mathcal{D} &= \overline{\alpha}\not{\partial}\gamma_5 \lambda.\end{aligned} \tag{1.25}$$

Similar to the chiral superfield, the three fields in the curl supermultiplet can be combined into a *curl superfield*. The curl superfield $\hat{W}_A(\hat{x})$ is a left-chiral spinor superfield, which, in the Wess-Zumino gauge, is given by

$$\hat{W}_A(\hat{x}) = \lambda_{LA}(\hat{x}) + \frac{1}{2}\gamma^\mu\gamma^\nu F_{\mu\nu A}(\hat{x})\theta_L - i\overline{\theta}\theta_L(\not{D}\lambda_R)_A - i\mathcal{D}_A(\hat{x})\theta_L. \tag{1.26}$$

The Lagrangian density of a renormalizable supersymmetric gauge theory can be found from the action. The action S includes an integral over superspace, given

by

$$S = -\frac{1}{4}\int d^4x d^4\theta \Big[\hat{\mathcal{S}}^\dagger e^{-2gt_A\hat{\Phi}_A}\hat{\mathcal{S}}\Big] \\ -\frac{1}{2}\Big[\int d^4x d^2\theta_L \hat{f}(\hat{\mathcal{S}} + h.c.)\Big] - \frac{1}{4}\int d^4x d^2\theta_L \overline{\hat{W}_A^c}\hat{W}_A. \tag{1.27}$$

Here, $\hat{\Phi}_A$ is a set of gauge potential superfields in which the vector potential resides and t_A are the matrix representations of the generators satisfying the Lie algebra $[t_A, t_B] = if_{ABC}t_C$. In addition, the action may include Fayet-Iliopoulus terms for each $U(1)$ factor of the gauge group which are not included in the above expression.

The contribution to the Lagrangian due to the first term of the action is found to be

$$\mathcal{L}_{gauge} = (D_\mu\mathcal{S})^\dagger(D^\mu\mathcal{S}) + \frac{i}{2}\overline{\psi}\not{D}\psi + \mathcal{F}^\dagger\mathcal{F} \\ - g\mathcal{S}^\dagger t\cdot\mathcal{D}\mathcal{S} + \Big(-\sqrt{2}\mathcal{S}_i^\dagger g t_A \overline{\lambda}_A \frac{1-\gamma_5}{2}\psi_i + h.c.\Big), \tag{1.28}$$

The covariant derivatives on $\mathcal{S}$ and ψ are given by

$$D_\mu\psi = \partial_\mu\psi + ig(t\cdot V_\mu)\psi_L - ig(t^*\cdot V_\mu)\psi_R, \\ D_\mu\mathcal{S} = \partial_\mu\mathcal{S} + igt\cdot V_\mu\mathcal{S} \tag{1.29}$$

The third term in the action gives rise to the Lagrangian of the gauge kinetic terms

$$\mathcal{L}_{GK} = -\frac{1}{4}F_{A\mu\nu}F_A^{\mu\nu} + \frac{i}{2}\overline{\lambda}_A\not{D}_{AC}\lambda_C + \frac{1}{2}\mathcal{D}_A\mathcal{D}_A, \tag{1.30}$$

where the covariant derivative on λ is given by

$$(\not{D}\lambda)_A = \not{\partial}\lambda_A + igf_{ABC}\not{V}_B\lambda_C. \tag{1.31}$$

Finally, the complete supersymmetric Lagrangian density of a renormalizable sypersymmetric gauge theory reads

$$
\begin{aligned}
\mathcal{L} &= \mathcal{L}_{GK} + \mathcal{L}_{gauge} + \mathcal{L}_{chiral} \\
&= (\partial_\mu \mathcal{S})^\dagger (\partial^\mu \mathcal{S}) + \frac{i}{2}\overline{\psi}\partial\!\!\!/\psi + \mathcal{F}^\dagger \mathcal{F} - \frac{1}{4} F_{A\mu\nu} F_A^{\mu\nu} + \frac{i}{2}\overline{\lambda}_A \not{D}_{AC} \lambda_C + \frac{1}{2}\mathcal{D}_A \mathcal{D}_A \\
&+ \sum_i \left[-\sqrt{2}\left(\mathcal{S}_i^\dagger g t_A \overline{\lambda}_A \frac{1-\gamma_5}{2}\psi_i + h.c. \right) + \mathcal{S}_i^\dagger g t_A \mathcal{S}_i \right] \\
&- i \sum_i \frac{\partial \hat{f}}{\partial \hat{\mathcal{S}}}\bigg|_{\hat{\mathcal{S}}=\mathcal{S}} \mathcal{F}_i - \frac{1}{2}\sum_{i,j} \frac{\partial^2 \hat{f}}{\partial \hat{\mathcal{S}}_i \partial \hat{\mathcal{S}}_i}\bigg|_{\hat{\mathcal{S}}=\mathcal{S}} \overline{\psi}_i \left(\frac{1-\gamma_5}{2} \right) \psi_j \\
&+ i \sum_i \left(\frac{\partial \hat{f}}{\partial \hat{\mathcal{S}}} \right)^\dagger \bigg|_{\hat{\mathcal{S}}=\mathcal{S}} \mathcal{F}_i^\dagger - \frac{1}{2}\sum_{i,j} \left(\frac{\partial^2 \hat{f}}{\partial \hat{\mathcal{S}}_i \partial \hat{\mathcal{S}}_i} \right)^\dagger \bigg|_{\hat{\mathcal{S}}=\mathcal{S}} \overline{\psi}_i \left(\frac{1+\gamma_5}{2} \right) \psi_j,
\end{aligned}
\tag{1.32}
$$

where i, j denote the matter field types and A is the gauge group index. As before, the Fayet-Iliopoulos terms are not included.

In any realistic SUSY theory, lepton and baryon numbers may not be conserved and one is forced to impose additional global symmetries. Matter parity, which is the same as R-parity, will remove B and L violating terms from the SUSY Lagrangian and is given by

$$
R \equiv (-1)^{3(B-L)+2s}, \tag{1.33}
$$

where s is the spin of the field. SUSY particles, or sparticles, are R-odd and do not mix with R-even SM particles. Furthermore, R-parity conservation implies that sparticles can only be pair produced in particle collisions and decay into an odd number of sparticles. Thus, the lightest supersymmetric particle (LSP) must be absolutely stable. For the remainder of this dissertation, R-parity is assumed

to be conserved in nature.

1.2.3 Soft SUSY Breaking

The fact that the quadratic divergencies cancel even if the fermion and boson masses are not equal is very crucial for phenomenological reasons. The lack of signals for the superpartners implies that supersymmetry is a broken summetry, giving larger masses to the superparticles. If the F or D term in the Lagrangian acquire a *vev* supersymmetry is broken spontaneously. This, however, disagrees with phenomenology for global SUSY models and one must move to supergravity (SUGRA) or local SUSY models. Here, SUSY is broken in some *hidden* sector which couples to the *visible* sector via messenger interactions. The most studied model using this method of SUSY breaking is *gravity mediation* which will be discussed in the following section. Gravity mediation is favored by the value of the Higgs mass which seems to require a large trilinear H-term.

Without knowing the actual supersymmetry breaking mechanism, it is possible to add new terms to the Lagrangian that do not re-introduce quadratic divergencies. Such terms are called *soft SUSY breaking* (SSB) terms. For example in the Wess-Zumino toy model, one may add

$$\mathcal{L}_{soft} = k(A^3 - 3AB^2) \tag{1.34}$$

to the Lagrangian in Eq. (1.19) without introducing a net quadratic divergence in the corrections to the one-point function of A. Here, k is a dimensional

coupling constant. Moreover, it can be shown that the following scenarios break supersymmetry softly to all orders in perturbation theory:

- scalar masses,
- gaugino masses, one for each gauge group (in gauge theories),
- linear terms in the scalar field $\mathcal{S}_i$,
- and bilinear or trilinear operators of the form $\mathcal{S}_i\mathcal{S}_j$ or $\mathcal{S}_i\mathcal{S}_j\mathcal{S}_k$.

1.2.4 The Minimal Supersymmetric Standard Model

The simplest phenomenologically viable supersymmetric theory is the Minimal Supersymmetric Standard Model (MSSM). It contains the fewest number of extra particles and interactions. As in the SM, the gauge symmetry of the MSSM is given by $SU(3)_C \times SU(2)_L \times U(1)_Y$. Supersymmetry is broken by adding allowed soft SUSY breaking terms to the theory. Table 1.2.4 lists the chiral supermultiplets for the first generation showing the SM particles and their superpartners. Superpartners of the quarks are called *squarks*, such as the stop, sbottom, etc. *Sleptons* are the SUSY partners to the leptons, including the selectron, sneutrino, etc. Together these are often referred to as *sfermions* and similar to the SM they appear in three generations. Table 1.2.4 shows the gauge supermultiplets with their fields which will be discussed later in this section. For a more detailed discussion on the MSSM see, for example, [25].

As discussed in Section 1.1.3, in the SM electroweak symmetry is broken via the Higgs mechanism, giving rise to mass terms for the fermions. In a supersymmetric

Field	spin 0	spin 1/2	$SU(3)_C$	$SU(2)_L$	$U(1)_Y$
$\hat{L} = \begin{pmatrix} \hat{\nu_{eL}} \\ \hat{e}_L \end{pmatrix}$	$(\tilde{\nu}\ \tilde{e}_L)$	$(\nu\ e_L)$	**1**	**2**	-1
$\hat{E}^C$	$\tilde{e}_R^*$	$\tilde{e}_R^\dagger$	**1**	**1**	2
$\hat{Q} = \begin{pmatrix} \hat{u_L} \\ \hat{d}_L \end{pmatrix}$	$(\tilde{u}_L\ \tilde{d}_L)$	$(u_L\ d_L)$	**3**	**2**	1/3
$\hat{U}^C$	$\tilde{u}_R^*$	$\tilde{u}_R^\dagger$	$\mathbf{3}^*$	**1**	-4/3
$\hat{D}^C$	$\tilde{d}_R^*$	$\tilde{d}_R^\dagger$	$\mathbf{3}^*$	**1**	2/3
$\hat{H}_u = \begin{pmatrix} \hat{h_u^+} \\ \hat{h}_u^0 \end{pmatrix}$	$(\tilde{h}_u^+\ \tilde{h}_u^0)$	$(h_u^+\ h_u^0)$	**1**	**2**	1
$\hat{H}_d = \begin{pmatrix} \hat{h_d^-} \\ \hat{h}_d^0 \end{pmatrix}$	$(\tilde{h}_d^-\ \tilde{h}_d^0)$	$(h_d^-\ h_d^0)$	**1**	$\mathbf{2}^*$	-1

Table 1.1: The MSSM chiral supermultiplets with their SM particles and superpartners for the first generation

Field	spin 1/2	spin 1	$SU(3)_C$	$SU(2)_L$	$U(1)_Y$
$\hat{g}_A,\ A = 1, ..., 8$	$\tilde{g}$	g	**8**	**1**	0
$\hat{W}_a,\ a = 1, 2, 3$	$\widetilde{W^\pm}\ \widetilde{W^0}$	$W^\pm\ W_0$	**1**	**3**	0
$\hat{B}$	$\tilde{B}$	B	**1**	**1**	0

Table 1.2: The MSSM gauge supermultiplets with the SM particles and superpartners

theory this is not possible. A doublet can only give mass to either the up-type or the down-type quarks, but not both. Thus, two Higgs doublet chiral supermultiplets $\hat{H}_u$ and $\hat{H}_d$ are needed, one interacting with $Y = 1/2$ fermions the other with $Y = -1/2$. These doublet fields consist of both the scalar/pseudo-scalar Higgs bosons and their superpartners, the higgsinos. Electroweak symmetry is broken when the up-type mass $m^2_{H_u}$ is driven to negative values via renormalization group equation (RGE) running. This mechanism is referred to as *radiative electroweak symmetry breaking* (REWSB) [26], since the RGE running is heavily dependent on the radiative corrections. The neutral scalar fields each acquire a *vev*, $\langle h^0_u \rangle \equiv v_u$ and $\langle h^0_d \rangle \equiv v_d$, which together define a new parameter,

$$\tan\beta \equiv \frac{v_u}{v_d}. \tag{1.35}$$

Usually the considered range is $\tan\beta \sim 3 - 60$. Too small $\tan\beta$ leads to too small values of m_h.

After electroweak symmetry breaking, five physical Higgs states and their superpartners remain: the light Higgs scalar h (typically taken as the SM Higgs), the heavy Higgs scalar H, two charged Higgs $H^{\pm}$, and the pseudo-scalar Higgs A. The superpotential in the MSSM is given by

$$\begin{aligned} \hat{f}_{MSSM} =& \mu(\hat{h}^0_u \hat{h}^0_d + \hat{h}^+_u \hat{h}^-_d) + f_u(\hat{u}\hat{h}^0_u - \hat{d}\hat{h}^+_u)\hat{U}^c \\ &+ f_d(\hat{u}\hat{h}^-_d + \hat{d}\hat{h}^0_d)\hat{D}^c + f_e(\hat{\nu}\hat{h}^-_d + \hat{e}\hat{h}^0_d)\hat{E}^c + ... \end{aligned} \tag{1.36}$$

Here, μ is the supersymmetric Higgs/higgsino bilinear term giving masses to the

gauge and Higgs bosons as well as their SUSY partners. Similarly, f_u, f_d and f_e are the coupling constants for the Yukawa interactions that give masses to the quarks and leptons of the first generation. The other generations have similar terms.

The gauge sector of the MSSM is made up of the three curl superfields, $\hat{B}_\mu$, $\hat{W}^a_\mu$, and $\hat{g}^A_\mu$ corresponding to the $U(1)_Y$, $SU(2)_L$, and $SU(3)_C$ symmetries, respectively. Supersymmetry is broken via soft SUSY breaking terms, which show up in the Lagrangian as gaugino mass terms:

$$\mathcal{L}_{mass} = -\frac{1}{2}[M_1\overline{\lambda}_0\lambda_0 + M_2(\overline{\lambda}_3\lambda_3 + 2\overline{\lambda}\lambda) + M_3\overline{\tilde{g}}\tilde{g}], \tag{1.37}$$

where M_1, M_2, and M_3 are the mass parameter of the bino, wino, and gluino, scalar mass terms and bilinear and trilinear terms. The gluino is a color octet fermion which cannot mix with any other fermions since $SU(3)_C$ is not broken. Hence, it is a mass eigenstate with $m_{\tilde{g}} = |M_3|$. The bino and wino mix with the higgsinos to form physical mass eigenstates, the four neutralinos ($\widetilde{Z}_{1,2,3,4}$), and the charginos ($\widetilde{W}^{\pm}_{1,2}$). Here, $\widetilde{Z}_1(\widetilde{W}_1)$ denote the lightest neutralino (chargino) and with increasing masses $\widetilde{Z}_4(\widetilde{W}_2)$ label the heaviest. Their masses depend on the mixing pattern of M_1, M_2, μ, and tanβ, and can be higgsino-like, gaugino-like, or some mixture. If $|\mu| \gg |M_{1,2}|, m_W$, then the lighter chargino and the two lighter neutralinos are gaugino-like, and the heavier chargino and two heavier neutralinos are higgsino-like. The situation is reversed if $|M_{1,2}| \gg |\mu|, m_W$. This will be important for the discussion in Chapter 4.

There are a total of 124 free parameters in the MSSM and one of its successes is the achievment of gauge coupling unification at the grand unified theory (GUT) scale, $m_{GUT} \simeq 2 \times 10^{16}$ GeV. Masses at the electroweak scale $Q = 1$ TeV remain stable under radiative corrections and allow the predictions of the MSSM to be extended to the high scale (HS) $Q = m_{GUT}$. Thus, one often assumes the MSSM is the correct effective field theory describing nature from the electroweak scale to the HS. Logarithmic divergences will, however, still remain, and calculations at the GUT-scale will contain terms proportional to $\frac{\alpha_i}{4\pi}\log(m_{GUT}/m_Z)$. These large logarithmic terms will play a role in Chapter 2, when discussing fine-tuning in SUSY.

Inspired by the universality of gravity and the need to suppress flavor-changing neutral current (FCNC) and CP violating processes, many early phenomenological studies adopted the universality hypothesis,

- $g = g' = g_S \equiv g_{GUT}$
- $m^2_{Q_i} = m^2_{U_i} = m^2_{D_i} = m^2_{L_i} = m^2_{E_i} = m^2_{H_u} = m^2_{H_d} \equiv m^2_0$
- $M_1 = M_2 = M_3 \equiv m_{1/2}$
- $A_t = A_b = A_\tau \equiv A_0$.

This assumption simplifies the parameter space to just five parameters, $m_0, m_{1/2}$, $A_0, sign(\mu), \tan\beta$, called mSUGRA (minimal SUperGRAvity)[3] or CMSSM (Constrained MSSM)[8] model. The $m^2_{H_u}$ term evolves from large m^2_0 at the GUT scale through zero to negative values at the weak scale, causing REWSB as mentioned

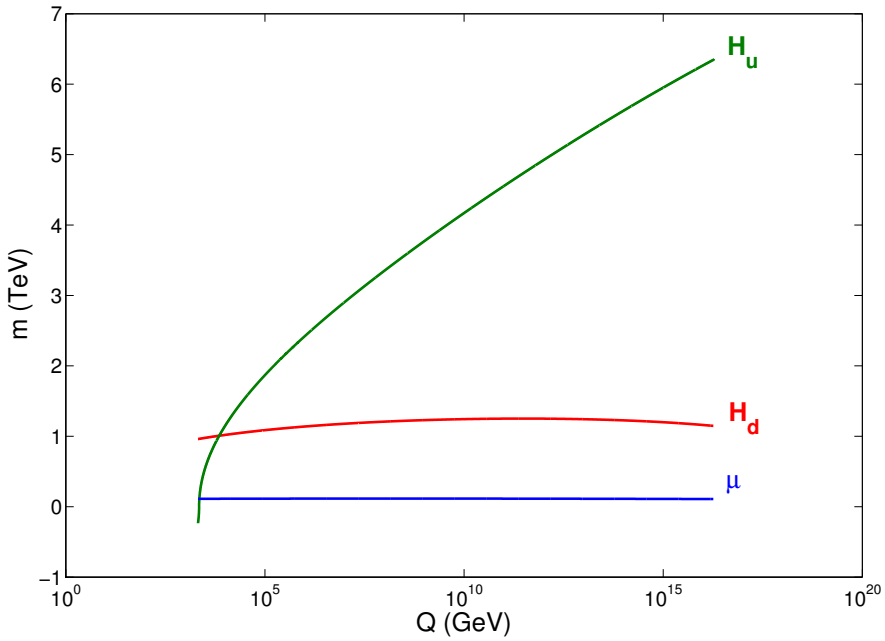

Figure 1.1: Renormalization group evolution of $sign(m^2_{H_u})\sqrt{|m^2_{H_u}|}$, $\sqrt{m^2_{H_d}}$ and μ versus energy scale Q for the RNS benchmark point from Ref. [27]. The value $m_A = 1$ TeV $\simeq m_{H_d}(weak)$ and $\mu(weak) = 110$ GeV.

before. The RG running of the soft term, as well as μ, versus the energy scale Q is shown in Fig. 1.1. Here, a radiatively-driven SUSY benchmark point from Ref. [27] was used, where $\mu = 110$ GeV and $\Delta_{EW} = 16$. The mSUGRA/CMSSM models belong to the class of supergravity models. Gravity mediated scenarios introduce a spin 2 gravity force carrier, called the graviton, which acts as the mediator between the hidden and the visible sector. Its superpartner is the spin 3/2 gravitino. Here, SUSY breaking can occur at a mass scale $m \sim 10^{11}$ GeV. This gives rise to particles called goldstinos, the superpartners of the Goldstone bosons. The gravitino gets its mass $m_{3/2}$ when the goldstinos' degrees of freedom are absorbed by the gravitino via the super Higgs mechanism. Then the SSB of

the visible sector are of order m^2/M_{Pl}, where $M_{Pl} \simeq 1.2 \times 10^{19}$ GeV is the Planck mass.

1.2.5 Alternatives and Extensions to mSUGRA

Another model included in the class of supergravity models is the Non-Universal Higgs Mass (NUHM) model. Here, one may choose additional free parameters such that the GUT scale Higgs masses differ from the common scalar mass m_0. For the discussions followed, NUHM models with one or two extra parameters are of interest:

- NUHM1[28], where $m_{H_u}^2 = m_{H_d}^2 \neq m_0^2$ at GUT scale and
- NUHM2[29], where $m_{H_u}^2 \neq m_{H_d}^2 \neq m_0^2$.

Also of interest is minimal Gauge Mediated Symmetry Breaking (mGMSB)[30, 31, 32], in which the hidden SUSY breaking sector communicates with the visible/MSSM sector via a sector of "messenger" fields. The mGMSB will be introduced in more detail in Chapter 3.

Another group of models are anomaly-mediated SUSY breaking models (AMSB)[33] which assume that the SUSY breaking sector is hidden away from the visible sector in extra-dimensional spacetime such that the dominant SSB contributions come from the superconformal anomaly. There are other alternatives to the AMSB, such as the HCAMSB[34] or gaugino-AMSB[35, 36], which also become of interest in Chapter 3.

1.2.6 Radiatively-driven Natural SUSY

Radiatively-driven natural SUSY (RNS) is based on the MSSM and may be valid up to the GUT scale. This model has two main qualities: 1) the superpotential higgsino mass is rather low with $|\mu| \sim 100 - 300$ GeV, and 2) it has a weak scale value of $-m_{H_u}^2 \sim m_Z^2$. Both these features are needed to allow for electroweak naturalness at the tree level. As in REWSB, $m_{H_u}^2$ is radiatively driven to low values and depends on large top quark Yukawa coupling. Thus, the RNS model has emerged as a way to reconcile low electroweak fine-tuning with lack of SUSY signals from recent LHC8 results and the presence of a rather large value of $m_h \sim 125$ GeV. It can not be realized within the mSUGRA/CMSSM framework since here μ is not a free parameter. It can, however be realized in the NUHM2 models with light higgsino-like $\widetilde{W}_1^{\pm}$ and $\widetilde{Z}_{1,2}$ and TeV-scale top squarks[19]. Generally natural SUSY[14] models solve the LHP with light higgsinos and moderate top squarks along with heavy first/second generation squarks and gluinos at the TeV-scale[15, 16, 17, 18]. Here, the problem of a too low value of m_h arises. The heavy stop masses in the RNS have large mixing and drive the mass of the light Higgs to ~ 125. These naively exacerbate fine-tuning due to the Little Hierarchy problem $m_{sparticle} \gg m_Z$, but the mass spectra of the NUHM2 allows for fine-tuning at the $3 - 10\%$ level. Chapter 3 will discuss the NUHM2 in comparison to a variety of other models.

Chapter 2

Measures of Naturalness[13, 37]

In soft SUSY breaking theories, with their ultra-violet properties, SUSY breaking appears near the weak scale, ensuring to be at most logarithmically sensitive to HS physics. Over the last three decades, weak scale SUSY embedded into a HS framework is subject to deep studies since it addresses the big hierarchy problem the SM fails to explain[38]. The question arises, how much fine-tuning is too much? Differently stated, are SUSY models unnatural and if so, how unnatural? Or, do these models remain natural for a certain range of parameter space? Thus, one main goal of collider[39, 40] and dark matter[41] search experiements is to examine all avenues in the search for natural SUSY. Some authors may argue that there is a great deal of subjectivity involved in contraints from naturalness. This chapter indroduces several different proposed measures of naturalness, which will be further discussed in Chapter 3.

2.1 Standard Model Fine-tuning

In the SM, the mass of the Higgs boson can be calculated as

$$m_h^2 = m_{h_{tree}}^2 + \delta m_{h_{rad}}^2 \tag{2.1}$$

where the tree-level squared mass $m^2_{h_{tree}} = 2\mu^2$ and the quadratically divergent radiative corrections

$$\delta m^2_{H_{SM}} \simeq \frac{3}{4\pi^2}\left(-\lambda_t^2 + \frac{g^2}{4} + \frac{g^2}{8\cos^2\theta_W} + \lambda\right)\Lambda^2 \tag{2.2}$$

are *independent* (here, λ_t is the SM top Yukawa coupling, g is the $SU(2)_L$ gauge coupling, λ is the SM Higgs quartic coupling and Λ is the effective theory energy cutoff scale). The λ_t and λ terms arise from the top loop and self-coupling, respectively. The terms proportional to g come from the W- and Z-loops. All four contributions are independently quadratically divergent.

A SM measure of EWFT can be defined by requiring that the radiative corrections δm_h^2 to the squared Higgs mass m_h^2 be not too large:

$$\Delta_{SM} = \delta m^2_{h_{rad}}/(m^2_{h_{tree}}/2) \lesssim \Delta^{max}_{SM}. \tag{2.3}$$

For large Λ, the large radiative corrections must be balanced by a fine-tuning of $2\mu^2$ such that m_h^2 maintains its physical value. Alternatively, to maintain naturalness, then $\delta m^2_{H_{SM}} \sim m_h^2$ which requires $\Lambda \lesssim 1$ TeV, *i.e.* the SM is only valid below about the $\Lambda \sim 1$ TeV scale.

2.2 Fine-tuning in Supersymmetry

In most supersymmetric models based on high scale input parameters– *i.e.* SUSY models with soft term boundary conditions imposed at a scale $\Lambda \gg m_{weak}$ where

Λ may range as high as $m_{GUT} \simeq 2 \times 10^{16}$ GeV or even the reduced Planck mass $M_P \simeq 2 \times 10^{18}$ GeV– the soft SUSY breaking terms are input at the scale Λ and then evolved to the electroweak scale $m_{weak} \sim 100$ GeV via renormalization group (RG) running. At the weak scale, the scalar potential is minimized and checked to ensure that EW symmetry is properly broken. The Higgs portion of the scalar potential is given by

$$V_{Higgs} = V_{tree} + V_{rad}, \tag{2.4}$$

where the portion of the neutral Higgs sector in the tree level is given by

$$\begin{aligned} V_{tree} =& (m_{H_u}^2 + \mu^2)|h_u^0|^2 + (m_{H_d}^2 + \mu^2)|h_d^0|^2 \\ & - B\mu(h_u^0 h_d^0 + h.c.) + \frac{1}{8}(g^2 + g'^2)(|h_u^0|^2|h_d^0|^2)^2 \end{aligned} \tag{2.5}$$

and the radiative corrections by

$$V_{rad} = \sum_i \frac{(-1)^{2s_i}}{64\pi^2}(2s_i + 1)c_i m_i^4 \Big[log(\frac{m_i^2}{Q^2} - \frac{3}{2}\Big]. \tag{2.6}$$

Here the sum runs over all fields that couple to Higgs fields, m_i^2 is the squared *Higgs field dependent* mass, $c_i = c_{char}c_{col}$, with $c_{char} = 3(1)$ for charged (neutral) particles and $c_{col} = 3(1)$ for colored (uncolored) particles and s_i is their spin quantum number. The radiative corrections that arise from the derivatives of V_{rad}

evaluated at the minimum are given by

$$\begin{aligned}
\Sigma_u^u &= \frac{\partial V_{rad}}{\partial |h_u|^2}\Big|_{min}, \\
\Sigma_d^d &= \frac{\partial V_{rad}}{\partial |h_d|^2}\Big|_{min}, \\
\Sigma_u^d &= \frac{\partial V_{rad}}{\partial (h_u h_d + c.c.)}\Big|_{min}.
\end{aligned} \tag{2.7}$$

These include contributions from various particles and sparticles with sizeable Yukawa and/or gauge couplings to the Higgs sector. The value of μ is then fixed in terms of the weak scale soft SUSY breaking terms $m_{H_u}^2$ and $m_{H_d}^2$ by requiring that the measured value of $m_Z \simeq 91.2$ GeV is obtained:

$$\frac{m_Z^2}{2} = \frac{m_{H_d}^2 + \Sigma_d^d - (m_{H_u}^2 + \Sigma_u^u)\tan^2\beta}{\tan^2\beta - 1} - \mu^2 \simeq -m_{H_u}^2 - \Sigma_u^u - \mu^2 \tag{2.8}$$

The biggest contributions to the radiative corrections come from the top squarks

$$\begin{aligned}
\Sigma_u^u(\tilde{t}_{1,2}) &= \frac{3}{16\pi^2} F(m_{\tilde{t}_{1,2}}^2)\Big[f_t^2 - g_Z^2 \mp \frac{f_t^2 A_t^2 - 8 g_Z^2 (\frac{1}{4} - \frac{2}{3}x_W)\Delta_t}{m_{\tilde{t}_2}^2 - m_{\tilde{t}_1}^2}\Big] \\
\Sigma_d^d(\tilde{t}_{1,2}) &= \frac{3}{16\pi^2} F(m_{\tilde{t}_{1,2}}^2)\Big[g_Z^2 \mp \frac{f_t^2 \mu_t^2 + 8 g_Z^2 (\frac{1}{4} - \frac{2}{3}x_W)\Delta_t}{m_{\tilde{t}_2}^2 - m_{\tilde{t}_1}^2}\Big],
\end{aligned} \tag{2.9}$$

where $F(m^2) = m^2(\log\frac{m^2}{Q^2} - 1)$, $g_Z^2 = (g^2 + g'^2)/8$, $x_W \equiv \sin^2\theta_W$ and $\Delta t = (m_{\tilde{t}_L}^2 - m_{\tilde{t}_R}^2)/2 + M_Z^2 \cos 2\beta(\frac{1}{4} - \frac{2}{3}x_W)$. The stop masses in the denominator of Eq. 2.9 are at tree level. More details on the radiative corrections to the minimization conditions of the Higgs potential can be found in Ref. [19].

Already at this point: if $-m_{H_u}^2(weak)$ in the right-hand-side of Eq. 2.8 is large positive ($\gg m_Z^2$), then the value of μ must be fine-tuned by hand to ensure

the measured value of m_Z^2 is obtained. Since most researchers these days run automated computer codes[42] to calculate the weak scale spectrum of SUSY and Higgs particles, this represents a *hidden* fine-tuning that ought to be accounted for.

Alternatively, if soft SUSY breaking terms *and* μ are input parameters, then much higher values of $m_Z \gg 91.2$ GeV are expected from scans over SUSY model parameter space. The 20 dimensional pMSSM parameter space includes

$$M_1,\ M_2,\ M_3, \tag{2.10}$$

$$m_{Q_1},\ m_{U_1},\ m_{D_1},\ m_{L_1},\ m_{E_1}, \tag{2.11}$$

$$m_{Q_3},\ m_{U_3},\ m_{D_3},\ m_{L_3},\ m_{E_3}, \tag{2.12}$$

$$A_t,\ A_b,\ A_\tau, \tag{2.13}$$

$$m_{H_u}^2,\ m_{H_d}^2,\ \mu,\ B. \tag{2.14}$$

The usual strategy is to use the EW minimization conditions[25] to trade the bilinear parameter B for the ratio of Higgs vevs $\tan\beta \equiv v_u/v_d$ and to exchange $m_{H_u}^2$ and $m_{H_d}^2$ for m_Z^2 and m_A^2[25]. This procedure reduces the number of free parameters to 19 (since m_Z is fixed) but hides the fine-tuning embedded in Eq. 2.8 since now either $m_{H_u}^2$ or μ^2 is an output.

Fig. 2.1 plots the value of m_Z which is generated from a scan over the pMSSM space for the range of scalar and gaugino mass soft terms from $0-10$ TeV, -10 TeV $< A_i < 10$ TeV, $\mu : 0-3$ TeV and $\tan\beta : 3-60$, while requiring the lightest neutralino $\widetilde{Z}_1$ as lightest SUSY particle (LSP) and $m_{\widetilde{W}_1} > 103.5$ GeV

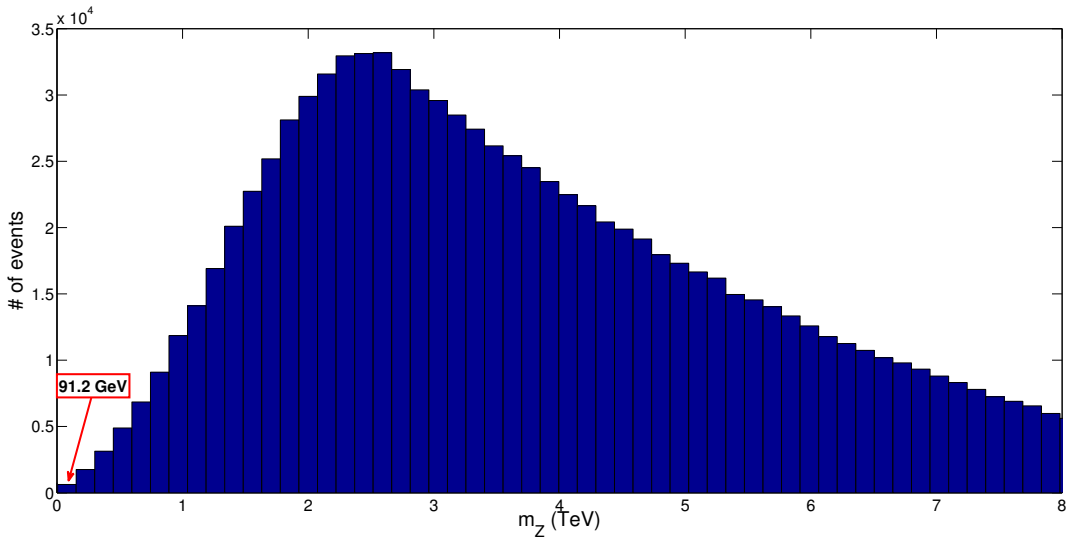

Figure 2.1: Plot of value of m_Z generated from a scan over pMSSM model parameter space while *not* implementing the m_Z^2 constraint.

(in accord with LEP2 constraints) [1] , but avoiding the m_Z^2 constraint. Here, one sees that the most probable value of m_Z is ~ 2.5 TeV with a large spread to both higher and lower values. It is highly unlikely to generate the measured value $m_Z = 91.2$ GeV. This is the essence of the Little Hierarchy problem: why is m_Z so small when the soft terms (which are proportional to $m_{3/2}$) are so large?

2.2.1 High-Scale Fine-Tuning Δ_{HS}

To include explicit dependence on the high scale Λ at which the SUSY theory may be defined, one may write the *weak scale* parameters $m_{H_{u,d}}^2$ and μ^2 in Eq. (2.8) as

$$m_{H_{u,d}}^2 = m_{H_{u,d}}^2(\Lambda) + \delta m_{H_{u,d}}^2; \qquad \mu^2 = \mu^2(\Lambda) + \delta\mu^2 \ , \tag{2.15}$$

[1] This limit diminishes to ~ 91.9 GeV in the case of a wino-like WIMP.

where $m^2_{H_{u,d}}(\Lambda)$ and $\mu^2(\Lambda)$ are the corresponding parameters renormalized at the high scale Λ.

If the MSSM is assumed to be valid up to the GUT scale, then the value of $\delta m^2_{H_u}$ can be found by integrating the renormalization group equation (RGE)[44]:

$$\frac{dm^2_{H_u}}{dt} = \frac{1}{8\pi^2}\left(-\frac{3}{5}g_1^2M_1^2 - 3g_2^2M_2^2 + \frac{3}{10}g_1^2S + 3f_t^2X_t\right) \tag{2.16}$$

where $t = \ln(Q^2/Q_0^2)$, $S = m^2_{H_u} - m^2_{H_d} + Tr\left[\mathbf{m}_Q^2 - \mathbf{m}_L^2 - 2\mathbf{m}_U^2 + \mathbf{m}_D^2 + \mathbf{m}_E^2\right]$ and where $X_t = m^2_{Q_3} + m^2_{U_3} + m^2_{H_u} + A_t^2$. By neglecting gauge terms and S ($S = 0$ in models with scalar soft term universality but can be large in models with non-universality), and also neglecting the $m^2_{H_u}$ contribution to X_t and the fact that f_t and the soft terms evolve under Q^2 variation, then this expression may be readily integrated from m_{SUSY} to the cutoff Λ to obtain

$$\delta m^2_{H_u} \sim -\frac{3f_t^2}{8\pi^2}(m^2_{Q_3} + m^2_{U_3} + A_t^2)\ln\left(\Lambda^2/m^2_{SUSY}\right). \tag{2.17}$$

Here, Λ may be taken as high as $m_{GUT} \simeq 2\times10^{16}$ GeV or even the reduced Planck mass $m_P \simeq 2.4\times10^{18}$ GeV. Also, $m^2_{SUSY} \simeq m_{\tilde{t}_1}m_{\tilde{t}_2}$ as this value minimizes the radiative corrections $\Sigma_u^u(\tilde{t}_{1,2})$. In this way, Eq. (2.8) becomes

$$\frac{m_Z^2}{2} = \frac{(m^2_{H_d}(\Lambda) + \delta m^2_{H_d} + \Sigma_d^d) - (m^2_{H_u}(\Lambda) + \delta m^2_{H_u} + \Sigma_u^u)\tan^2\beta}{\tan^2\beta - 1} - (\mu^2(\Lambda) + \delta\mu^2)\,. \tag{2.18}$$

One can now define a high scale fine-tuning measure by requiring that each of the

terms on the right-hand-side of Eq. (2.18) (normalized again to $m_Z^2/2$) be smaller than a value

$$\Delta_{\rm HS} \equiv max_i|B_i|/(m_Z^2/2) \ , \tag{2.19}$$

with $B_{H_d} \equiv m_{H_d}^2(\Lambda)/(\tan^2\beta - 1)$, $B_{H_u} = -m_{H_u}^2(\Lambda)\tan^2\beta/(\tan^2\beta - 1)$ and $B_\mu = -\mu^2(\Lambda)$. Also, $B_{\Sigma_u^u(k)} = -\Sigma_u^u(k)\tan^2\beta/(\tan^2\beta - 1)$ and $B_{\Sigma_d^d(k)} = \Sigma_d^d(k)/(\tan^2\beta - 1)$, where k labels the various loop contributions included in Eq. 2.18

By requiring[14, 15, 16, 45] $\Delta_{HS} \sim \delta m_{H_u}^2/(m_h^2/2) \lesssim 10$ one then expects $m_{\tilde{t}_{1,2},\tilde{b}_1} \lesssim 600$ GeV. Using the Δ_{HS} measure along with $m_h \simeq 125$ GeV then one finds some popular SUSY models to be electroweak fine-tuned to 0.1%[69].

2.2.2 Barbieri-Giudice Fine-Tuning Δ_{BG}

The more traditional measure Δ_{BG} was proposed by Ellis *et al.*[4] and later investigated more thoroughly by Barbieri and Giudice[5]. Here,

$$\Delta_{BG} \equiv max_i\left[c_i\right] \quad \text{where} \quad c_i = \left|\frac{\partial \ln m_Z^2}{\partial \ln a_i}\right| = \left|\frac{a_i}{m_Z^2}\frac{\partial m_Z^2}{\partial a_i}\right| \tag{2.20}$$

where the a_i constitute the fundamental parameters of the model and the c_i are known as *sensitivity coefficients*[46].

The starting point is to express m_Z^2 in terms of weak scale SUSY parameters as in Eq. 2.8:

$$m_Z^2 \simeq -2m_{H_u}^2 - 2\mu^2 \tag{2.21}$$

where the partial equality obtains for moderate-to-large $\tan\beta$ values and where we

assume for now the radiative corrections are small. An advantage of Δ_{BG} over the previous large-log measure is that it maintains the correlation between $m_{H_u}^2(\Lambda)$ and $\delta m_{H_u}^2$ by replacing $m_{H_u}^2(m_{weak}) = \left(m_{H_u}^2(\Lambda) + \delta m_{H_u}^2\right)$ by its expression in terms of high scale parameters. To evaluate Δ_{BG}, one needs to know the explicit dependence of $m_{H_u}^2$ and μ^2 on the fundamental parameters. Semi-analytic solutions to the one-loop renormalization group equations for $m_{H_u}^2$ and μ^2 can be found for instance in Ref's [47]. For the case of $\tan\beta = 10$, then[48, 49, 46]

$$\begin{aligned} m_Z^2 \simeq & -2.18\mu^2 + 3.84M_3^2 + 0.32M_3M_2 + 0.047M_1M_3 - 0.42M_2^2 \\ & +0.011M_2M_1 - 0.012M_1^2 - 0.65M_3A_t - 0.15M_2A_t \\ & -0.025M_1A_t + 0.22A_t^2 + 0.004M_3A_b \\ & -1.27m_{H_u}^2 - 0.053m_{H_d}^2 \\ & +0.73m_{Q_3}^2 + 0.57m_{U_3}^2 + 0.049m_{D_3}^2 - 0.052m_{L_3}^2 + 0.053m_{E_3}^2 \\ & +0.051m_{Q_2}^2 - 0.11m_{U_2}^2 + 0.051m_{D_2}^2 - 0.052m_{L_2}^2 + 0.053m_{E_2}^2 \\ & +0.051m_{Q_1}^2 - 0.11m_{U_1}^2 + 0.051m_{D_1}^2 - 0.052m_{L_1}^2 + 0.053m_{E_1}^2, \end{aligned} \quad (2.22)$$

where all terms on the right-hand-side are understood to be GUT scale parameters.

Then, the proposal is that the variation in m_Z^2 with respect to parameter variation be small. Thus, Δ_{BG} measures the fractional change in m_Z^2 due to fractional variation in high scale parameters a_i.

The requirement of low Δ_{BG} is then equivalent to the requirement of no large cancellations on the right-hand-side of Eq. 2.22 since (for linear terms) the

logarithmic derivative just picks off coefficients of the relevant parameter. For instance, $c_{m^2_{Q_3}} = 0.73 \cdot (m^2_{Q_3}/m^2_Z)$. If one allows $m_{Q_3} \sim 3$ TeV (in accord with requirements from the measured value of m_h) then one obtains $c_{m^2_{Q_3}} \sim 800$ and so $\Delta_{BG} \geq 800$. In this case, SUSY would be electroweak fine-tuned to about 0.1%. If instead one sets $m_{Q_3} = m_{U_3} = m_{H_u} \equiv m_0$ as in models with scalar mass universality, then the various scalar mass contributions to m^2_Z largely *cancel* and $c_{m^2_0} \sim -0.017 m^2_0/m^2_Z$: the contribution to Δ_{BG} from scalars drops by a factor ~ 50.

The above argument illustrates the extreme model-dependence of Δ_{BG} for multi-parameter SUSY models. The value of Δ_{BG} can change radically from theory to theory even if those theories generate exactly the same weak scale sparticle mass spectrum.

2.3 Δ_{EW} and its implications

The fact that $m_Z = 91.2$ GeV along with $m_h \simeq 125.5$ GeV tells us from Eq. 2.8 that to naturally generate the measured value of m_Z (and m_W) and m_h, then

- $|\mu| \sim m_Z \sim 100 - 200$ GeV
- $m^2_{H_u}$ should be driven to small negative values such that $-m^2_{H_u} \sim 100 - 200$ GeV at the weak scale and
- that the radiative corrections are not too large: $\Sigma^u_u \lesssim 100 - 200$ GeV

The first two of these conditions are shown in Fig. 1.1 as soft term and μ RG running versus Q for a radiatively-driven natural SUSY benchmark point from

Ref. [27] where $\mu = 110$ GeV and $\Delta_{EW} = 16$.

Formally, these conditions arise from requiring the *electroweak fine-tuning measure* Δ_{EW} be not too large, where

$$\Delta_{EW} \equiv max_i \left|C_i\right| / (m_Z^2/2) \ , \tag{2.23}$$

may be constructed, with $C_{H_d} = m_{H_d}^2/(\tan^2\beta - 1)$, $C_{H_u} = -m_{H_u}^2 \tan^2\beta/(\tan^2\beta - 1)$ and $C_\mu = -\mu^2$. Also, $C_{\Sigma_u^u(k)} = -\Sigma_u^u(k)\tan^2\beta/(\tan^2\beta - 1)$ and $C_{\Sigma_d^d(k)} = \Sigma_d^d(k)/(\tan^2\beta - 1)$, where k labels the various loop contributions included in Eq. 2.8.

The largest of the radiative corrections comes from the top squark sector $\Sigma_u^u(\tilde{t}_{1,2})$. These radiative corrections can be minimized for large stop mixing from a large trilinear A_t parameter, which also raises up the value of m_h to the 125 GeV regime for top squark masses in the 1-4 TeV range[18].

An advantage of Δ_{EW} is that it is model-independent in the sense that any model which yields the same weak scale mass spectrum will generate the same value of Δ_{EW}.

2.4 Naturalness in the SUGRA19 Model

In previous studies, the radiative natural SUSY model has emerged as a way to reconcile low EWFT with lack of SUSY signals at LHC8 and the presence of a light Higgs scalar with mass $m_h \sim 125$ GeV. The RNS model cannot be realized within the restrictive mSUGRA/CMSSM framework, but can be realized

within the context of NUHM2 models (which depend on 6 input parameters) and where μ can be a free input value. In RNS models, Δ_{EW} as low as ~ 10 can be generated while Δ_{HS} as low as 10^3 can be found. One may wonder if the extra 13 parameters in the SUGRA19 model allow for even lower values of Δ_{EW}.

2.4.1 SUSY mass spectrum calculation

In this section, the Isajet 7.83 [50] SUSY spectrum generator Isasugra[51] was used to calculate superparticle mass spectra in the SUGRA19 model. Isasugra begins the calculation of the sparticle mass spectrum with input $\overline{DR}$ gauge couplings and f_b, f_τ Yukawa couplings at the scale $Q = M_Z$ (f_t running begins at $Q = m_t$) and evolves the 6 couplings up in energy to scale $Q = M_{\rm GUT}$ (defined as the value Q where $g_1 = g_2$) using two-loop renormalization group equations (RGEs). The exact unification condition $g_3 = g_1 = g_2$ at $M_{\rm GUT}$ is not enforced, since a few percent deviation from unification can be attributed to unknown GUT-scale threshold corrections [52]. Next, the SSB boundary conditions at $Q = M_{\rm GUT}$ are imposed and the set of 26 coupled two-loop MSSM RGEs [53, 54] evolve back down in scale to $Q = M_Z$. Full two-loop MSSM RGEs are used for soft term evolution, and the gauge and Yukawa coupling evolution includes threshold effects in the one-loop beta-functions, so the gauge and Yukawa couplings transition smoothly from the MSSM to SM effective theories as different mass thresholds are passed. In Isasugra, the values of SSB terms which mix are frozen out at the scale $Q = m_{SUSY} = \sqrt{m_{\tilde{t}_L} m_{\tilde{t}_R}}$, while non-mixing SSB terms are frozen out at their own mass scale [51]. The scalar potential is minimized using the RG-

improved one-loop MSSM effective potential evaluated at an optimized scale $Q = m_{SUSY} \sim \sqrt{m_{\tilde{t}_L} m_{\tilde{t}_R}}$ to account for leading two-loop effects [55]. Once the tree-level sparticle mass spectrum is obtained, one-loop radiative corrections are calculated for all sparticle and Higgs boson masses, including complete one-loop weak scale threshold corrections for the top, bottom and tau masses at scale $Q = m_{SUSY}$ [56]. Since Yukawa couplings are modified by the threshold corrections, the solution must be obtained iteratively, with successive up-down running until a convergence at the required level is found.

2.4.2 Scan calculations

First a *broad-based* scan is performed to search for models with low Δ_{EW} and low Δ_{HS}. The randomized scan ranges over the following SUGRA19 parameters:

- Gaugino masses: $M_1,\ M_2,\ M_3 : 0 - 3.5$ TeV
- First/second generation scalar masses: m_{Q_1}, m_{U_1}, m_{D_1}, m_{L_1}, m_{E_1}: $0 - 3.5$ TeV,
- Third generation scalar masses: m_{Q_3}, m_{U_3}, m_{D_3}, m_{L_3}, m_{E_3}: $0 - 3.5$ TeV,
- Higgs soft masses: $m_{H_u},\ m_{H_d} :\ 0 - 3.5$ TeV,
- trilinear soft terms: $A_t,\ A_b,\ A_\tau$:-3.5 TeV $\rightarrow 3.5$ TeV,
- ratio of weak scale Higgs vevs $\tan\beta :\ 2 - 60$.

A common mass for first and second generation scalars is adopted so as to avoid the most stringent SUSY FCNC constraints[57].

The solutions are to satisfy the following conditions:

- electroweak symmetry be radiatively broken (REWSB),
- the neutralino $\widetilde{Z}_1$ is the lightest MSSM particle,
- the light chargino mass obeys the model independent LEP2 limit, $m_{\widetilde{W}_1} > 103.5$ GeV[58] and
- $123 < m_h < 128$ GeV.

Limits from any LHC sparticle searches are not imposed since the general scan can produce compressed spectra which in many cases can easily elude LHC gluino and squark searches. Points which satisfy the above constraints are plotted as blue circles in the following scatter plots.

Also, for each point generated the values of $BF(b \to s\gamma)$[59, 60] and $BF(B_S \to \mu^+\mu^-)$[61] are calculated. The measured value of $BF(b \to s\gamma)$ is found to be $(3.55 \pm 0.26) \times 10^{-4}$ [62]. For comparison, the SM prediction[63] is $BF^{SM}(b \to s\gamma) = (3.15 \pm 0.23) \times 10^{-4}$. Also, recently the LHCb collaboration has found an excess over the background for the decay $B_s \to \mu^+\mu^-$[65]. They find a branching fraction of $BF(B_s \to \mu^+\mu^-) = 3.2^{+1.5}_{-1.2} \times 10^{-9}$ which is in accord with the SM prediction of $(3.2 \pm 0.2) \times 10^{-9}$.[2] Points with $BF(b \to s\gamma)$ within 3σ of its measured value $BF(b \to s\gamma) = (2.5 - 4.5) \times 10^{-4}$ and points with $BF(B_s \to \mu^+\mu^-) = (2 - 4.7) \times 10^{-9}$ will be labeled as light blue, showing that these points are also in accord with B-physics constraints.

[2]Soon after this study was performed, CMS[66] measured events interpreted as $B_s \to \mu^+\mu^-$ giving a combined branching fraction of $BF(B_s \to \mu^+\mu^-) = (2.9 \pm 0.7) \times 10^{-9}$.

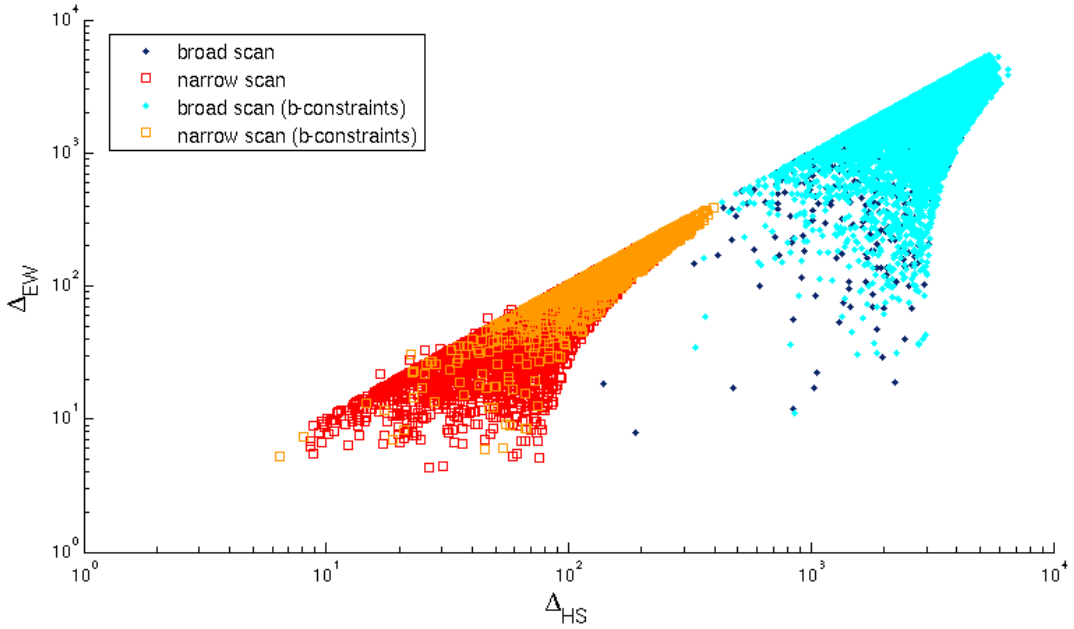

Figure 2.2: Plot of Δ_{HS} vs. Δ_{EW} from a broad (dark/light blue) and focused (red/orange) scan over SUGRA19 model parameter space. The orange and light blue points satisfy B-decay constraints while the dark blue and red points do not.

The first set of results are shown in Fig. 2.2. The broad scan points are shown in blue. One can see that the bulk of generated points yield Δ_{EW} and $\Delta_{HS} \gtrsim 10^3$, so would qualify as highly EW finetuned in generating $m_Z = 91.2$ GeV. The points with the lowest Δ_{EW} values come in with $\Delta_{EW} \sim 10$, which is similar to that which can be achieved in the more restrictive NUHM2, but which is much better than what can be achieved in mSUGRA.

The lowest Δ_{EW} point has $\Delta_{EW} = 7.9$, while the corresponding $\Delta_{HS} = 190$. The SUGRA19 parameters associated with this point are listed in Table 2.1 in the column labeled as EW1. The point has the required low $\mu \sim 180$ GeV and $m^2_{H_u}(m_{weak}) \sim -(171 \text{ GeV})^2$. In addition, the large top-squark mixing $A_t/m_Q(3) \sim -2.1$ softens the top squark radiative corrections $\Sigma^u_u(\tilde{t}_{1,2})$ whilst

raising m_h up to 123.5 GeV.

The corresponding sparticle mass spectra are listed in Table 2.2. The gluinos and squarks are $\sim 2-3$ TeV: well beyond current LHC reach. The $\widetilde{W}_2^{\pm}$ and $\widetilde{Z}_{1,2}$ are dominantly higgsino-like with a mass gap $m_{\widetilde{Z}_2} - m_{\widetilde{Z}_1} \simeq 3$ GeV. Thus, even though the higgsinos can be produced with large cross sections at LHC, the very soft visible energy release from their decays makes them difficult to detect[67]. The light higgsinos should be straightforward to detect at a linear e^+e^- collider with $\sqrt{s} \gtrsim 400$ GeV. The lightest top squark $\tilde{t}_1$ has mass less than 1 TeV: typically below values generated from radiative natural SUSY models[19]. This leads to a somewhat anomalous branching fraction $BF(b \to s\gamma) \sim 2.5 \times 10^{-4}$, below the measured value of $(3.55 \pm 0.26) \times 10^{-4}$ [62].

Next, to hone in on SUGRA19 solutions with low Δ_{HS}, a narrow, dedicated scan about the lowest Δ_{HS} solution is performed:

- $M_1:\ 3-3.5$ TeV, $M_2:\ 2.7-3.2$ TeV, $M_3:\ 0.8-1.3$ TeV
- $m_Q(1,2):\ 0.9-1.4$ TeV, $m_U(1,2):\ 2.2-2.7$ TeV, $m_D(1,2):\ 1.25-1.75$ TeV, $m_L(1,2):\ 0.4-0.9$ TeV, $m_E(1,2):\ 0.7-1.2$ TeV,
- $m_Q(3):\ 0-0.5$ TeV, $m_U(3):\ 0-0.5$ TeV, $m_D(3):\ 2.7-3.2$ TeV, $m_L(3):\ 0.1-0.5$ TeV, $m_E(3):\ 1-2$ TeV,
- $m_{H_u}:\ 0.05-0.55$ TeV, $m_{H_d}:\ 2.9-3.4$ TeV,
- $A_t:\ -1.3 \to -0.8$ TeV, $A_b:\ 2.9-3.4$ TeV, $A_\tau:\ 1.7-2.2$ TeV,

with $\tan\beta$ still $2-60$ as before.

parameter	EW1	HS1	HS2
$M_1(m_{GUT})$	2822.1	3266.2	3416.4
$M_2(m_{GUT})$	3385.3	2917.8	3091.3
$M_3(m_{GUT})$	884.9	1095.7	1085.8
$m_Q(1)$	2484.7	1192.6	978.5
$m_U(1)$	2506.2	2468.3	2440.6
$m_D(1)$	2342.1	1508.9	1404.2
$m_L(1)$	1820.4	623.8	754.8
$m_E(1)$	1731.2	936.1	915.8
$m_Q(3)$	698.3	6.6	371.3
$m_U(3)$	1552.8	233.9	23.2
$m_D(3)$	1498.5	2946.0	3052.4
$m_L(3)$	3339.3	341.1	451.3
$m_E(3)$	2114.9	1268.7	1247.5
m_{H_u}	871.3	314.0	125.4
m_{H_d}	2205.3	3160.4	2964.9
A_t	-1509.6	-1024.4	-801.3
A_b	2301.7	3121.6	3294.3
A_τ	3307.3	1932.0	1754.5
$\tan\beta$	27.0	51.1	29.0
μ	181.4	242.8	98.0
Δ_{EW}	7.9	17.9	5.2
Δ_{HS}	190.0	32.0	6.4

Table 2.1: Input parameters (GUT scale) in GeV for one low Δ_{EW} point and two low Δ_{HS} points. We take $m_t = 173.2$ GeV.

mass (GeV)	EW1	HS1	HS2
$m_{\tilde{g}}$	2042.9	2436.7	2428.8
$m_{\tilde{u}_L}$	3650.7	2991.9	2968.5
$m_{\tilde{u}_R}$	2980.5	3214.8	3191.6
$m_{\tilde{e}_R}$	2196.3	1763.6	1786.1
$m_{\tilde{t}_1}$	879.5	1033.2	892.4
$m_{\tilde{t}_2}$	2305.1	1958.3	2394.9
$m_{\tilde{b}_1}$	2121.8	1961.4	2418.0
$m_{\tilde{b}_2}$	2327.7	2916.1	3495.8
$m_{\tilde{\tau}_1}$	2219.6	1049.5	1748.3
$m_{\tilde{\tau}_2}$	3865.8	1467.5	1911.3
$m_{\tilde{\nu}_\tau}$	3884.8	1464.9	1911.4
$m_{\widetilde{W}_2}$	2802.2	2393.0	2538.3
$m_{\widetilde{W}_1}$	192.1	255.5	104.1
$m_{\widetilde{Z}_4}$	2810.2	2386.8	2530.3
$m_{\widetilde{Z}_3}$	1261.2	1448.0	1513.5
$m_{\widetilde{Z}_2}$	187.8	251.2	102.4
$m_{\widetilde{Z}_1}$	184.7	247.9	99.3
m_A	2759.7	2242.6	3176.4
m_h	123.5	123.6	123.1
$\Omega^{std}_{\widetilde{Z}_1}h^2$	0.007	0.013	0.003
$BF(b \to s\gamma) \times 10^4$	2.5	1.8	2.6
$BF(B_s \to \mu^+\mu^-) \times 10^9$	3.9	4.5	3.8
$\sigma^{SI}(\widetilde{Z}_1 p)$ (pb)	2.9×10^{-10}	3.7×10^{-10}	2.5×10^{-10}

Table 2.2: Sparticle masses in GeV and observables for one low Δ_{EW} and two low Δ_{HS} points as in Table 2.1. The measured values of the branching fractions are $BF(b \to s\gamma) = (3.55 \pm 0.26) \times 10^{-4}$ and $BF(B_s \to \mu^+\mu^-) = 3.2^{+1.5}_{-1.2} \times 10^{-9}$.

The results from the narrow scan are shown in Fig. 2.2 as red squares, while points that obey B-constraints are labeled as orange squares. The more focused sampling over lucrative parameter ranges has produced points with much lower Δ_{EW} values ranging down to ~ 5, and also solutions with Δ_{HS} as low as 6. The $\Delta_{HS} = 6.4$ solution is presented in Tables 2.1 and 2.2 as benchmark model HS2. While point HS2 has μ of just 98 GeV, the lightest chargino mass is $m_{\widetilde{W}_1} = 104.1$ GeV, slightly beyond the limit from LEP2 searches. Since gluino and squark masses are in the several TeV range, the point is also safe from LHC8 searches. The mass gaps $m_{\widetilde{W}_1} - m_{\widetilde{Z}_1} = 4.8$ GeV and $m_{\widetilde{Z}_2} - m_{\widetilde{Z}_1} = 3.1$ GeV so again there will be only tiny visible energy release from the higgsino decays.

To display the sort of parameter choices leading to low Δ_{HS}, Fig. 2.3 shows the values of Δ_{EW} (blue points) and Δ_{HS} (red/orange points) versus superpotential higgsino mass μ from the broad (diamonds) and narrow (squares) scan. From the plot, one sees unambiguously that low $|\mu| \sim m_Z$ is a necessary, but not sufficient, condition to obtain *both* low Δ_{EW} and low Δ_{HS}. This translates into the solid prediction that four light higgsinos should lie within reach of a linear e^+e^- collider with $\sqrt{s} > 2|\mu|$.

Fig. 2.4 shows Δ_{HS} and Δ_{EW} vs. $m_{H_u}(m_{GUT})$ from the broad and narrow scans over SUGRA19 parameter space. Here, low Δ_{EW} solutions can be obtained over a large range of $m_{H_u}(m_{GUT})$ values, as expected from radiative natural SUSY results[19] which allow for a large cancellation between $m^2_{H_u}(m_{GUT})$ and $\delta m^2_{H_u}$. However, the low Δ_{HS} solutions are only obtained for $m_{H_u}(m_{GUT})$ not too far from m_Z, as required by Eq. 2.18.

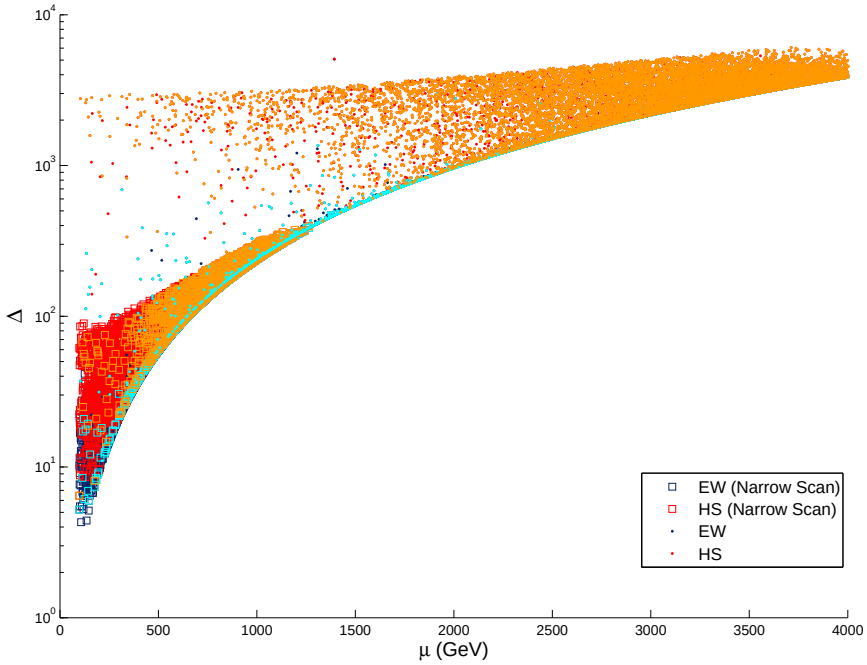

Figure 2.3: Plot of Δ_{HS} and Δ_{EW} vs. μ from scan over SUGRA19 model parameter space. Color coding as in Fig. 2.2.

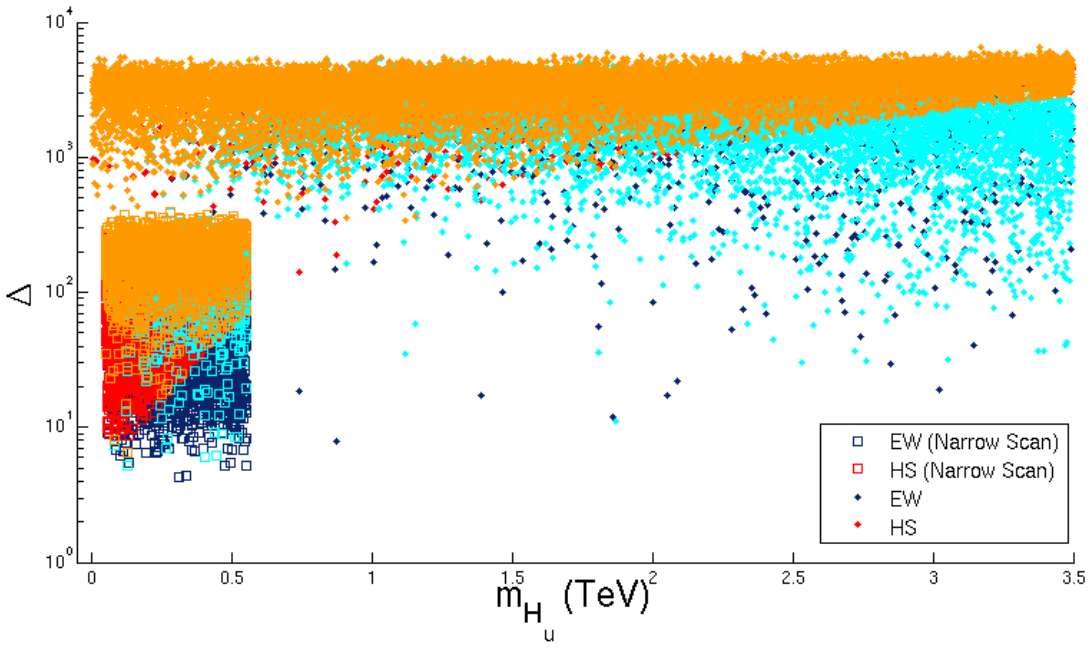

Figure 2.4: Plot of Δ_{HS} and Δ_{EW} vs. $m_{H_u}(m_{GUT})$ from scan over SUGRA19 model parameter space. Color coding as in Fig. 2.2.

Fig. 2.5 plots Δ_{HS} and Δ_{EW} vs. M_3, where it is noted that $m_{\tilde{g}} \simeq |M_3|$ up to radiative corrections. Low Δ_{EW} values allow for $M_3 \sim 1-3$ TeV, in accord with LHC searches which require $m_{\tilde{g}} \gtrsim 1$ TeV for not-too-compressed spectra.

In Fig. 2.6, Δ_{EW} and Δ_{HS} are plotted vs. $BF(b \to s\gamma)$. Also shown is the measured central value and both 1 and 3-σ error bars. SUSY contributions to the $b \to s\gamma$ decay rate come mainly from chargino-stop loops and the W and charged Higgs loops, and so are large when these particles are light and when $\tan\beta$ is large[59, 60]. In the case shown here, the low Δ_{HS} solutions which require third generation squarks somewhat heavier than generic Natural SUSY but somewhat lighter than radiative Natural SUSY, one finds the bulk of low Δ_{HS} solutions to lie a couple standard deviations below the measured value.

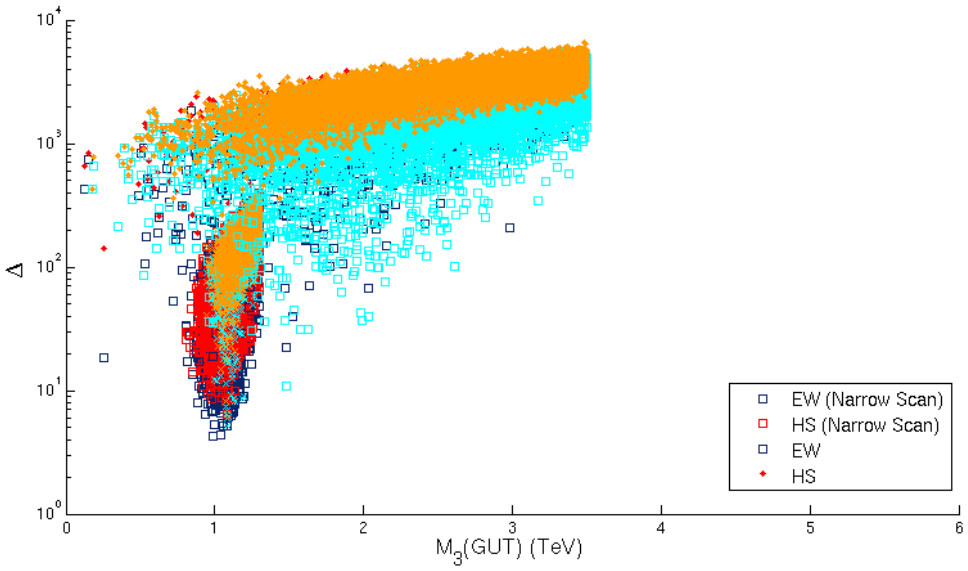

Figure 2.5: Plot of Δ_{HS} and Δ_{EW} vs. M_3 ($\sim m_{\tilde{g}}$) from scan over SUGRA19 model parameter space. Color coding as in Fig. 2.2.

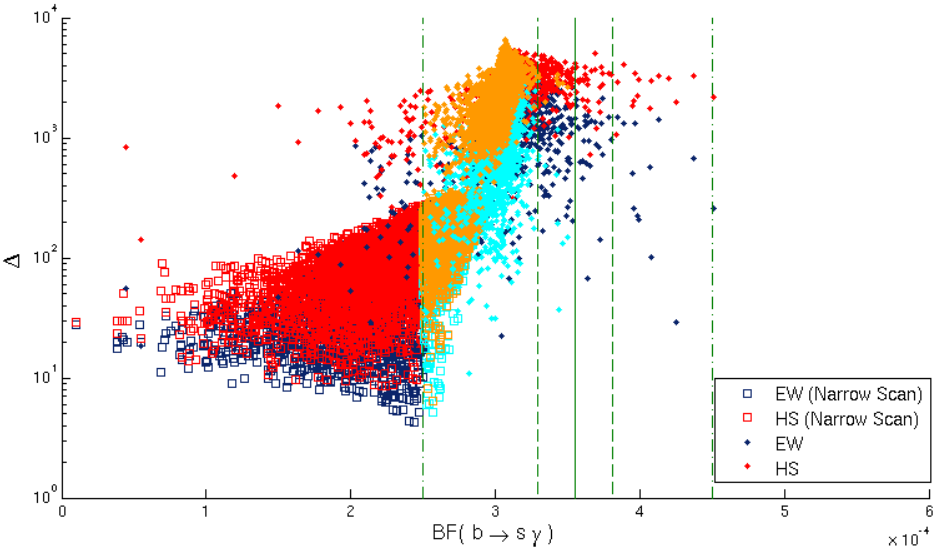

Figure 2.6: Plot of Δ_{EW} and Δ_{HS} vs. $BF(b \to s\gamma)$ from a 19 parameter scan. Color coding as in Fig. 2.2. The vertical solid line is the measured value and the dashed lines are the 1σ and 3σ uncertainties.

2.5 The Problem with Δ_{HS}

In the previous section, scans over the most general minimal flavor- and minimal CP-violating GUT scale SUSY model – SUGRA19 – were implemented with two goals in mind. The first goal was to check if the additional freedom of 13 extra parameters over NUHM2 models allows for much lower Δ_{EW} solutions. In previous work – by proceeding from mSUGRA to NUHM2 models – a reduction in the minimum of Δ_{EW} of at least a factor of 10 was found[68, 19]. The present work, does not show any substantial reduction in the minimal Δ_{EW} value by proceeding from the NUHM2 model to SUGRA19. The parameter freedom of NUHM2 appears sufficient to minimize Δ_{EW} to its lowest values of $\sim 5-10$.

The second goal was to check whether the additional parameter freedom can improve on the high scale EWFT parameter Δ_{HS}. In this regard, improvements by factors ranging up to ~ 150 were found. In order to generate low values of Δ_{HS}, one must generate $\mu \sim 100-300$ GeV as usual, but also one must start with $m_{H_u}^2 \sim m_Z^2$ at the GUT scale, and then generate relatively little change $\delta m_{H_u}^2$ during evolution from m_{GUT} to m_{weak}. Small values of $\delta m_{H_u}^2$ can be found if one begins with electroweak gaugino masses $M_{1,2} \sim 3M_3$ at the GUT scale so that gaugino-induced RG evolution dominates at high $Q \sim m_{GUT}$. The RG running of gaugino masses and selected soft scalar masses for HS1 are shown in Fig. 2.7. In frame *a*), we see that indeed M_1 and M_2 start at ~ 3 TeV values and decrease, whilst M_3 starts small at $Q = m_{GUT}$ and sharply increases. The gaugino mass boundary conditions then influence the running of the soft scalar masses in frame

b). Most important is the running of $m_{H_u}^2$, which starts near m_Z^2 at m_{GUT}, runs up to about the TeV scale at $Q \sim 10^{10}$ GeV, and then is pushed to small negative values by $Q \sim m_{weak}$. Also, $m_U(3)$ and $m_Q(3)$ start small, which aides the high Q gaugino dominance in the running of $m_{H_u}^2$. By $Q \sim m_{weak}$, these third generation squark soft terms have been pushed to the TeV scale. Thus, top squarks are not so heavy and the radiative corrections $\Sigma_u^u(\tilde{t}_{1,2})$ are under control. Top-Yukawa terms dominate the running of $m_{H_u}^2$, leading to broken electroweak symmetry, but also to not much net change in $m_{H_u}^2$ during its evolution from m_{GUT} to m_{weak}.

The solutions with low Δ_{HS} are characterized by the presence of four light higgsinos $\widetilde{W}_1^{\pm}$ and $\widetilde{Z}_{1,2}$ similar to RNS models. However, in contrast to RNS models, the third generation squarks tend to be lighter (although not as light as generic natural SUSY which favors $m_{\tilde{t}_{1,2}} \lesssim 500$ GeV). The lighter third generation squarks lead to significant SUSY contributions to the decay $b \to s\gamma$, and seem to be disfavored by the measured value of this branching fraction.

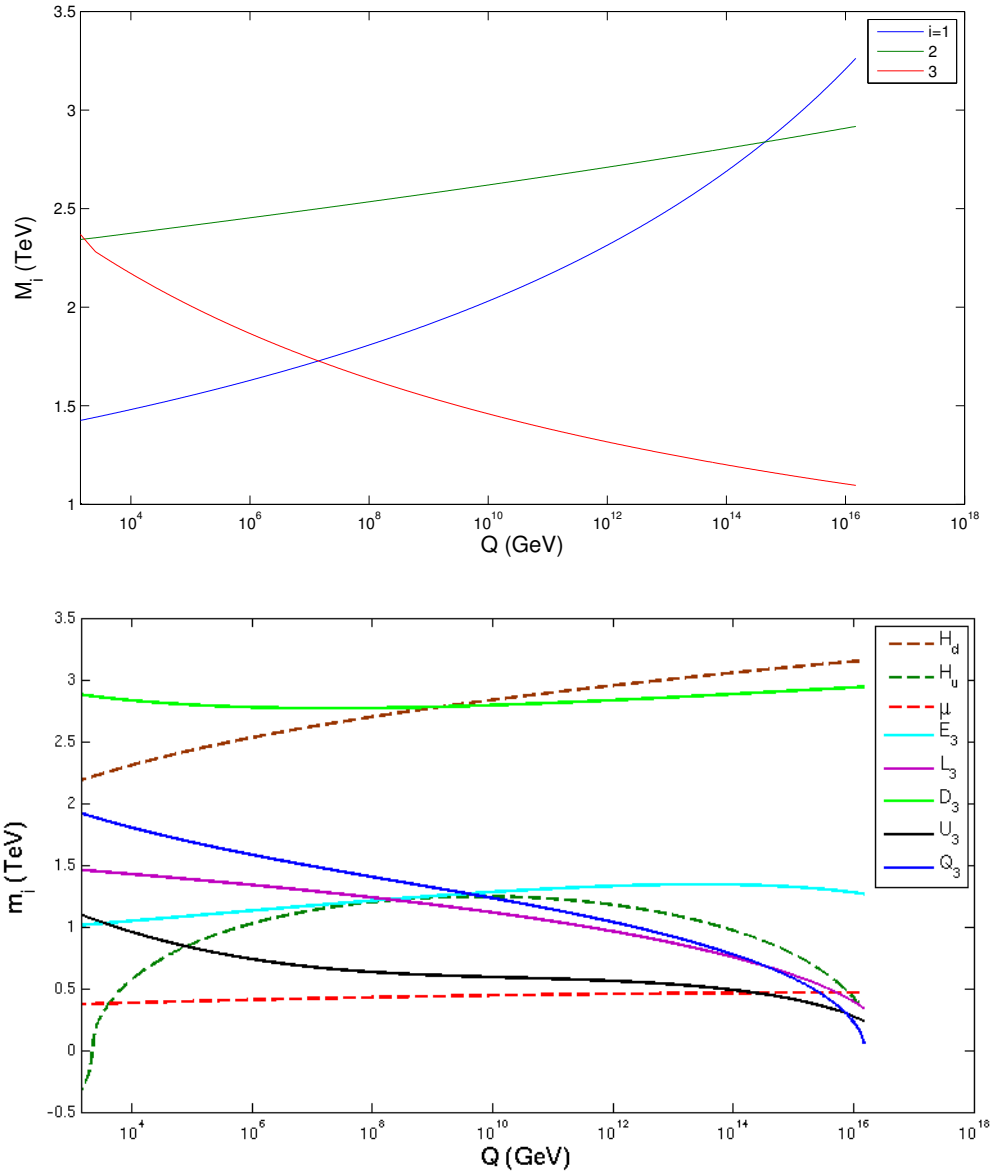

Figure 2.7: Plot of *a*) running gaugino masses and *b*) running scalar masses vs. Q from model HS1 with $\Delta_{HS} = 32$.

Chapter 3

Supersymmetry under siege[37]

Two pitfalls occur within the approach of Sec. 2.2.1 when defining Δ_{HS}.

- The first is that $m_{H_u}^2(\Lambda)$ and $\delta m_{H_u}^2$ are *not* independent: the value of $m_{H_u}^2$ feeds directly into evaluation of $\delta m_{H_u}^2$ via the X_t term in Eq. (2.16). It also feeds indirectly into $\delta m_{H_u}^2$ by contributing to the evolution of the $m_{Q_3}^2$ and $m_{U_3}^2$ terms. In fact, the larger the value of $m_{H_u}^2(\Lambda)$, then the larger is the cancelling correction $\delta m_{H_u}^2$.

- The second is that whereas $SU(2)_L \times U(1)_Y$ gauge symmetry can be broken at tree level in the SM, in the SUGRA case where SUSY is broken in a hidden sector via the superHiggs mechanism then $m_{H_u}^2 \sim m_{3/2}^2 > 0$ and EW symmetry is not even broken until one includes radiative corrections. For SUSY models valid up to some high scale $\Lambda \gg m_{weak}$, EW symmetry is broken radiatively by $m_{H_u}^2$ being driven to large negative values by the large top quark Yukawa coupling[26].

The first point brings up the problem that any observable O may look finetuned if $O = O + b - b$ and b is large but combining dependent terms leaves O *not* finetuned. In order to ascertain when a claim of fine-tuning is legitimate, we have proposed a simple **Fine-tuning Rule** which may act as a guide:

> *When evaluating fine-tuning, it is not permissible to claim fine-tuning of* **dependent** *quantities one against another.*

The over-estimates of EWFT by conventional measures such as seen in chapter 2 come from violations of this rule.

To be explicit, most theories contain several, perhaps many, parameters. Some of these may be set equal to measured values, while others may be undetermined or at least constrained, but may vary over a wide range of values. The parameters are frequently introduced to parametrize our ignorance of more fundamental physics, and their variation allows one to encompass a wide range of possibilities. We can think of each parameter as a dial, capable of being adjusted to specific, or alternatively a wide range of values. If some contribution to a measured quantity (*e.g.* m_h^2 or m_Z^2 in this text) in a theory blows up, and we have an adjustable parameter which may be dialed independently to compensate, then we may legitimately evaluate fine-tuning: is a huge, unnatural cancellation required? Alternatively, if a dial/parameter is driven to large, opposite-sign compensating values as a consequence of one related contribution blowing up, then any claimed fine-tuning would violate our rule (the quantities would be *dependent*) and some regrouping of terms into independent quantities should be found. We will meet some clarifying examples in the subsequent sections of this chapter.

3.1 All naturalness measures agree

3.1.1 When is Δ_{HS} a reliable measure of naturalness?

The fine-tuning measure Δ_{HS} introduced in Sec. 2.2.1 is a good example of the violation of the Fine-tuning Rule. Using this measure could lead to the incorrect

conclusion the model is fine-tuned since as stated in Sec. 2.5, $m^2_{H_u}(\Lambda)$ and $\delta m^2_{H_u}$ are *not* independent.

If instead dependent terms are combined, one finds a regrouping[18, 19]

$$m_h^2|_{phys} = \mu^2 + \left(m^2_{H_u}(\Lambda) + \delta m^2_{H_u}\right) \tag{3.1}$$

where now μ^2 and $\left(m^2_{H_u}(\Lambda) + \delta m^2_{H_u}\right)$ are each independent so each should be comparable to m_h^2 in order to avoid fine-tuning. It is often claimed that under such a regrouping, then the SM Higgs mass would also not be fine-tuned. But here we see that in the MSSM case – since the $m^2_{H_u}$ and $\delta m^2_{H_u}$ terms are dependent – the situation is different from the SM and one must group dependent terms together. The regrouping in Eq. 3.1 of contributions to m_h^2 into independent terms leads back to the Δ_{EW} measure defined in Sec. 2.3.

3.1.2 When is Δ_{BG} a reliable measure of naturalness?

The model dependence of Δ_{BG} mentioned in Sec. 2.2.2 likewise arises due to a violation of the Fine-tuning Rule: one must combine dependent terms into independent quantities before evaluating EW fine-tuning.

In Ref. [69], it was argued that in an ultimate theory (UTH), where all soft parameters are correlated, then Δ_{BG} should be a reliable measure of naturalness. For any fully specified hidden sector, one expects each soft supersymmetry breaking

(SSB) term to be some multiple of $m_{3/2}$[70, 71, 72]: *e.g.*

$$m_{H_u}^2 = a_{H_u} \cdot m_{3/2}^2, \tag{3.2}$$

$$m_{Q_3}^2 = a_{Q_3} \cdot m_{3/2}^2, \tag{3.3}$$

$$A_t = a_{A_t} \cdot m_{3/2}, \tag{3.4}$$

$$M_i = a_i \cdot m_{3/2}, \tag{3.5}$$

$$\cdots. \tag{3.6}$$

Here, the coefficients a_i parametrize our ignorance of the exact model for SUSY breaking. By using several adjustable parameters, we cast a wide net which encompasses a large range of hidden sector SUSY breaking possibilities.

Plugging the soft terms 3.2-3.6 into Eq. 2.22, one arrives at the expression

$$m_Z^2 = -2.18\mu^2 + a \cdot m_{3/2}^2, \tag{3.7}$$

where the value of a is now just some number which is the sum of all the coefficients of the terms $\propto m_{3/2}^2$ and μ is assumed to be independent of $m_{3/2}$.

In this case, the sensitivity coefficients can be computed:

$$c_{m_{3/2}^2} = |a \cdot (m_{3/2}^2/m_Z^2)| \text{ and} \tag{3.8}$$

$$c_{\mu^2} = |-2.18(\mu^2/m_Z^2)|. \tag{3.9}$$

For Δ_{BG} to be $\sim 1-10$ (natural SUSY with low fine-tuning), then Eq. 3.9 implies

- $\mu^2 \sim m_Z^2$

and also Eq. 3.8 implies

- $a \cdot m_{3/2}^2 \sim m_Z^2$.

The first of these conditions implies light higgsinos with mass $\sim 100 - 200$ GeV, the closer to m_Z the better. The second condition can be satisfied if $m_{3/2} \sim m_Z$[5] *or* if a is quite small. The former seems highly unlikely due to a lack of LHC8 SUSY signal and the rather large value of m_h. In the latter case, the SUSY soft terms conspire such that there are large cancellations amongst the various coefficients of $m_{3/2}^2$ in Eq. 2.22: this is what is called radiatively-driven natural SUSY[18, 19] since in this case a large high scale value of $m_{H_u}^2$ can be driven radiatively to small values $\sim -m_Z^2$ at the weak scale.

Furthermore, one can equate the value of m_Z^2 in terms of weak scale parameters with the value of m_Z^2 in terms of GUT scale parameters:

$$m_Z^2 \simeq -2\mu^2(weak) - 2m_{H_u}^2(weak) \simeq -2.18\mu^2(GUT) + a \cdot m_{3/2}^2. \tag{3.10}$$

Since μ hardly evolves under RG running (the factor 2.18 is nearly 2), then the BG condition for low fine-tuning states

$$-m_{H_u}^2(weak) \sim a \cdot m_{3/2}^2 \sim m_Z^2, \tag{3.11}$$

i.e. that the value of $m_{H_u}^2$ must be driven to *small* negative values $\sim -m_Z^2$ at the weak scale. These are exactly the conditions required by the model-independent

EWFT measure Δ_{EW}: *i.e.* one finds

$$\lim_{n_{SSB}\to 1} \Delta_{BG} \to \Delta_{EW} \tag{3.12}$$

where n_{SSB} is the number of *independent* soft SUSY breaking terms. Therefore, this approach also reconciles the Δ_{HS} measure (with appropriately regrouped independent terms) with the Δ_{BG} measure (when applied to models with a single independent soft breaking term such as $m_{3/2}$).

3.2 Electroweak fine-tuning in various SUSY models

In the following Section, we will evaluate EW fine-tuning for a variety of SUSY models using the case where all three measures agree since as shown above the Higgs mass fine-tuning and the BG measure both reduce to Δ_{EW} once dependent contributions to m_Z^2 or m_h^2 are combined into independent terms.

For each model, random sets of parameter values over the range listed in each subsection are generated. Then supersymmetric sparticle and Higgs mass spectra are generated using the Isasugra[51] subprogram of Isajet[50]. Each solution satisfies the following requirements:

- electroweak symmetry be radiatively broken (REWSB),
- the neutralino $\widetilde{Z}_1$ is the lightest MSSM particle,
- the light chargino mass obeys the model independent LEP2 limit $m_{\widetilde{W}_1} >$ 103.5 GeV[58] ($m_{\widetilde{W}_1} > 91.9$ GeV in the case of a wino-like chargino) and

- $m_h = 125.5 \pm 2.5$ GeV.

As in the SUGRA19 study, LHC sparticle search limits are not imposed since these general scans can produce compressed spectra which in many cases can easily elude LHC gluino and squark searches. Also no WIMP dark matter constraints are imposed since for cases with a standard thermal WIMP underabundance, the WIMP abundance might be augmented by late decaying cosmological relics (*e.g.* axinos, saxions, moduli, $\cdots$) or in the case of an overabundance, the WIMPs might decay to yet lighter particles (*e.g.* into light axino LSPs) or be diluted by late time entropy injection[73].

For each point generated, the values of $BF(b \to s\gamma)$[59, 60] and $BF(B_S \to \mu^+\mu^-)$[61] are calculated (as well as other B decay observables which turn out to be far less constraining). As discussed in Sec. 2.4, the measured value of $BF(b \to s\gamma)$ is found to be $(3.55 \pm 0.26) \times 10^{-4}$ [62] and the SM prediction[63] is $BF^{SM}(b \to s\gamma) = (3.15 \pm 0.23) \times 10^{-4}$. Also, for $B_s \to \mu^+\mu^-$ the combined branching fraction from both the LHCb collaboration[65] and CMS[66] is determined to be $(2.9\pm0.7)\times10^{-9}$ which is in rough accord with the SM prediction of $(3.2\pm0.2)\times10^{-9}$. Here, SUSY model points with

- $BF(b \to s\gamma) = (3.03 - 4.08) \times 10^{-4}$

and

- $BF(B_s \to \mu^+\mu^-) = (1.5 - 4.3) \times 10^{-9}$

will be labeled as satisfying B-physics constraints.

3.2.1 mSUGRA/CMSSM

The first scan is over the paradigm mSUGRA[3] or CMSSM[8] model with parameter ranges given by

- $m_0 : 0 - 15$ TeV,
- $m_{1/2} : 0 - 2$ TeV,
- $-2.5 < A_0/m_0 < 2.5$:
- $\tan\beta : 3 - 60$,

and for both signs of μ. The results of this scan have been shown previously in Ref. [74] for all $\tan\beta$ and in Ref. [69] for $\tan\beta = 10$. Here it is presented for completeness so that the reader may more readily compare these results against other SUSY models, and because now more restrictive B-decay constraints are imposed.

The value of Δ_{EW} is shown vs. m_0 in Fig. 3.1 where blue dots comprise all solutions while red dots also respect B-decay constraints. For low m_0, the value of Δ_{EW} is around 10^3, indicating EWFT at the $\Delta_{EW}^{-1} \sim 0.1\%$ level. As m_0 increases, the value of Δ_{EW} can drop sharply into the 10^2 range for $m_0 \sim 7 - 10$ TeV. This is the case of the hyperbolic branch/focus-point region (denoted HB/FP) where μ becomes small[75, 76]. The value of Δ_{EW} doesn't drop to arbitrarily small values because at such large m_0 values then the top squark masses become $\sim 5 - 10$ TeV and the radiative corrections $\Sigma_u^u(\tilde{t}_{1,2})$ become large. In fact, as m_0 increases beyond 7 TeV, then the minimum of Δ_{EW} also increases due to the increasing

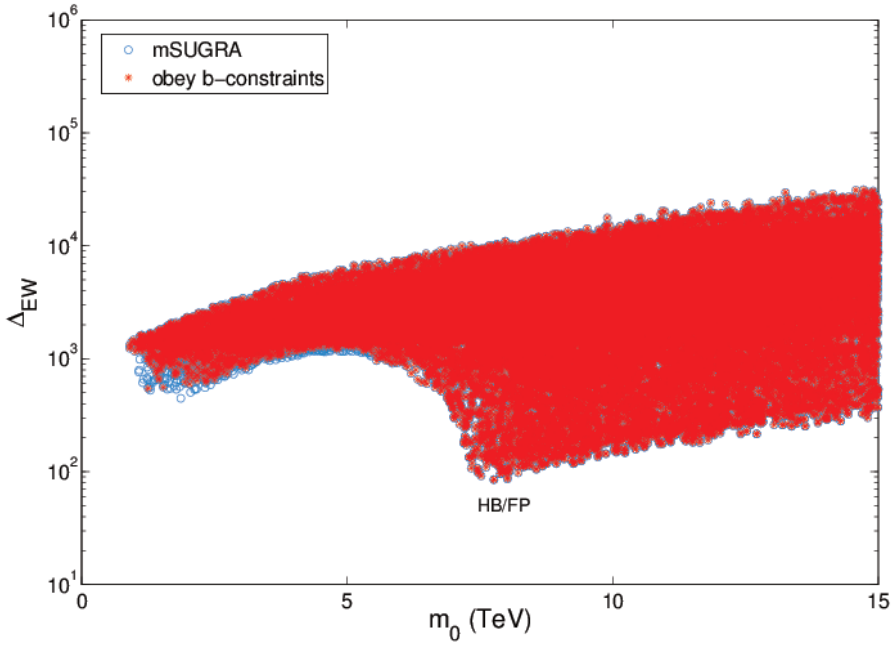

Figure 3.1: Plot of Δ_{EW} vs. m_0 from a scan over mSUGRA/CMSSM parameters space whilst maintaining $m_h = 125.5 \pm 2.5$ GeV and whilst obeying B-decay constraints. The location of the hyperbolic branch/focus point regions is labelled as HB/FP.

radiative corrections. With such a high minimum value of Δ_{EW}, one would expect mSUGRA/CMSSM probably does not describe nature.

3.2.2 NUHM1

The NUHM1 model[28] is inspired by $SO(10)$ SUSY GUT models where the Higgs doublets live in the 10-dimensional fundamental representation while the matter scalars inhabit the 16-dimensional spinor representation. In this case, the parameter set is expanded by one and the scan now ranges over

- $m_0 : 0 - 15$ TeV,
- $m_{H_u} = m_{H_d} \equiv m_H : 0 - 15$ TeV,

- $m_{1/2} : 0 - 2$ TeV,
- $-2.5 < A_0/m_0 < 2.5$:
- $\tan\beta : 3 - 60$.

By increasing $m_H \gg m_0$, then $m_{H_u}^2$ is only driven to small instead of large negative values, while if $m_{H_u}^2$ is increased too much, then $m_{H_u}^2$ is never driven negative and electroweak symmetry is not broken. If m_H is taken smaller than m_0, even with $m_H^2 < 0$ as a possibility, then $m_{H_d} \sim m_A$ can be decreased while $m_{H_u}^2$ is driven to very large negative values. In the former case, where $m_{H_u}^2$ is driven to small negative values, then μ also decreases– since its value is set to yield the measured Z mass via Eq. 2.8. In such cases, we expect reduced values of Δ_{EW}.

In the scan results shown in Fig. 3.2, this is indeed bourne out, as one sees that the minimal value of Δ_{EW} reaches as low as ~ 30, which is much less fine-tuned than mSUGRA. Values of Δ_{EW} in the $30 - 50$ range which obey B-decay constraints and $m_h \sim 125$ can be found for $m_0 \sim 3 - 10$ TeV. With such large m_0 values, then the top squarks also tend to be in the $3 - 10$ TeV regime and the top squark radiative corrections prevent Δ_{EW} from reaching below ~ 30.

3.2.3 NUHM2

The NUHM2 model[29] is inspired by $SU(5)$ SUSY GUTs where each of the MSSM Higgs doublets live in separate 5 and $\overline{5}$ representations, or by $SO(10)$ SUSY GUTs with D-term scalar mass splitting. In such a case, the mSUGRA parameter space expands to include $m_{H_u}^2$ and $m_{H_d}^2$ as soft SUSY breaking terms

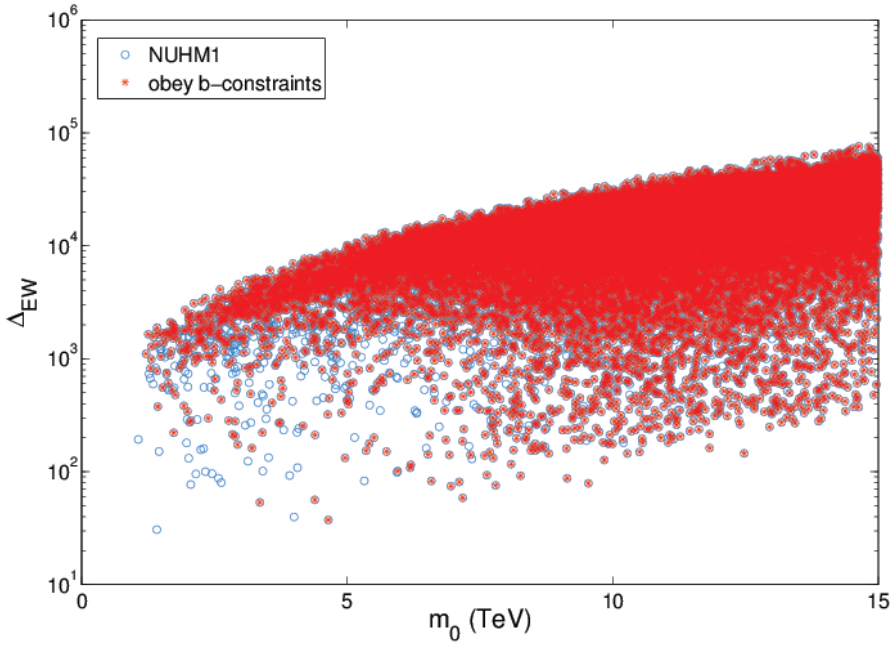

Figure 3.2: Plot of Δ_{EW} vs. m_0 from a scan over NUHM1 parameters space whilst maintaining $m_h = 125.5 \pm 2.5$ GeV.

which are independent of m_0. Using weak scale mass relations, then $m^2_{H_u}$ and $m^2_{H_d}$ can be traded for the more convenient weak scale parameters μ and m_A.

The case of NUHM2, in accord with Ref. [19], scans over

- $m_0: \ 0 - 20$ TeV,
- $m_{1/2}: \ 0.3 - 2$ TeV,
- $-3 < \ A_0/m_0 < 3$
- $\mu: \ 0.1 - 1.5$ TeV,
- $m_A: \ 0.15 - 1.5$ TeV,
- $\tan\beta : 3 - 60$,

lead to results shown in Fig. 3.3. Here, one sees that Δ_{EW} can reach values as low as 10, corresponding to $\Delta_{EW}^{-1} \sim 10\%$ EWFT. Even lower values ~ 7 have been generated in Ref. [69] for a fixed $\tan\beta = 10$ value. The key here is that low μ values $\sim 100 - 200$ GeV can be input by hand while top squarks can occur in the $1 - 5$ TeV regime with large mixing, which also acts to reduce the radiative corrections $\Sigma_u^u(\tilde{t}_{1,2})$[18]. The required GUT scale values of m_{H_u} are about $1.2m_0$ while $m_{H_d}(m_{GUT})$ can be anywhere in the TeV-range[19]. As m_0 increases beyond about 7 TeV, then the min of Δ_{EW} slowly increases due to increasing top squark radiative corrections. For the model examined in Ref. [19] with split generations, then $2 - 4$ TeV top squarks are allowed in accord with $10 - 30$ TeV first/second generation scalars: this situation offers at least a partial decoupling solution to the SUSY flavor and CP problems[77].

3.2.4 mGMSB

In minimal gauge mediated supersymmetry breaking (mGMSB)[30, 31, 32], a sector of "messenger" fields is hypothesized which communicates between the hidden SUSY breaking sector and the visible/MSSM sector. Visible sector scalar fields acquire a mass $m_i^2 \propto (\alpha_i/4\pi)^2\Lambda^2$ while gauginos acquire a mass $M_i = (\alpha_i/4\pi)\Lambda$ where Λ parametrizes the induced SUSY breaking scale in the messenger sector. The trilinear SSB a-terms are suppressed by an additional loop factor and hence are expected to be small. This latter effect leads to only small amounts of stop mixing: consequently huge stop masses are required in mGMSB in order to

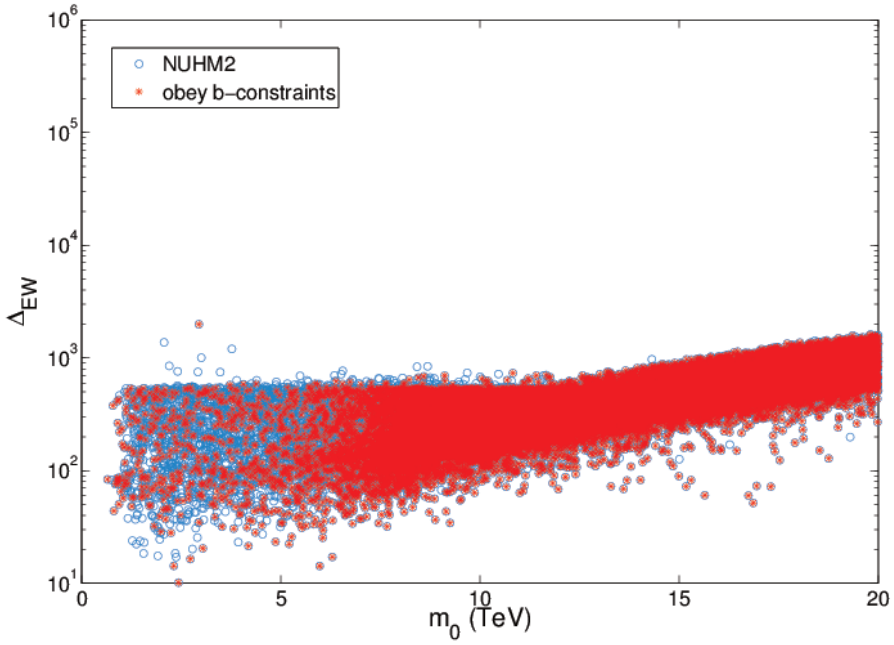

Figure 3.3: Plot of Δ_{EW} vs. m_0 from a scan over NUHM2 parameters space whilst maintaining $m_h = 125.5 \pm 2.5$ GeV.

generate $m_h \sim 125$ GeV. Furthermore, the hierarchy of mass values in mGMSB

$$M_1 < m_E < M_2 < m_L = m_{H_u} = m_{H_d} \ll M_3 < m_{\tilde{q}} \tag{3.13}$$

means that the $m_{H_u}^2$ boundary condition is already suppressed at the messenger scale M_{mes}, and then is strongly driven to large negative values due to the large values of m_{Q_3} and m_{U_3} contributing to the X_t term in Eq. 2.16. The upshot is that for allowed parameter ranges, $m_{H_u}^2$ is driven to large negative values at the weak scale, and the value of μ must be large positive (fine-tuned) to obtain the measured value of m_Z.

Fig. 3.4 where Δ_{EW} is plotted versus Λ shows results from a scan over values

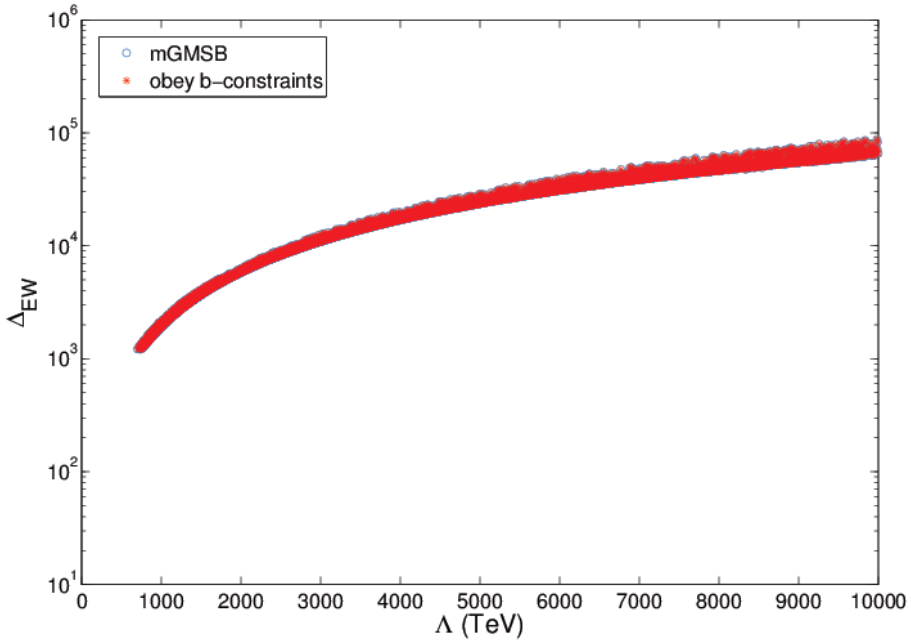

Figure 3.4: Plot of Δ_{EW} vs. Λ from a scan over mGMSB parameters space whilst maintaining $m_h = 125.5 \pm 2.5$ GeV.

- $\Lambda: \ 10^2 - 10^4$ TeV,
- $M_{mes} = 2\Lambda$,
- $\tan\beta : 3 - 60$,
- $sign(\mu) = \pm$.

From the plot, one sees that requiring $m_h : 123 - 128$ GeV then requires $\Lambda \gtrsim 500$ TeV, which results in very heavy top squarks and large fine-tuning, with the minimum of Δ_{EW} at 10^3, or 0.1% EWFT. Here, one would conclude that at least minimal GMSB is not likely to describe nature.

3.2.5 mAMSB

In anomaly-mediated SUSY breaking(AMSB) models[33], it is assumed that the SUSY breaking sector is sequestered from the visible sector – perhaps in extra spacetime dimensions – so that the dominant soft SUSY breaking contribution comes from the superconformal anomaly. In this case, gaugino masses $M_i = c_i(g_i^2/16\pi^2)m_{3/2}$ with $c_i = (33/5, 1, -3)$ for the $U(1)$, $SU(2)$ and $SU(3)$ groups respectively. Thus, multi-TeV values of $m_{3/2}$ are required which also ameliorates the so-called cosmological gravitino problem[78]. Also, the lightest gauginos are wino-like with a neutral wino as LSP. Due to tachyonic slepton masses in pure AMSB, an additional universal contribution m_0^2 is invoked in order to gain a phenomenologically viable spectrum of matter scalars. Since the trilinear a parameter is small, mAMSB has trouble generating $m_h \sim 125$ GeV unless top squarks are in the multi-TeV regime.

A scan over mAMSB parameter space is performed according to

- $m_{3/2}:\ 20 - 1000$ TeV,
- $m_0:\ 0 - 10$ TeV,
- $\tan\beta : 3 - 60$,
- $sign(\mu) = \pm$.

Results are shown in Fig. 3.5. Here, one sees that the minimal value of Δ_{EW} occurs at $m_{3/2} \sim 100$ TeV and has a value ~ 100, or 1% EWFT.

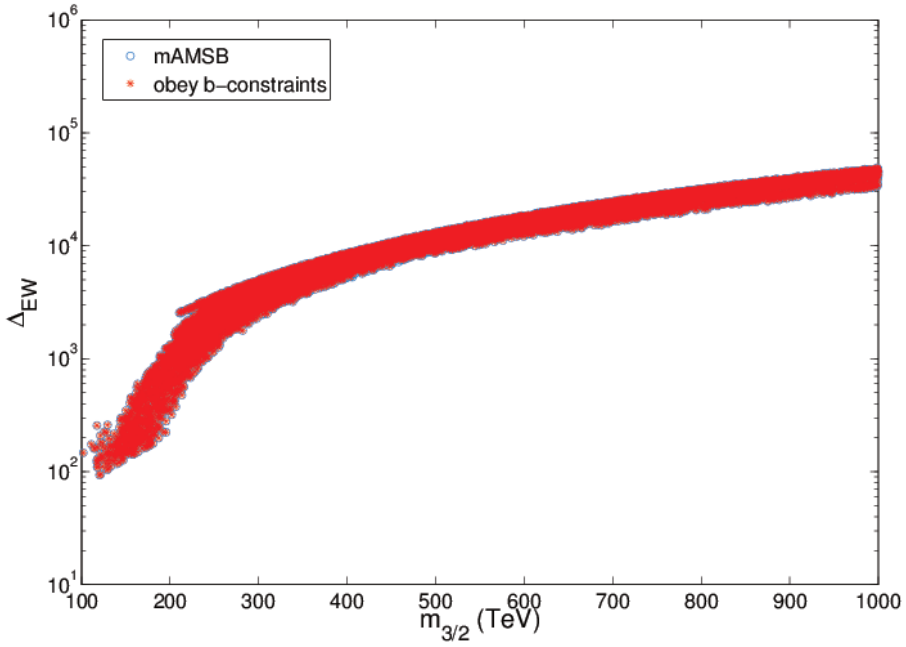

Figure 3.5: Plot of Δ_{EW} vs. $m_{3/2}$ from a scan over mAMSB parameters space whilst maintaining $m_h = 125.5 \pm 2.5$ GeV.

3.2.6 HCAMSB

An alternative set-up for AMSB, known as hypercharged anomaly-mediation (HCAMSB), has been advocated in Ref. [34]. It is a string motivated scenario which uses a similar construction to the one envisioned for AMSB. In HCAMSB, SUSY breaking is localized at the bottom of a strongly warped hidden region, geometrically separated from the visible region where the MSSM resides. The warping suppresses contributions due to tree-level gravity mediation so that anomaly mediation can become the dominant source of SUSY breaking in the visible sector. Possible exceptions to this sequestering mechanism are gaugino masses of U(1) gauge symmetries. Thus, in the MSSM, the mass of the bino (the gaugino of $U(1)_Y$) can be the only soft SUSY breaking parameter not determined

by anomaly mediation. Depending on its size, the bino mass M_1 can lead to a small perturbation to the spectrum of anomaly mediation, or it can be the largest soft SUSY breaking parameter in the visible sector. As a result of RG evolution, its effect on other soft SUSY breaking parameters can dominate the contribution from anomaly mediation. In extensions of the MSSM, additional $U(1)$s can also communicate SUSY breaking to the MSSM sector.

In HCAMSB, the SSB terms are of the same form as AMSB except for the $U(1)_Y$ gaugino mass:

$$M_1 = \tilde{M}_1 + \frac{b_1 g_1^2}{16\pi^2} m_{3/2}, \tag{3.14}$$

where $\tilde{M}_1 = \alpha m_{3/2}$. The large $U(1)_Y$ gaugino mass can cause $m_{H_u}^2$ to first run to large positive values before it is driven negative so that EW symmetry is broken. This potentially leads to lower fine-tuning since then $m_{H_u}^2$ may be driven to just small negative values.

The scan is over the HCAMSB parameter space

- $m_{3/2}: \ 25 - 2000$ TeV,
- $\alpha: \ -0.25 - 0.25$,
- $\tan\beta : 3 - 60$,
- $sign(\mu) = \pm$

with the LEP2 chargino mass limit reduced to $m_{\widetilde{W}_1} > 91.9$ GeV as appropriate for a wino-like LSP. Results are shown in Fig. 3.6 where Δ_{EW} is plotted versus $m_{3/2}$. Here, one finds a minimal value of $\Delta_{EW} \sim 100$ for $m_{3/2} \sim 400$ TeV.

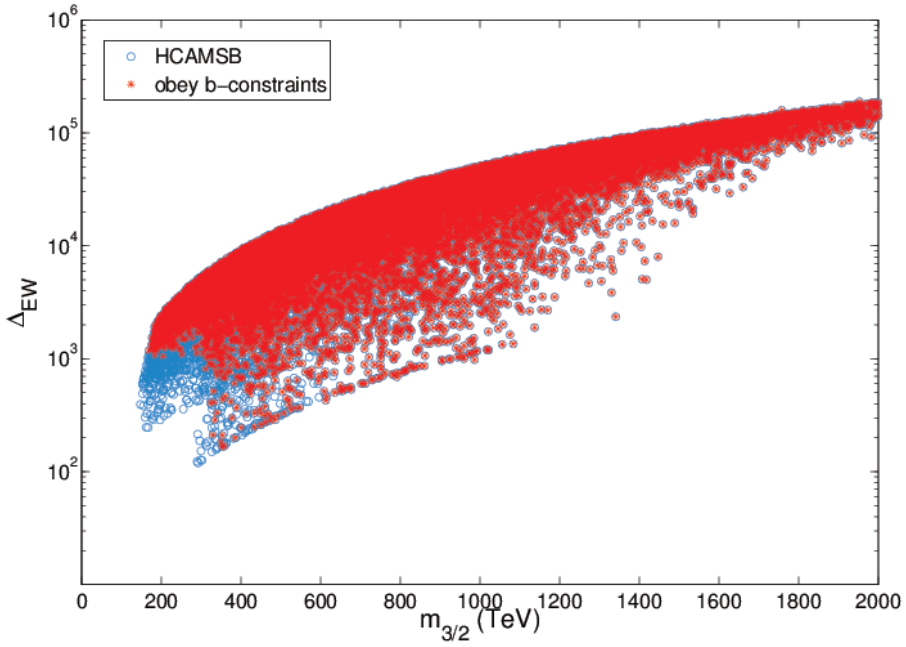

Figure 3.6: Plot of Δ_{EW} vs. $m_{3/2}$ from a scan over HCAMSB parameters space whilst maintaining $m_h = 125.5 \pm 2.5$ GeV.

3.2.7 inoAMSB

A third alternative related to AMSB is known as gaugino-AMSB or inoAMSB for short[35, 36]. The main assumption here is that the high energy theory which generates SUSY breaking is of the sequestered type[33] so that the classical gaugino and scalar masses and A-terms are highly suppressed relative to the gravitino mass scale. Nevertheless, in contrast to what is usually advocated in AMSB, it has been argued [70] that only *gaugino masses* are generated by Weyl anomalies. In inoAMSB, the scalar masses are then generated by renormalization group (RG) running as in what is often called gaugino mediation[79] or simple no-scale SUSY breaking models[80]. The inoAMSB model then avoids both the generic FCNC problems of gravity mediated scenarios and also the tachyonic slepton problem of

the traditional AMSB construct. The inoAMSB model then depends on just two parameters: the gravitino mass $m_{3/2}$ which sets the scale for all sparticle masses, and $\tan\beta$ while $m_0 = A_0 \equiv 0$.

Here a scan over the following inoAMSB parameter space is performed:

- $m_{3/2}:\ 100 - 1000$ TeV,
- $\tan\beta : 3 - 60$,
- $sign(\mu) = \pm$

with the LEP2 chargino mass limit given by $m_{\widetilde{W}_1} > 91.9$ GeV as appropriate for a wino-like LSP.

Results are shown in Fig. 3.7 plotting Δ_{EW} vs. $m_{3/2}$. One finds a minimal value of $\Delta_{EW} \sim 350$ for $m_{3/2} \sim 420$ TeV so this model is highly electroweak fine-tuned over the parameter range which generates a value of m_h in accord with measurement. The reason is that by setting $m_{H_u}^2 = 0$ at $Q = m_{GUT}$, then it can only be driven to large negative values resulting in high EW fine-tuning.

3.2.8 Mixed moduli-anomaly mediation

These models, known as mixed moduli-anomaly mediated SUSY breaking (MMAMSB), or mirage mediation, are based on the KKLT construction[81] of string compactification with fluxes, which produce the necessary de Sitter vacuum. In the KKLT construct, one first introduces nonzero fluxes in the Type IIB string theory compactified on a Calabi-Yau manifold. Due to the nonzero fluxes, the complex structure moduli and the dilaton are completely fixed but

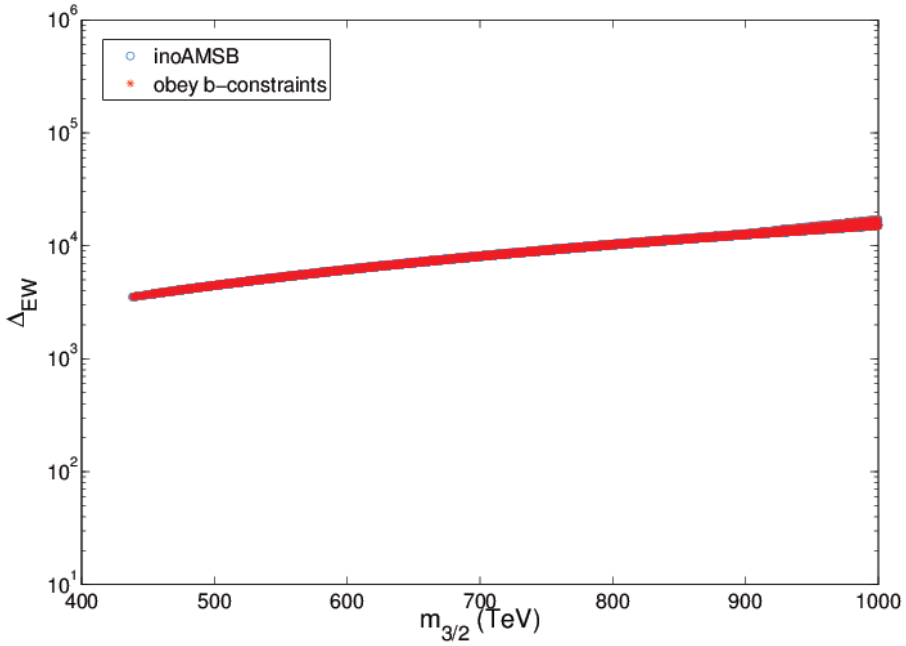

Figure 3.7: Plot of Δ_{EW} vs. $m_{3/2}$ from a scan over inoAMSB parameters space whilst maintaining $m_h = 125.5 \pm 2.5$ GeV.

the size modulus T remains a flat direction. To fix this, KKLT invoked non-perturbative effects, such as gaugino condensation on D7 branes. At this stage, all moduli are fixed, but one ends up with supersymmetric vacua and negative vacuum energy. The final step in the construction is to include anti D-branes yielding the desired de-Sitter vacua (with positive vacuum energy) and breaking supersymmetry. Because of the presence of branes and fluxes, the models have generically warped compactifications. Due to the warping, the addition of the anti D-brane breaks supersymmetry by a very small amount.

The phenomenology of KKLT-inspired models is distinctive in that moduli fields and the Weyl anomaly make comparable contributions to SUSY breaking effects in the observable sector of fields[82]. The contribution of each can be

parametrized by α which yields pure AMSB for $\alpha = 0$ but which tends to pure moduli (gravity) mediation as α becomes large. The phenomenology also depends on the so-called modular weights which in turn depend on the location of various fields in the extra dimensions: $n_i = 0$ (1) for matter fields located on D7 (D3) branes; fractional values $n_i = 1/2$ are also possible for matter living at brane intersections. It is claimed that MMAMSB models have the potential to be minimally EW fine-tuned[83, 84].

The parameter space of MMAMSB models is given by

- $m_{3/2}:\ 10 - 100$ TeV,
- $\alpha:\ -15 \to 15$,
- $\tan\beta : 3 - 60$,
- $sign(\mu) = \pm$,

along with

- $n_H,\ n_m = 0,\ 1/2$ or 1.

Many of the following results can be understood by inspection of the α vs. $m_{3/2}$ plane plots available for each modular weight combination and shown in Ref. [85].

3.2.9 Cases with $n_H = 0$

First results for MMAMSB are shown in Fig. 3.8 in the Δ_{EW} vs. $m_{3/2}$ frame for cases with *a*). $(n_H, n_m) = (0, 0)$, *b*). $(n_H, n_m) = (0, \frac{1}{2})$ and *c*). $(n_H, n_m) = (0, 1)$. The case with $(n_H, n_m) = (0, 0)$ finds a minimal value of $\Delta_{EW} \simeq 437$ which occurs

at $m_{3/2} \sim 35$ TeV. At this point, $m_{\tilde{g}} \sim m_{\tilde{q}} \sim 1.8$ TeV which might be expected to be ruled out by LHC8 searches. However, the compressed spectra with gaugino masses $M_1, M_2, M_3 \sim 800, 1000, 1800$ GeV leads to softer visible energy than might be otherwise expected. The value of $\mu \sim 1200$ GeV produces the large value of Δ_{EW}. While much less tuned spectra are possible, they only occur with very low m_h values and so are ruled out by the LHC8 Higgs discovery.

The case with $(n_H, n_m) = (0, \frac{1}{2})$ has a minimal value of $\Delta_{EW} = 314$ and so also is EW fine-tuned. In this case, the minimum occurs for $m_{3/2} = 95$ TeV which leads to $m_{\tilde{g}} = 3.6$ TeV. The large $\mu = 1.1$ TeV value leads to high EW fine-tuning. Here, the LSP is the lightest higgsino with mass $m_{\widetilde{Z}_1} \sim \mu$. Models exist with $m_h \sim 125$ GeV and much lower fine-tuning reaching to $\Delta_{EW} \sim 30$ (blue points) but these all violate B-decay constraints due to rather light top squarks.

For the case with $(n_H, n_m) = (0, 1)$, then the lowest Δ_{EW} value is found to be ~ 91, a considerable improvement but still nine times greater than the min from NUHM2. In this case, the solutions form two distinct branches– the upper with $\alpha < 0$ while the lower has $\alpha > 0$. The lowest $\Delta_{EW} = 91$ point actually has $\mu \sim 150$ GeV, but with $m_{3/2} \sim 50$ TeV, then the top squarks have mass $m_{\tilde{t}_{1,2}} \sim 2.1,\ 2.8$ TeV and not enough mixing so the values of $\Sigma_u^u(\tilde{t}_{1,2})$ dominate the fine-tuning.

3.2.10 Cases with $n_H = 1/2$

Results for MMAMSB for cases with *a*). $(n_H, n_m) = (\frac{1}{2}, 0)$, *b*). $(n_H, n_m) = (\frac{1}{2}, \frac{1}{2})$ and *c*). $(n_H, n_m) = (\frac{1}{2}, 1)$ are shown in Fig. 3.9 in the Δ_{EW} vs. $m_{3/2}$ plane. For

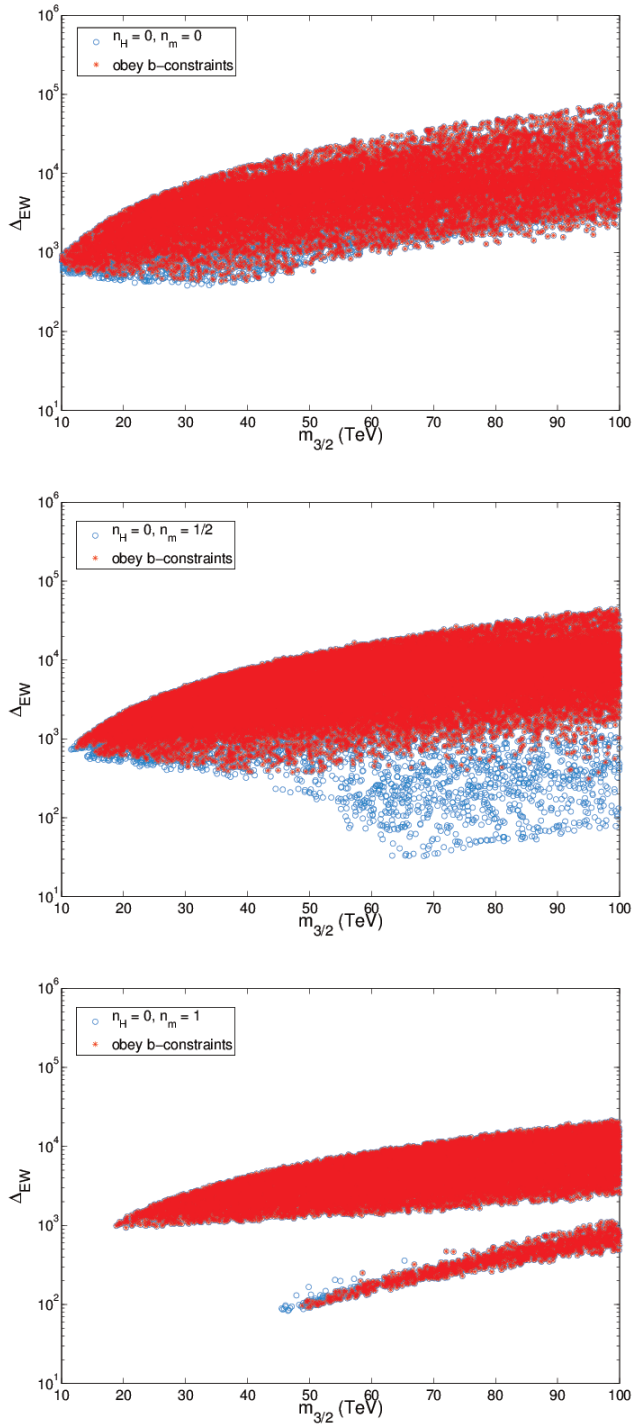

Figure 3.8: Plot of Δ_{EW} vs. $m_{3/2}$ from a scan over MMAMSB parameter space with $n_H = 0$ whilst maintaining $m_h = 125.5 \pm 2.5$ GeV.

frame *a*)., we find a minimum $\Delta_{EW} = 457$ at $m_{3/2} = 98$ TeV where a spectrum with $m_{\tilde{g}} \sim m_{\tilde{q}} \sim 2$ TeV but with $\mu = 1.4$ TeV. The LSP is a neutral higgsino with mass ~ 1.34 TeV and $\Omega_{\widetilde{Z}_1} h^2 \sim 0.15$. Even lower Δ_{EW} solutions reaching values of ~ 100 occur at very high $m_{3/2}$, but these blue points are excluded by B-decay constraints.

For the $(n_H, n_m) = (\frac{1}{2}, \frac{1}{2})$ case in frame *b*)., the lowest value of Δ_{EW} is found to be 375 at $m_{3/2} = 83$ TeV. Here again, $\mu \simeq 1.25$ TeV which gives a higgsino-like LSP and rather compressed spectra.

For the $(n_H, n_m) = (\frac{1}{2}, 1)$ case shown in frame *c*)., then Δ_{EW} can reach as low as ~ 100 at the high $m_{3/2} \sim 80$ TeV point. For this point, μ drops as low as 589 GeV and the LSP is again higgsino-like with a thermal underabundance of neutralino dark matter. The gluino and squark masses cluster around $3.5 - 4.5$ TeV, beyond LHC reach.

3.2.11 Cases with $n_H = 1$

The MMAMSB cases with *a*). $(n_H, n_m) = (1, 0)$, *b*). $(n_H, n_m) = (1, \frac{1}{2})$ and *c*). $(n_H, n_m) = (1, 1)$ are shown in Fig. 3.10. For the first case with $(1, 0)$, then the min of Δ_{EW} is 859 at $m_{3/2} = 90$ TeV. The large EWFT is generated by the large $\mu = 1.9$ TeV value. Even so, the LSP is mainly bino with mass $m_{\widetilde{Z}_1} \sim 1.7$ TeV.

For frame *b*). with $(n_H, n_m) = (1, \frac{1}{2})$, then the min of Δ_{EW} is 1178 at $m_{3/2} = 76$ TeV where $m_{\tilde{g}} \sim 3.9$ TeV and the bino-like LSP has mass ~ 1.8 TeV.

Finally, frame *c*). shows the $(n_H, n_m) = (1, 1)$ case where a min of Δ_{EW} is found to be 1643 at $m_{3/2} = 27$ TeV. Here, gluino and squark masses tend to

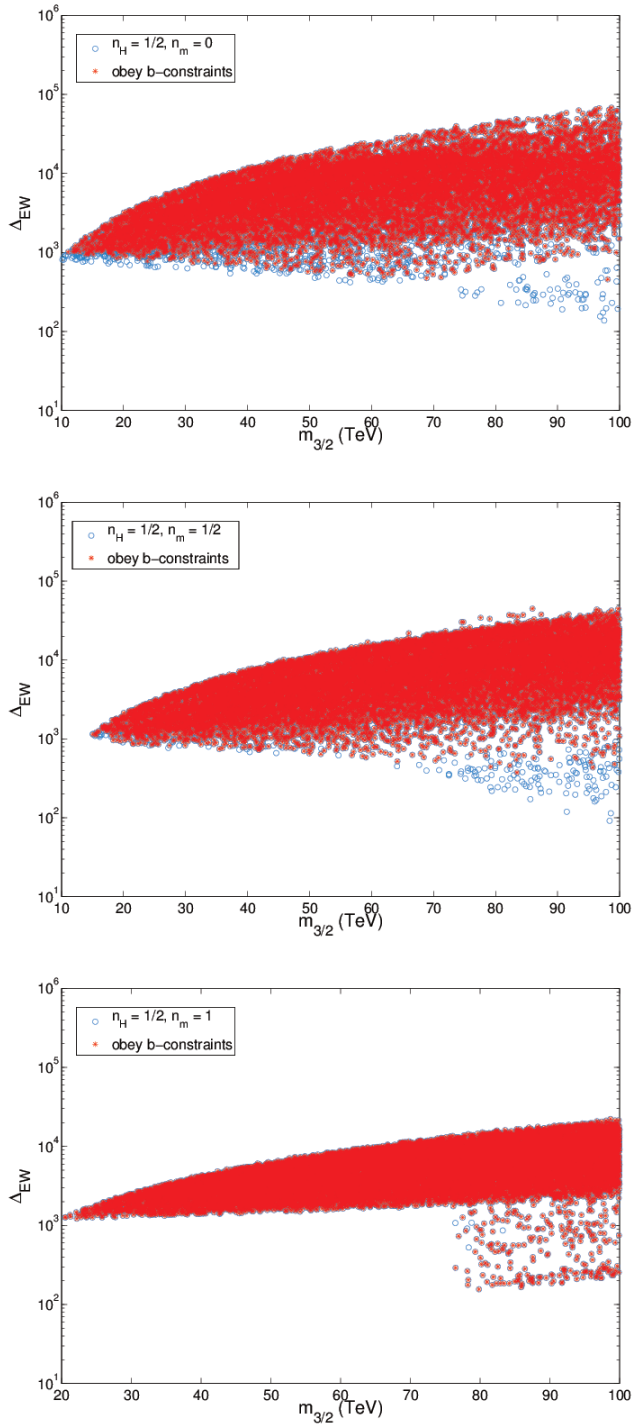

Figure 3.9: Plot of Δ_{EW} vs. $m_{3/2}$ from a scan over MMAMSB parameter space with $n_H = 1/2$ whilst maintaining $m_h = 125.5 \pm 2.5$ GeV.

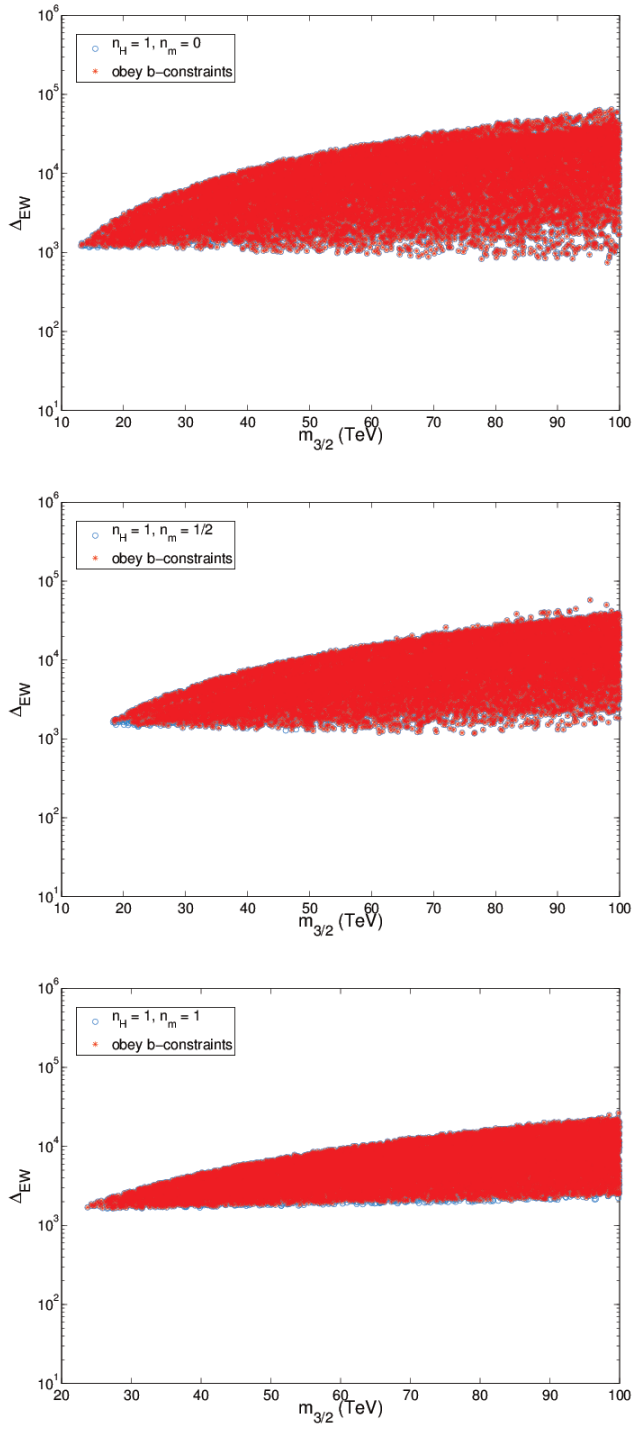

Figure 3.10: Plot of Δ_{EW} vs. $m_{3/2}$ from a scan over MMAMSB parameters space with $n_H = 1$ whilst maintaining $m_h = 125.5 \pm 2.5$ GeV.

exceed 4 TeV whilst $\mu \sim 2.6$ TeV which leads to the large EW fine-tuning.

3.3 16 Models in One View

This chapter, has re-examined electroweak fine-tuning in light of recent LHC results on the Higgs discovery with $m_h \simeq 125.5$ GeV and the lack of any sort of signal for sparticles. This situation has lead to various claims that the MSSM is no longer viable, or at least highly fine-tuned in the EW sector. Alternatively, it has been claimed that conventional measures, applied conventionally, overestimate EWFT[69].

To clarify the situation, we have proposed a Rule of Fine-tuning: When evaluating fine-tuning, it is not permissible to claim fine-tuning of *dependent* quantities one against another. Following this rule it is shown that Δ_{BG} and Δ_{HS} both reduce to the model-independent electroweak measure Δ_{EW}.

For low Δ_{EW}, then it is required that 1. $\mu \sim 100 - 300$ GeV, 2. $m_{H_u}^2$ is radiatively driven to small negative values $\sim m_Z$ and 3. the top-squarks are in the few TeV range with large mixing. The large mixing reduces top-squark radiative contributions to Δ_{EW} while lifting m_h into the 125 GeV range.

Δ_{EW} values from a scan over parameters of 16 models have been evaluated: mSUGRA, NUHM1, NUHM2, mGMSB, mAMSB, HCAMSB, inoAMSB and nine cases of mixed moduli-anomaly (mirage) mediated SUSY breaking. The overall results are summarized in Fig. 3.11 which shows the range of Δ_{EW} generated on the y-axis versus models on the x-axis. Only one model– NUHM2– reaches to the

rather low $\Delta_{EW} \sim 10$ values, indicating just 10% EWFT. This can be so because the freedom in the soft Higgs sector allows arbitrarily low values of μ (subject to LEP2 constraints) to be generated while at the same time driving $m_{H_u}^2$ to just small negative values, while also accommodating TeV-scale top squarks with large mixing. For the remaining models, their inherent constraints make satisfying these conditions with $m_h \sim 125$ GeV very difficult unless they are highly fine-tuned. The best of the remainder models include $NUHM1$ which allows for min Δ_{EW} as low as 30. Thus, Δ_{EW} does indeed put SUSY models under seige.

Luckily, at least NUHM2 and its generalizations survive, and even thrive. In the case of the surviving NUHM2 spectra (those with $\Delta_{EW} \lesssim 30$), a discovery at LHC14 might take place provided $m_{\tilde{g}} \lesssim 2$ TeV[86]: this reach covers about half of parameter space[19]. The definitive search for SUSY would have to take place at a linear e^+e^- collider where $\sqrt{s}$ could extend beyond $2m(higgsino)$ – in this case $\sqrt{s} \sim 500 - 600$ GeV is required for a thorough search. Such a machine would either discover SUSY or rule out SUSY naturalness[88]. We may also expect an ultimate discovery of a higgsino-like WIMP and a DFSZ-type axion, since models such as SUSY DFSZ solve the strong CP fine-tuning problem and the μ problem while at the same time allowing naturally for a Little Hierarchy of $f_a \ll m_{hidden}$, where $m_{hidden} \sim 10^{11}$ GeV represents the mass scale usually associated with hidden sector SUSY breaking. That hierarchy is then reflected by the hierarchy $\mu \ll m_{3/2}$ which seems to be what naturalness combined with LHC data is telling us.

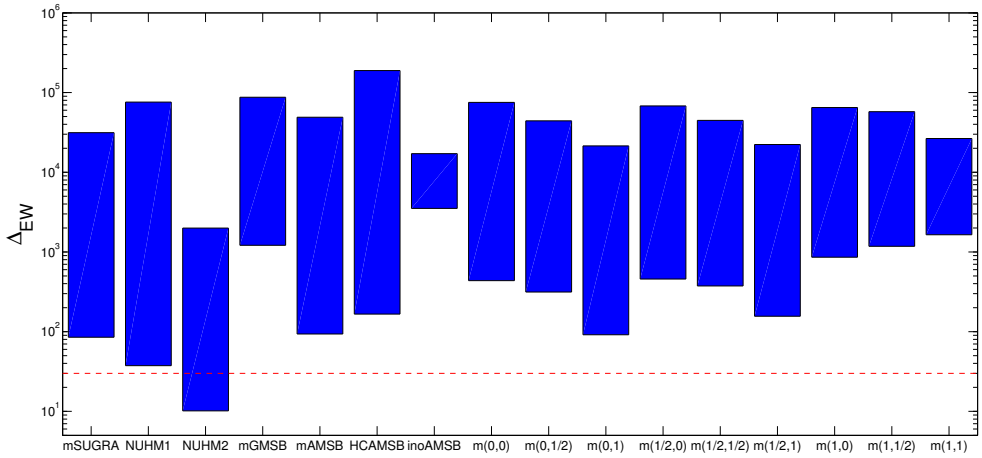

Figure 3.11: Histogram of range of Δ_{EW} values generated for each SUSY model considered in the text. We would consider $\Delta_{EW} \lesssim 30$– the lower the better– as acceptable values for EW fine-tuning. This region is located below the dashed red line.

Chapter 4

Variation on NUHM2[89]

Inspired by gauge coupling unification, these previous studies had assumed gaugino mass unification as well as naturalness. From gaugino mass unification, $M_1 = M_2 = M_3$ at $Q = m_{GUT}$, one expects from RG evolution at the weak scale that $M_1 \sim M_3/7$ and $M_2 \sim 2M_3/7$ so that the LHC8 lower bound on M_3 ($M_3 \sim m_{\tilde{g}} \gtrsim 1.3$ TeV) also provides a lower bound on M_1 and M_2. In this case, for natural SUSY which respects LHC8 bounds, one expects the mass hierarchy $|\mu| < M_1 < M_2 < M_3$ to occur. Thus, in the RNS model, taken as the paradigm case for the study of natural SUSY, one expects four light higgsino states with mass $m_{\widetilde{W}_1^{\pm}},\ m_{\widetilde{Z}_{1,2}} \sim |\mu|$ where the lightest higgsino $\widetilde{Z}_1$ acts as the lightest-SUSY-particle or LSP. In particular, mixed higgsino-bino or higgino-wino LSPs are not allowed if the gluino is heavy.

Collider signals as well as cosmology depend sensitively on the nature of the LSP. For instance, in the RNS framework with gaugino masses near the TeV range, one expects the light electroweak -inos $\widetilde{W}_1^{\pm}$ and $\widetilde{Z}_{1,2}$ to be dominantly higgsino-like with typically small $m_{\widetilde{W}_1} - m_{\widetilde{Z}_1}$ and $m_{\widetilde{Z}_2} - m_{\widetilde{Z}_1}$ mass splittings of order 10-20 GeV [19]. Such a small mass splitting results in only soft visible energy release from the heavier higgsino three-body decays to the $\widetilde{Z}_1$. This situation makes pair production of higgsinos very difficult to detect at LHC [90, 91, 92, 106, 107] in spite of their relatively small masses and correspondingly large production cross sections; other superpartners may be very heavy, and possibly beyond the reach

of the LHC. In contrast, in models with light gauginos and heavy higgsinos, the mass gap between the bino and wino-like states tends to be large (if gaugino mass unification is assumed), and signals from wino pair production followed by their decays to bino-like LSPs should be readily detectable. The celebrated clean trilepton signature arising from $\widetilde{W}_1\widetilde{Z}_2$ production followed by $\widetilde{W}_1 \to l\overline{\nu_l}\widetilde{Z}_1$ and $\widetilde{Z}_2 \to l\bar{l}\widetilde{Z}_1$ is perhaps the best-known example.

The phenomenology of dark matter is even more sensitive to the content of the LSP. Higgsino and wino-like LSPs lead to an under-abundance of thermally-produced LSPs whereas a bino-like LSP leads to overproduction of WIMPs (weakly interacting massive particles) unless the neutralino annihilation rate is dynamically enhanced, *e.g.* via an s-channel resonance or via co-annihilation, or their density is diluted by entropy production late in the history of the Universe. In the wino- or higgsino-LSP cases, if one solves the strong CP problem via a quasi-visible axion [93], then the dark matter is expected to occur as an axion-neutralino admixture, *i.e.* two dark matter particles [94]. Another consideration is the occurance of large mixings of higgsinos and gauginos. Then, one can get the so-called well-tempered bino/higgsino or bino/wino, a neutralino which saturates the measured DM abundance.

Gaugino mass unification – well-motivated as it may be – is by no means sacrosanct. Phenomenologically, while the high scale value of M_3 is required to be large by LHC8 constraints on $m_{\tilde{g}}$, M_1 and/or M_2 may well have much smaller magnitudes without impacting naturalness. Motivated by these conditions, this chapter examines how the phenomenology of natural SUSY models with

$|\mu| \sim 100 - 300$ GeV may be altered if we give up the gaugino mass unification assumption and allow for the possibility that the bino or/and wino also happens to be light. The LSP (and possibly also other electroweak-inos) would then be mixtures of higgsinos and electroweak gauginos, or may even be very nearly bino- or wino-like, resulting in very different mass and mixing patterns from expectations within the RNS framework. A mixed bino-higgsino LSP could well lead to the observed relic-density for thermally produced neutralinos. Small values of gaugino mass parameters would have to be regarded as fortuitous from the perspective of naturalness. Nevertheless since light winos/binos do not jeapordize naturalness, in the absence of any compelling theory of the origin of SSB parameters, a phenomenological study of this situation seems justified by the philosophy that it is best to examine all avenues in the search for natural SUSY at the LHC.

Non-universal gaugino masses (NUGM) can occur in GUT models wherein the gauge kinetic function transforms non-trivially as the direct product of two adjoints [95, 96]. Or, it may be that GUTs play no role, and that unification occurs within the string-model context. Models with mixed anomaly- and gravity-mediation contributions to gauginos masses also lead to non-universal gaugino mass parameters [97]. Investigation of how the phenomenology of natural SUSY models is modified from RNS expectations forms the subject of this chapter. Naturalness in the context of non-universal gaugino masses has also been considered in Refs. [98] and [99].

4.1 Natural SUSY benchmark scenarios

This study begins by exhibiting a sample benchmark point within the framework of the canonical 2-extra-parameter non-universal Higgs model (NUHM2) with *unified* gaugino mass parameters and a higgsino-like LSP under the column RNSh in Table 4.1. This point has parameters $m_0 = 5000$ GeV, $m_{1/2} = 700$ GeV, $A_0 = -8000$ GeV and $\tan\beta = 10$ with $(\mu,\ m_A) = (200, 1000)$ GeV. The RNSh point has $\Delta_{\rm EW} = 9.6$ corresponding to about 10% electroweak fine-tuning, and $m_h = 124.3$ GeV while $m_{\tilde{g}} \simeq 1.8$ TeV with $m_{\tilde{q}} = 5.2$ TeV. It is safely beyond LHC8 reach. The lightest neutralino is dominantly higgsino-like (higgsino-wino-bino composition is listed as $v_h^{(1)} \equiv \sqrt{v_1^{(1)2} + v_2^{(1)2}}$, $v_w^{(1)}$ and $v_b^{(1)}$ defined similarly to Ref. [25]) and has mass $m_{\widetilde{Z}_1} = 188$ GeV and thermally-produced neutralino relic density [100] $\Omega_{\widetilde{Z}_1}h^2 = 0.013$. SUSY contributions to the branching fraction for $b \to s\gamma$ are negligible so that this is close to its SM value [101] and in accord with experiment [102]. The spin-independent neutralino-proton scattering cross section shown in the third-last row of the table naively violates the bound $\sigma^{SI}(\widetilde{Z}_1 p) \lesssim (2-3)\times 10^{-9}$ pb from the LUX experiment [103], but this bound is obtained assuming that the neutralino comprises *all* of the cold dark matter. In the case studied here, the thermal neutralino contribution is just about 10% of the total DM contribution, and this point is in accord with the constraint upon scaling the expected event rate by $\xi = \Omega_{\widetilde{Z}_1}h^2/0.12$. Also shown is the spin-dependent neutralino-nucleon scattering cross-section. The IceCube experiment currently has the best sensitivity to this quantity by searching for high energy neutrinos arising

from neutralinos which are captured by the sun and annihilated in the solar core. The current IceCube limit [105], lies around $\sigma^{SD}(\widetilde{Z}_1 p) \lesssim 1.5 \times 10^{-4}$ pb so that the RNSh point would seem to be excluded by this bound. For this analysis, the neutralino density in the solar core is obtained by assuming equilibration between the capture rate and the annihilation rate of neutralinos. Since the capture rate scales *linearly* with the neutralino relic density, the predicted event rates also need to be scaled by ξ before comparing with IceCube. After re-scaling, we see that the RNSh point is an order of magnitude away from the IceCube upper limit of $\sim 1.5 \times 10^{-4}$ pb that is obtained assuming the neutralinos dominantly annihilate via $\widetilde{Z}_1\widetilde{Z}_1 \to WW$. The other columns display natural SUSY benchmark points where the bino or the wino mass parameters are dialed to relatively low values resulting in natural SUSY models with either a bino-like (RNSb) or wino-like (RNSw) LSP. These cases will be discussed in detail in the following sections.

4.2 Natural SUSY with a bino-like LSP

This section examines how the phenomenology of natural SUSY models is altered if one allows for non-universal gaugino mass parameters, and lets the GUT scale bino mass vary independently. To this end, the RNSh benchmark point from Table 4.1 has been adopted, but now allowing M_1 to be a free parameter, positive or negative. To generate spectra and the value of $\Delta_{\rm EW}$, the Isajet 7.84 spectrum generator [50] has been used. In Fig. 4.1, we show by red circles the value of $\Delta_{\rm EW}$ versus the GUT scale value of M_1. One sees that – aside from numerical

parameter	RNSh	RNSb	RNSw
M_1(GUT)	700	380	700
M_2(GUT)	700	700	175
M_3(GUT)	700	700	700
$m_{\tilde{g}}$	1795.8	1796.2	1809.8
$m_{\tilde{u}_L}$	5116.2	5116.2	5100.7
$m_{\tilde{u}_R}$	5273.3	5271.3	5277.4
$m_{\tilde{e}_R}$	4809.0	4804.4	4806.7
$m_{\tilde{t}_1}$	1435.1	1438.1	1478.3
$m_{\tilde{t}_2}$	3601.2	3603.3	3584.9
$m_{\tilde{b}_1}$	3629.4	3631.5	3611.6
$m_{\tilde{b}_2}$	5003.9	5003.6	5007.4
$m_{\tilde{\tau}_1}$	4735.6	4731.1	4733.9
$m_{\tilde{\tau}_2}$	5071.9	5070.8	5053.9
$m_{\tilde{\nu}_\tau}$	5079.2	5078.1	5060.8
$m_{\widetilde{W}_2}$	610.9	611.0	248.4
$m_{\widetilde{W}_1}$	205.3	205.3	121.5
$m_{\widetilde{Z}_4}$	621.4	621.5	322.1
$m_{\widetilde{Z}_3}$	322.0	217.9	237.8
$m_{\widetilde{Z}_2}$	209.3	209.8	211.8
$m_{\widetilde{Z}_1}$	187.8	149.5	114.2
m_h	124.3	124.2	124.3
$v_h^{(1)}$	0.96	0.57	0.60
$v_w^{(1)}$	-0.14	0.07	-0.80
$v_b^{(1)}$	0.24	-0.82	0.08
$\Delta_{\rm EW}$	9.6	9.6	10.8
$\Omega^{std}_{\widetilde{Z}_1}h^2$	0.013	0.11	0.0015
$BF(b\to s\gamma)$	3.3×10^{-4}	3.3×10^{-4}	3.3×10^{-4}
$\sigma^{SI}(\widetilde{Z}_1p)$ (pb)	1.6×10^{-8}	1.7×10^{-8}	4.3×10^{-8}
$\sigma^{SD}(\widetilde{Z}_1p)$ (pb)	1.7×10^{-4}	2.8×10^{-4}	8.9×10^{-4}
$\langle\sigma v\rangle\vert_{v\to0}$ (cm^3/sec)	2.0×10^{-25}	1.8×10^{-26}	1.7×10^{-24}

Table 4.1: Input parameters and masses in GeV units for three Natural SUSY benchmark points with $\mu = 200$ GeV and $m_A = 1000$ GeV. We also take $m_0 = 5000$ GeV, $A_0 = -8000$ GeV and $\tan\beta = 10$. Also shown are the values of several non-accelerator observables.

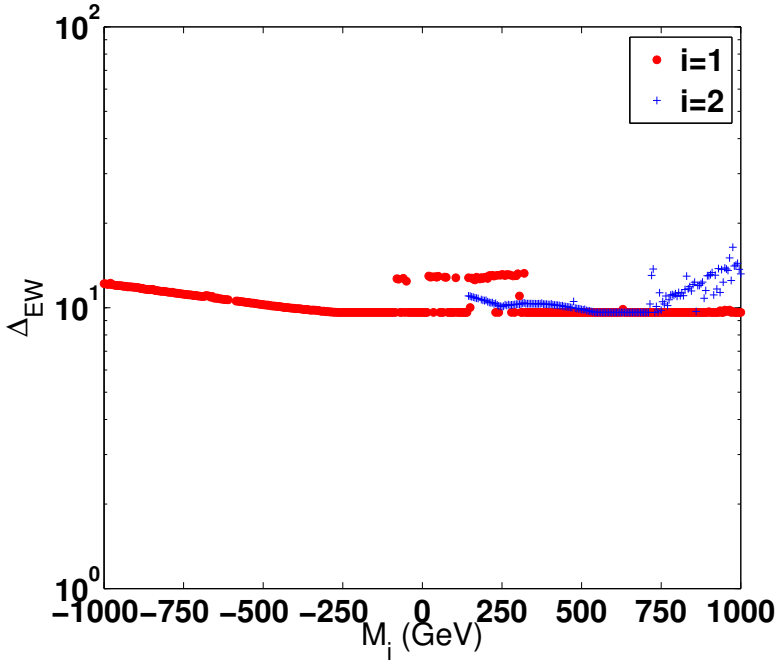

Figure 4.1: Variation in fine-tuning measure $\Delta_{\rm EW}$ vs. M_1 (red circles) or M_2 (blue pluses), with all other parameters fixed at their values for the RNS SUSY benchmark model point in Table 4.1. Here, and in subsequent figures the M_i on the horizontal axis is the value of the corresponding gaugino mass parameter renormalized at the GUT scale. We cut the graphs off if the lighter chargino mass falls below 100 GeV.

instabilities arising from the iterative solution to the SUSY RGEs – the value of $\Delta_{\rm EW}$ stays nearly constant so that, as anticipated, varying M_1 hardly affects the degree of electro-weak fine-tuning.

Fig. 4.2 shows the mass values of the charginos and neutralinos as M_1 is varied between -700 GeV to 700 GeV. For $M_1 = 700$ GeV, the gaugino mass unification point, we find that $\widetilde{W}_1$ and $\widetilde{Z}_{1,2}$ are all higgsino-like with mass values clustered around $\mu = 200$ GeV while the bino-like $\widetilde{Z}_3$ lies near 300 GeV and the wino-like $\widetilde{Z}_4$ and $\widetilde{W}_2$ lie at ~ 600 GeV. As M_1 is lowered, then the bino component of $\widetilde{Z}_1$ increases while the bino-component of $\widetilde{Z}_3$ decreases. The mass eigenvalues track

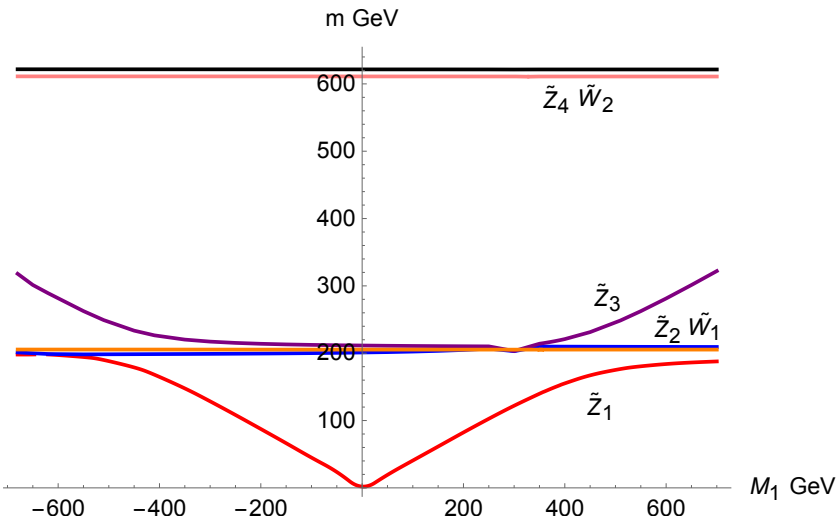

Figure 4.2: Variation of electroweak-ino masses vs. M_1 for a general RNS SUSY benchmark model with variable M_1 and $M_2 = M_3$

the gaugino/higgsino content, and when passing through $M_1 = 300$ GeV, the $\widetilde{Z}_1$ and $\widetilde{Z}_3$ exchange identities and interchange from being bino-like to higgsino-like. A similar level crossing is seen on the negative M_1 side of the figure. Since there is no charged bino, the values of $m_{\widetilde{W}_{1,2}}$ remain constant (at μ and M_2(weak)) with variation of M_1. Since the value of $m_{\widetilde{Z}_1}$ is decreasing as M_1 decreases, then the mass gaps $m_{\widetilde{W}_1} - m_{\widetilde{Z}_1}$ and $m_{\widetilde{Z}_2} - m_{\widetilde{Z}_1}$ also increase. The mass gaps reach values of ~ 150 GeV for M_1 as small as 50 GeV. This should render signals from $\widetilde{W}_1\widetilde{Z}_2$ and $\widetilde{W}_1\widetilde{W}_1$ production much easier to detect at the LHC as compared to the RNSh case.

In Fig. 4.3, one sees the thermally-produced neutralino relic density as calculated using the IsaReD program [100]. The value of $\Omega_{\widetilde{Z}_1}h^2$ begins at ~ 0.01 for $|M_1| = 700$ GeV which is typical for a higgsino-like LSP of mass 200 GeV. As $|M_1|$ decreases, then the bino content of $\widetilde{Z}_1$ becomes larger – reducing the

annihilation cross section – so that the thermal relic density correspondingly increases. For $|M_1| \simeq 380$ GeV, the value of $\Omega_{\widetilde{Z}_1}h^2$ reaches 0.12, *i.e.* it saturates the measured DM abundance, and one gets the so-called well-tempered neutralino. For even lower values of $|M_1|$, then neutralinos are unable to annihilate efficiently and $\Omega_{\widetilde{Z}_1}h^2$ exceeds 1 except for special values where the neutralino annihilation cross-section is resonance-enhanced. For $|M_1| \sim 150$ GeV, then the bino-like neutralino has mass $m_{\widetilde{Z}_1} \sim m_h/2$ so that neutralinos can efficiently annihilate through the light Higgs resonance. The annihilation rate at resonance is not quite symmetric for the two signs of M_1. For even lower values of $|M_1|$, then $m_{\widetilde{Z}_1} \sim M_Z/2$ so that neutralinos efficiently annihilate through the Z boson pole. Values of $|M_1| < 100$ GeV move below the Z-resonance and due to the increasing bino content of $\widetilde{Z}_1$, the LSP annihilation cross section becomes even smaller, leading to an even larger thermal relic density.

Table 4.1 displays the SUSY spectrum for $M_1(\text{GUT}) = 380$ GeV as RNSb, the value for which the thermal neutralino relic density $\Omega^{TP}_{\widetilde{Z}_1}h^2$ essentially saturates the measured abundance so that $\Omega_{\widetilde{Z}_1}h^2 = 0.12$. In this case, the $\widetilde{Z}_1$ is a bino-higgsino admixture albeit already it is dominantly bino-like. The mass gap $m_{\widetilde{W}_1} - m_{\widetilde{Z}_1}$ is ~ 56 GeV while the mass gap $m_{\widetilde{Z}_2} - m_{\widetilde{Z}_1}$ is ~ 60 GeV.

4.2.1 Implications for LHC13

The possibility of non-universal gaugino mass parameters has important implications for discovery of natural SUSY at LHC13.

Since squarks are very heavy, the multijet + E_T^{miss} signal mainly arises from

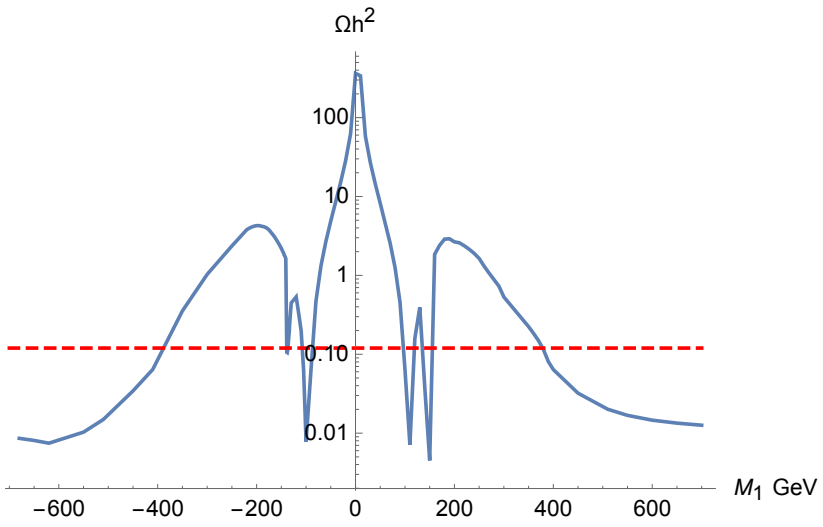

Figure 4.3: Variation of $\Omega^{TP}_{\widetilde{Z}_1}h^2$ vs. M_1 for a general RNS SUSY benchmark model with variable M_1 and $M_2 = M_3$. The dashed line shows the measured value of the cold dark matter relic density.

$pp \to \tilde{g}\tilde{g}X$ followed by gluino cascade decays mainly via $\tilde{g} \to tb\widetilde{W}_j$ and $t\bar{t}\widetilde{Z}_i$. For a fixed $m_{\tilde{g}}$, but varying M_1, one still expects multi-lepton plus multi-jet+$E_T^{\rm miss}$ events at a rate which mainly depends on the value of $m_{\tilde{g}}$. For discovery via gluino pair production, the LHC13 reach – which extends to about $m_{\tilde{g}} \sim 1.7$ TeV (for $m_{\tilde{g}} \ll m_{\tilde{q}}$) for 100 fb^{-1} of integrated luminosity [90] – tends to be dominated by multi-jet+$E_T^{\rm miss}$ channel and so changes little compared to the case of universal gaugino masses. For the RNS point in question, the gluino dominantly decays via $\tilde{g} \to \tilde{t}_1 t$, and the $\tilde{t}_1$ subsequently decays via $\tilde{t}_1 \to b\widetilde{W}_1, t\widetilde{Z}_{1,2,3}$. Within the gluino pair cascade decay events, the isolated multi-lepton content should increase with decreasing M_1 due to the increased mass gap between $\widetilde{W}_1 - \widetilde{Z}_1$ and $\widetilde{Z}_{2,3} - \widetilde{Z}_1$ since one may also obtain energetic leptons from $\widetilde{W}_1 \to \ell\nu_\ell\widetilde{Z}_1$ and $\widetilde{Z}_2 \to \widetilde{Z}_1\ell^+\ell^-$ three body decays in addition to those from top or $\widetilde{Z}_3$ decays. If M_1 is sufficiently small,

then the two-body decays $\widetilde{W}_1 \to \widetilde{Z}_1 W$ and $\widetilde{Z}_2 \to \widetilde{Z}_1 Z,\ \widetilde{Z}_1 h$ open up. The latter two decays, if open, tend to occur at comparable rates in natural SUSY with a bino-like LSP since the lighter -inos tend to be a gaugino-higgsino admixture. The isolated opposite-sign/same flavor (OS/SF) dileptons present in cascade decay events will have mass edges located at $m_{\widetilde{Z}_2} - m_{\widetilde{Z}_1}$ for three-body decays, or else real $Z \to \ell^+\ell^-$ or $h \to b\bar{b}$ pairs will appear in the case of two-body decays of $\widetilde{Z}_2$ and $\widetilde{Z}_3$:

For electroweak-ino pair production, allowing non-universality in the gaugino sector changes the situation quite dramatically. In the case of RNS with gaugino mass unification, the higgsino pair production reactions $pp \to \widetilde{W}_1^+\widetilde{W}_1^-$ and $\widetilde{W}_1\widetilde{Z}_{1,2}$ are largely invisible due to the small mass gaps [90]. It may, however, be possible to detect higgsino pair production making use of initial state QCD radiation and specially designed analyses if the higgsino mass is below $\sim 170 - 200$ GeV, depending on the integrated luminosity [106, 107].

The wino pair production process $pp \to \widetilde{W}_2\widetilde{Z}_4 X$ can lead to a characteristic same-sign diboson signature [39] arising from $\widetilde{W}_2^{\mp} \to \widetilde{Z}_1 W^{\mp}$ and $\widetilde{Z}_4 \to \widetilde{W}_1^{\pm} W^{\mp}$ decays, where the higgsinos decay to only soft visible energy and are largely invisible.

In contrast, as M_1 diminishes, then the growing $\widetilde{W}_1 - \widetilde{Z}_1$ and $\widetilde{Z}_2 - \widetilde{Z}_1$ mass gaps give rise increasingly to visible decay products and a richer set of electroweak -ino signals. In Fig. 4.4, one finds the NLO cross sections obtained using Prospino [108] for various electroweak-ino pair production reactions versus variable $M_1(GUT)$

for the RNS benchmark case.[1] As M_1 falls to lower values, the chargino pair rates remain constant since μ and M_2 do not change. The $\widetilde{W}_1\widetilde{W}_2$ cross section in the topmost frame is small because squarks are very heavy, and the $Z\widetilde{W}_1\widetilde{W}_2$ coupling is dynamically suppressed. Although the $\widetilde{W}_1 \to f\bar{f}'\widetilde{Z}_1$ decay products become more energetic with reducing $|M_1|$, the chargino pair signals are typically challenging to extract from large SM backgrounds such as W^+W^- production.

For $\widetilde{W}_1\widetilde{Z}_{1,2}$ production, the cross sections can be large but the decays give only soft visible energy for $M_1 \sim 700$ GeV. But as M_1 is lowered, the cross section for $\widetilde{W}_1\widetilde{Z}_2$ remains large but the mass gaps increase. Ultimately, the clean trilepton signature should become visible against SM backgrounds [109, 110]. Also, the reaction $pp \to \widetilde{W}_1\widetilde{Z}_3$ has an increasing cross section as M_1 decreases and should give rise to $\ell + Z$ events: trileptons where one pair reconstructs a real Z [111], as is the case for the RNSb benchmark point: see also Ref's. [112, 113]. Ultimately, the $\widetilde{Z}_3 \to \widetilde{Z}_1 h$ mode also opens up, reducing the trilepton signal but potentially offering an opportunity for a search via the Wh channel [114].

In models with heavy squarks, higgsino pair production reactions make the main contribution to neutralino pair production processes. In many models, $|\mu|$ is large, making neutralino pair production difficult to see at hadron colliders. Natural SUSY models with non-universal gaugino masses are an exception as can be seen from the bottom frame of Fig. 4.4 where cross-sections for various neutralino pair production processes are shown. The bino-higgsino level crossing

[1]Since, as seen in the previous figures the mixing patterns are roughly symmetric about $M_1 = 0$, and because it is relatively time-consuming to run Prospino, only results for positive values of M_1 are shown.

that was mentioned earlier is also evident: for large M_1 the $\widetilde{Z}_1$ and $\widetilde{Z}_2$ are higgsino-like states and $\widetilde{Z}_1\widetilde{Z}_2$ production (solid squares) dominates, whereas for small M_1 then $\widetilde{Z}_2$ and $\widetilde{Z}_3$ are higgsino-like and $\widetilde{Z}_2\widetilde{Z}_3$ production (left-pointing triangles) is dominant even though the $\widetilde{Z}_1\widetilde{Z}_2$ and $\widetilde{Z}_1\widetilde{Z}_3$ reactions are kinematically favoured. Also $\widetilde{Z}_1\widetilde{Z}_2$ and $\widetilde{Z}_2\widetilde{Z}_3$ production can lead to dilepton and four-lepton final states which may be visible, and to ZZ, Zh and $hh + E_T^{\rm miss}$ final states if $|M_1|$ is sufficiently small.

4.2.2 Implications for ILC physics

The prospects for SUSY discovery and precision measurements in the RNS model have been examined for an International Linear e^+e^- Collider (ILC) with $\sqrt{s} \sim 250 - 1000$ GeV in Ref. [115]. Such a machine is a higgsino factory in addition to a Higgs factory and even with small (10 GeV) inter-higgsino mass gaps, SUSY signals should stand out above SM backgrounds. The clean environment, together with the availability of polarized electron beams, also allows for precision measurements that point to the higgsino origin of these events. The main reactions of import are $e^+e^- \to \widetilde{W}_1^+\widetilde{W}_1^-$ and $\widetilde{Z}_1\widetilde{Z}_2$ production.

In the case where M_1 is low enough so that one obtains a bino-like LSP, the second higgsino state $\widetilde{Z}_3$ also becomes accessible, and reactions involving $\widetilde{Z}_3$ provide even richer prospects for SUSY discovery. Various SUSY pair production cross sections are shown in Fig. 4.5 versus variable M_1 and for $\sqrt{s} = 500$ GeV. The electron and positron beams are taken to be unpolarized in this figure. Once again the level crossings between bino and higgsino-like states are evident. For

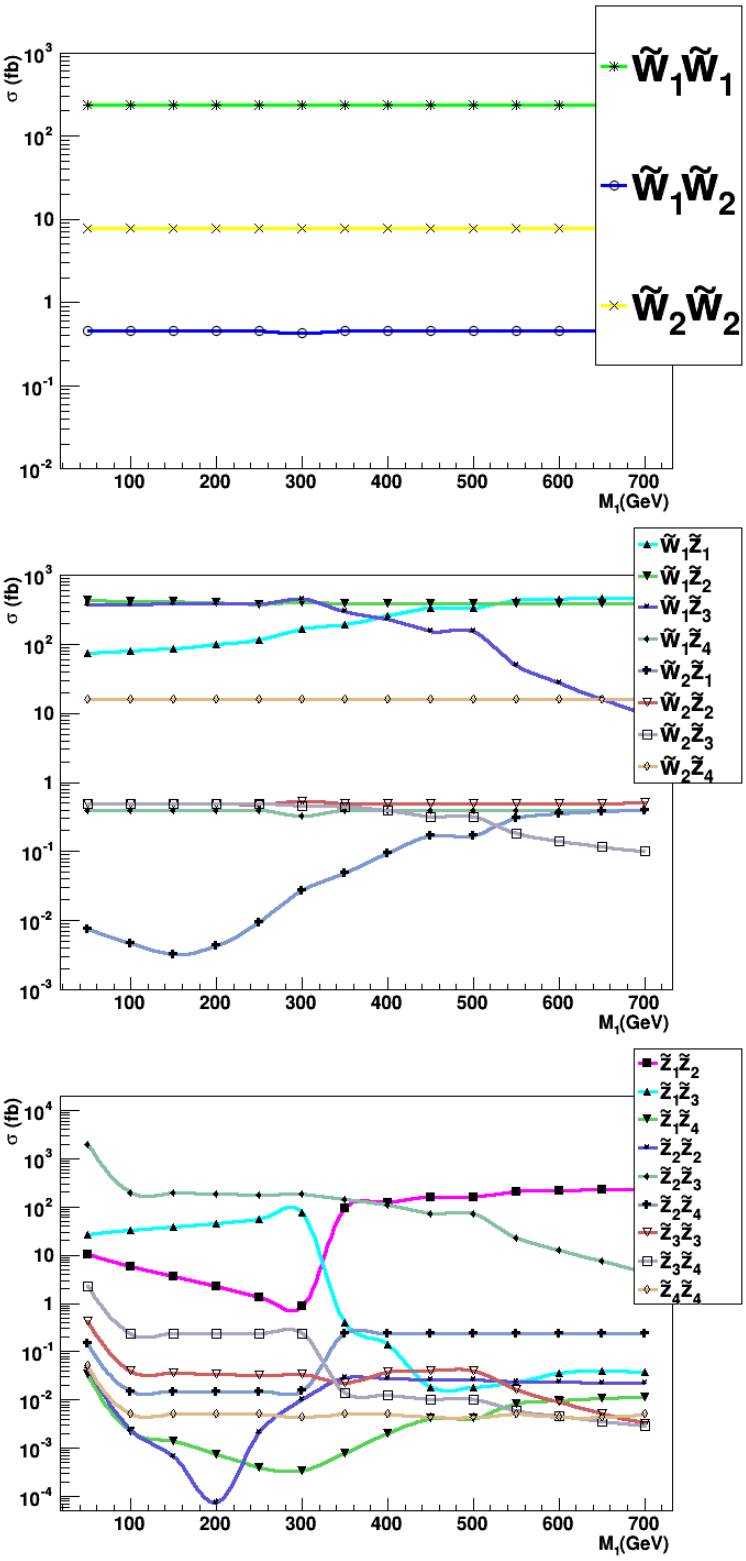

Figure 4.4: Electroweak -ino pair production cross sections versus M_1 for the RNS SUSY benchmark model with variable M_1 but with $M_2 = M_3$

the case of unified gaugino masses with $M_1 = 700$ GeV, then indeed only $\widetilde{W}_1\widetilde{W}_1$ and $\widetilde{Z}_1\widetilde{Z}_2$ are available. However, as $|M_1|$ is lowered, then $\sigma(\widetilde{W}_1\widetilde{W}_1)$ remains constant although the decay products of $\widetilde{W}_1$ become more energetic once the LSP becomes bino-like and lighter than the higgsino. The dijet mass spectrum from $\widetilde{W}_1 \to \widetilde{Z}_1 q\bar{q}'$ decay allow for precision extraction of $m_{\widetilde{W}_1}$ and $m_{\widetilde{Z}_1}$ and also extraction of the weak scale SUSY parameters μ and also M_1, if the bino mass is small enough [116, 117, 115].

Turning to neutralino production, one sees that higgsino pair production – $\widetilde{Z}_1\widetilde{Z}_2$ production if $|M_1|$ is large, and $\widetilde{Z}_2\widetilde{Z}_3$ production for small values of $|M_1|$ – dominates the neutralino cross section just as in the LHC case. Notice that for $0 < M_1 < 300$ GeV, $\widetilde{Z}_1\widetilde{Z}_3$ production also occurs at an observable rate, falling with reducing M_1 because of the increasing bino content of $\widetilde{Z}_1$. The strong dip in $\sigma(\widetilde{Z}_1\widetilde{Z}_3)$ around $M_1 \simeq 500$ GeV is due to an accidental cancellation in the $Z\widetilde{Z}_1\widetilde{Z}_3$ coupling. $\widetilde{Z}_2\widetilde{Z}_3$ and $\widetilde{Z}_1\widetilde{Z}_3$ production should lead to interesting event topologies, including $Z + E_T^{\rm miss}$ and $h + E_T^{\rm miss}$ events where the missing mass does *not* reconstruct to M_Z, depending on the decay modes of the neutralinos. On the negative M_1 side, the $\widetilde{Z}_1\widetilde{Z}_3$ cross section is small, except beyond the level crossing at $M_1 \simeq -600$ GeV.

4.2.3 Implications for dark matter searches

In SUSY, the LSP is a dark matter candidate which would fill all space as a non-relativistic gas. The LSPs would gravitationally clump to form a galactic halo and it is the goal of direct detection experiements to detect this halo of weakly

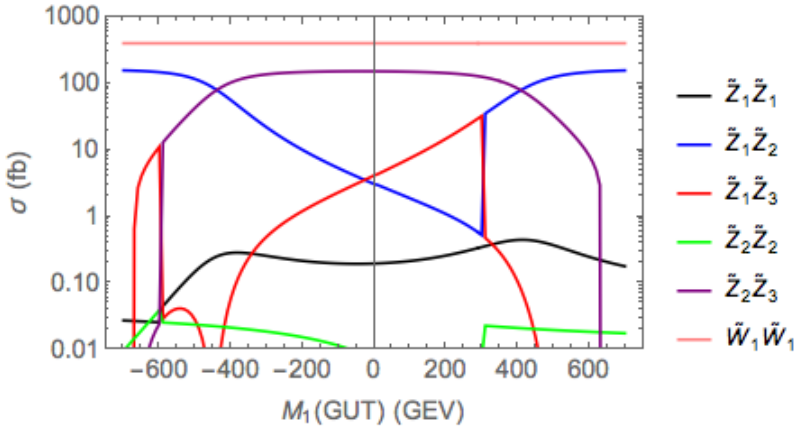

Figure 4.5: Chargino and neutralino production cross sections at a linear e^+e^- collider with $\sqrt{s} = 500$ GeV with unpolarized beams for the RNS SUSY benchmark model with variable M_1 but with $M_2 = M_3$

interacting massive particles (WIMPs). The basic idea of these experiments is that as the earth rotates through this halo, relic WIMPs will deposit small amounts of energy when scattering off the nuclei in some detector material.

In the RNS model with unified gaugino masses and a higgsino-like LSP, the relic density of thermally produced neutralinos is much smaller than the observed density of cold dark matter. This allows for a contribution from axions [93] that must be present if nature adopts the Peccei-Quinn solution to the strong CP problem. In the case of DFSZ axions [118], one also gains a solution to the SUSY μ problem and can allow for a natural value of $\mu \sim 100 - 200$ GeV via radiative PQ breaking [119]. In such models, the DM tends to be axion-dominated [120] with a local abundance of neutralino WIMPs reduced by factors of 10-15 from usual expectations. The reduced local abundance makes direct detection more difficult since detection rates depend linearly on the local neutralino abundance.

Indirect detection rates from WIMP halo annihilations depend on the square of the local abundance so are even more suppressed in models where the WIMPs only make up a fraction of the dark matter [41].

For the more general model where $|M_1|$ may be lower than expected from gaugino mass unification, the thermally-produced neutralino abundance is increased, and consequently one expects a greater fraction of neutralino dark matter compared to axions, assuming there are no other processes that affect the neutralino relic density. The increased local neutralino abundance leads to more favorable prospects for WIMP direct and indirect detection.

The spin-independent (SI) WIMP-proton scattering cross section from IsaReS [121] is shown in Fig. 4.6. The curve with red dots shows the case of variable M_1. As M_1 decreases from large, positive values, then the LSP becomes more of a bino-higgsino admixture. Since the SI cross sections proceeds mainly through light Higgs h exchange, and the Higgs-neutralino coupling is proportional to a product of gaugino times higgsino components [25], then the SI direct detection cross section increases by up to a factor of ~ 2 for lowered M_1. As M_1 is lowered even further, then the LSP becomes more purely bino-like, and the SI direct detection cross section drops sharply. The sharp dip at $M_1 \simeq -110$ GeV is due to the reduction of the $h\widetilde{Z}_1\widetilde{Z}_1$ coupling, and also the cancellation between the neutralino scattering through the exchange of the light CP-even Higgs and that through the exchange of the heavy CP- even Higgs, denoted as the blind spot in dark matter direct detection [25, 122, 123]. The kink at $M_1 \sim -600$ GeV occurs due to a change in the composition of the LSP: one sees from Fig. 4.2 that the

levels are getting very close, and the -inos may be switching composition.

One may be concerned that the cross-section in Fig. 4.6 seemingly violated the upper limits from LUX (Ref. [103]) of $\sim (1-2) \times 10^{-9}$ pb for neutralinos in the mass range 20-200 GeV. As mentioned previously, one should remember that these limits assume that the LSP saturates the observed density of cold dark matter, which is certainly *not the case* for a higgsino-like LSP (large $|M_1|$ values in the figure). Scaling by the expected fraction of the thermal relic density makes the large $|M_1|$ region safe, though on the edge of observability of the LUX experiment, *if thermal production is assumed to be the complete story of the neutralino relic density.* For smaller values of $|M_1|$, where it may also appear that the direct detection bound is violated, this clearly is not the case. One should, however, keep in mind that for these ranges of M_1, the direct detection rate from which the bound in Ref. [103] is inferred cannot be reliably calculated because the physics processes responsible for bringing the neutralino relic density to its final value lie outside the present framework. Put differently, one needs to be cautious against unilaterally excluding model parameters (including the RNSb model) based on these considerations, because this frequently requires other assumptions about the cosmological history of the Universe that have no impact upon collider physics.[2] While WIMP discovery would be unambiguous, interpretation of the physics underlying any signal would require a careful specification of all underlying assumptions.

The expected spin-dependent (SD) proton-neutralino direct detection cross

[2]What is clear from the data is that neutralinos with a large higgsino content (including the well-tempered neutralino) cannot be the bulk of the local dark matter.

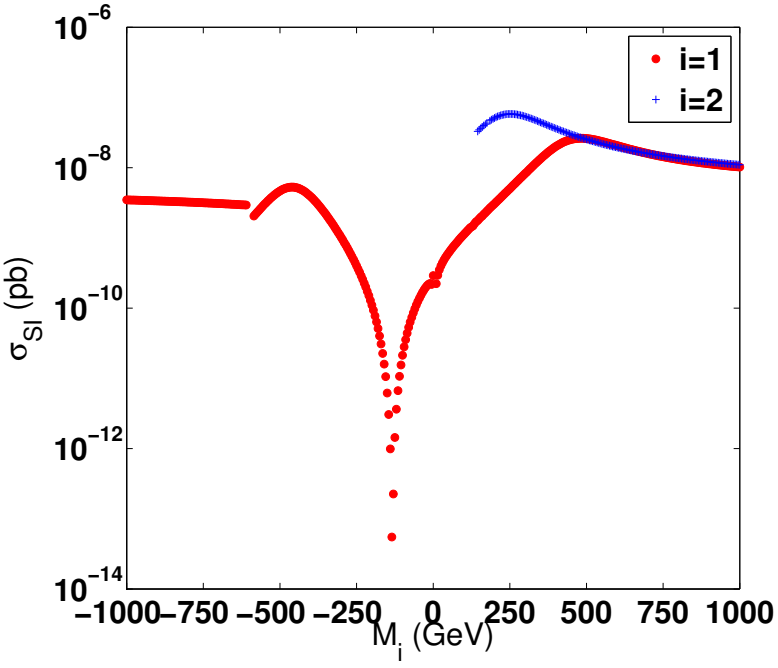

Figure 4.6: Spin-independent $p\widetilde{Z}_1$ scattering cross section vs. M_1 (red dots) or M_2 (blue pluses) for the RNS benchmark point.

section is plotted versus the gaugino mass parameter in Fig. 4.7. In this case, the scattering occurs dominantly via Z-exchange. The $Z\widetilde{Z}_1\widetilde{Z}_1$ coupling (Eq. 8.101 of Ref. [25]) is proportional to a difference in square of higgsino components of the neutralino. For M_1 large and positive, both higgsino components are comparable and there is a large cancellation in the coupling. As M_1 decreases, the higgsino components of $\widetilde{Z}_1$ decrease, but the up-type higgsino content more so than the down type. There is less cancellation and the coupling increases. As M_1 decreases further, the bino component increases and the smallness of the higgsino components decreases the coupling. The negative M_1 side shows more or less similar features until we reach $M_1 \simeq -600$ GeV where the flip in the identity of the neutralino mentioned in the previous figure results in the jump.

As far as WIMP detection goes, the SD cross section would influence IceCube [105] detection rates the most since the WIMP abundance in the solar core is determined by equilibration between the capture rate and the annihilation rate of WIMPs in the sun. The scattering/ capture rate of the Sun depends mainly on the Hydrogen-WIMP scattering cross section which proceeds more through the SD interaction since there is no nuclear mass enhancement. While some of the predicted values (red points) might well be marginally excluded by the IceCube search, the main message is that for the most part the model with $\mu = 200$ GeV is on the edge of detectability, as long as neutralinos dominantly annihilate to W pairs and assuming that neutralinos essentially saturate the entire cold dark matter relic density.

Fig. 4.8 shows the thermally-averaged neutralino annihilation cross section

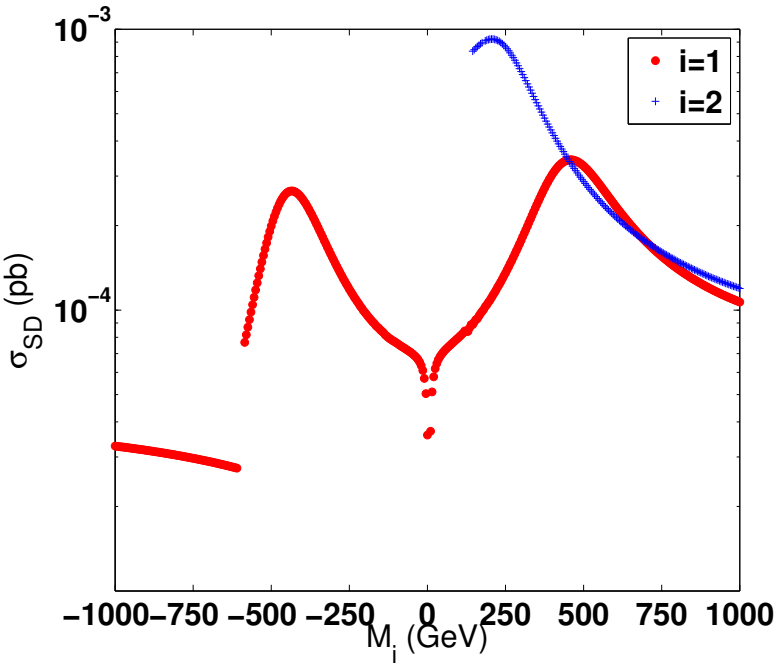

Figure 4.7: Spin-dependent $p\widetilde{Z}_1$ scattering cross section vs. M_1 (red circles) or M_2 (blue pluses) for the RNS benchmark point.

times relative velocity evaluated as $v \to 0$. This quantity enters the halo WIMP annihilation rate, and detection rate for galactic positrons, anti-protons and gamma rays from WIMP halo annihilations are proportional to this factor. In the case of gaugino mass unification where the neutralino is higgsino-like, then the local abundance is reduced and the expected detection rate is reduced by the square of the WIMP underabundance: ξ^2 where $\xi = \Omega_{\widetilde{Z}_1} h^2/0.12$. From the figure, one sees that while the local abundance increases as $|M_1|$ is reduced (Fig. 4.3), the annihilation rate decreases because annihilation to WWs occurs mainly via the (reducing) higgsino component of the LSP. Once this channel is closed (around $|M_1| \simeq 200$ GeV), annihilation to fermions takes over and the rate drops further. The FERMI-LAT collaboration has obtained upper limits located at about a few $\times 10^{-26} cm^3/s$ ($\sim 2 \times 10^{-25}\ cm^3/s$) for annihilation to $b\bar{b}$ (WW pairs) [124]. Assuming a Navarro-Frenk-White profile for dwarf galaxies in the analysis, models with a larger cross section would have led to a flux of gamma rays not detected by the experiment. Even without the ξ^2 scaling noted above, and certainly after the scaling, these bounds do not exclude any of the points in the figure. All the caveats that have been discussed for the applicability of direct detection bounds are also applicable in this case, and one must use caution in excluding ranges of parameters even if the Fermi Collaboration obtains tighter bounds in the future.

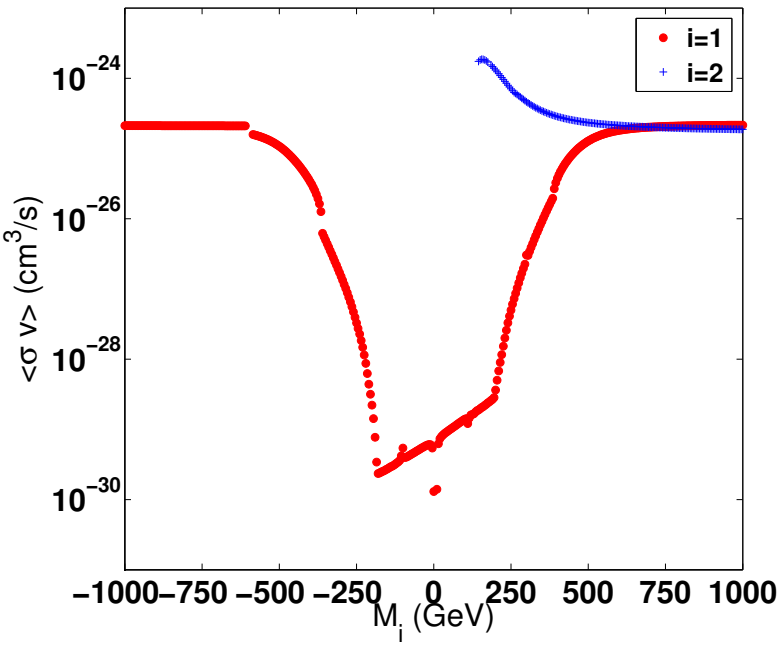

Figure 4.8: Thermally-averaged neutralino annihilation cross section times velocity at $v = 0$ vs. M_1 (red dots) or M_2 (blue pluses) for the RNS benchmark point.

4.3 Natural SUSY with a wino-like LSP

This section examines the phenomenological implications of altering the $SU(2)$ gaugino mass parameter M_2 while keeping $M_1 = M_3 = 700$ GeV. The variation of $\Delta_{\rm EW}$ with M_2 is shown in Fig. 4.1 as blue pluses. Again, one sees that $\Delta_{\rm EW}$ is relatively insensitive to M_2 except for the largest values of this parameter. This is due to the increasing contribution of winos to $\Sigma_u^u(\widetilde{W}_{1,2})$. Thus, models with $M_2 \ll M_{1,3}$ lead to a wino-like LSP at little cost to naturalness. For $M_2 < 150$ GeV the chargino becomes lighter than 100 GeV (roughly the chargino mass bound from LEP2). Here, and in subsequent figures, negative values of M_2 are not considered as these lead to a chargino LSP: $m_{\widetilde{W}_1} < m_{\widetilde{Z}_1}$.

In Fig. 4.9, one sees how the masses of charginos and neutralinos change as M_2 is reduced from its unified value. Starting with the RNSh spectra at $M_2 = 700$ GeV, where the $\widetilde{W}_2$ and $\widetilde{Z}_4$ are essentially winos, and $\widetilde{Z}_1$, $\widetilde{Z}_2$ and $\widetilde{W}_1$ are higgsinos, one sees that as M_2 is lowered, the mass of the wino-like states reduces whereas the higgsino-like states remain with the mass fixed close to μ. The mass of the bino-like $\widetilde{Z}_3$ also remains nearly constant. This behaviour persists until $\widetilde{Z}_3$ and $\widetilde{Z}_4$ switch identities and the bino-wino level crossing is reached near $M_2 \simeq 350$ GeV. For still lower values of M_2, one sees another level crossing between the charged as well as neutral wino-like and higgsino-like states. For $M_2 < 200$ GeV, the lighter chargino as well as the LSP are wino-like, the heavier chargino and the neutralinos $\widetilde{Z}_{2,3}$ are higgsino-like, and $\widetilde{Z}_4$ is mainly a bino. The mass gap $m_{\widetilde{W}_1} - m_{\widetilde{Z}_1}$ has actually decreased with decreasing M_2 since these wino-like states have very tiny

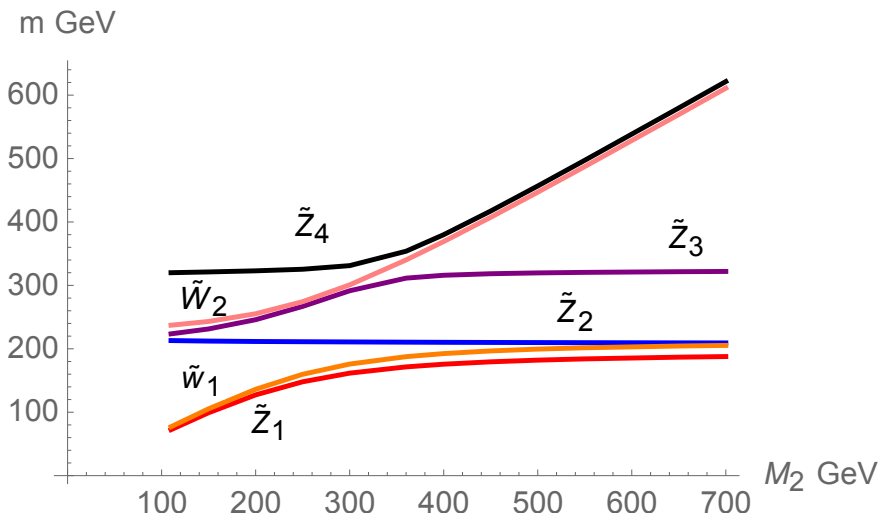

Figure 4.9: Variation of chargino and neutralino masses vs. M_2 for the RNS SUSY benchmark model with variable M_2 but with $M_1 = M_3$

mass splittings. The mass gaps $m_{\widetilde{W}_2} - m_{\widetilde{Z}_1}$ and $m_{\widetilde{Z}_2} - m_{\widetilde{Z}_1}$ greatly *increase* with decreasing M_2, reflecting the widening higgsino-wino mass difference. This should make their visible decay products harder so that these states are easier to detect at the LHC.

The thermally-produced neutralino relic density $\Omega_{\widetilde{Z}_1}h^2$ versus M_2 is shown in Fig. 4.10. Starting with $M_2 = 700$ GeV for which $\Omega_{\widetilde{Z}_1}h^2 \sim 0.01$, one sees that $\Omega_{\widetilde{Z}_1}h^2$ steadily decreases with decreasing M_2 and reaches a value $\Omega_{\widetilde{Z}_1}h^2 \sim 0.001$ for very low values of M_2 where the $\widetilde{Z}_1$ is nearly pure wino. This is because wino annihilation proceeds via the larger SU(2) triplet coupling to electroweak gauge bosons while annihilation of higgsinos proceeds via the smaller doublet coupling – the cross section for annihilation to W pairs, which is dominated by the t-channel chargino exchange, goes as the fourth power of this coupling. Thus, in the case of low M_2 with a wino-like neutralino, we might expect an even more reduced local

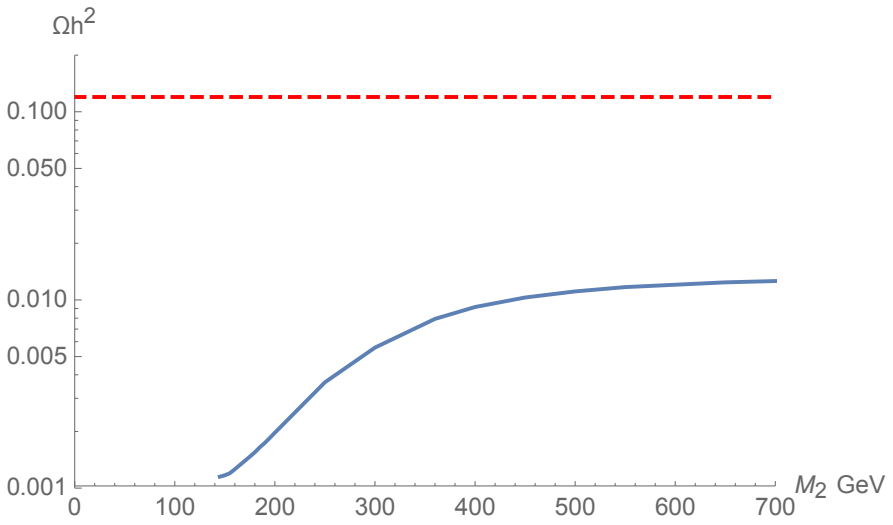

Figure 4.10: Variation of $\Omega^{TP}_{\widetilde{Z}_1}h^2$ vs. M_2 (blue curve) for the RNS SUSY benchmark model with variable M_2 but with $M_1 = M_3$. We cut the graph off at the low end because $m_{\widetilde{W}_1}$ falls below its LEP2 bound.

abundance from *thermally produced LSPs*. The balance may be made up either by axions or other relics, or by LSPs produced by late decays of heavier particles. The graph is cut off when $m_{\widetilde{W}_1}$ falls below its LEP2 bound. We do not see any dips corresponding to s-channel h or Z resonance annihilation as these fall in the LEP2 excluded region.

An RNS benchmark point with a wino-like LSP is shown in Table 4.1 and is labelled as RNSw. All input parameters for RNSw are the same as for RNSh except now M_2 is chosen to be 175 GeV. The $\widetilde{W}_1 - \widetilde{Z}_1$ mass gap has decreased to just 7.3 GeV while the $\widetilde{Z}_2 - \widetilde{Z}_1$ mass gap has increased beyond the RNSh value up to ~ 97 GeV, large enough so that both $\widetilde{Z}_2 \to \widetilde{Z}_1 Z$ and $\widetilde{Z}_2 \to \widetilde{W}_1^{\pm} W^{\mp}$ decays are now allowed. In such a scenario, one would expect LHC SUSY cascade decay events to be rich in content of real Z bosons that could be searched for at

the LHC. In fact, the CMS [125] and ATLAS [126] collaborations have already obtained bounds on chargino and neutralino masses from an analysis of about 20 fb^{-1} of LHC8 data. These limits are obtained in simplified models from an analysis of expectations from $\widetilde{W}_1\widetilde{Z}_2$ and $\widetilde{W}_1\widetilde{W}_1$ production at LHC8, assuming that $m_{\widetilde{W}_1} = m_{\widetilde{Z}_2}$ and that the charginos (neutralinos) decay 100% of the time to W bosons (Z bosons or Higgs bosons). While these limits are not directly applicable to pair produced $\widetilde{W}_1$ and $\widetilde{Z}_2$ for the RNSw scenario in the table, the reader may be concerned that *higgsino-pair production* processes $pp \to \widetilde{W}_2\widetilde{Z}_{2,3}X, \widetilde{W}_2\widetilde{W}_2X$ would lead to final states similar to what the LHC searches look for. The RNSw scenario, with $m_{\widetilde{Z}_1} = 114$ GeV is clearly allowed by current searches; data from the LHC13 run should, however, decisively probe this benchmark point.

4.3.1 Implications for LHC13

As discussed in Sec. 4.2.1, the discovery reach of LHC13 for gluino pairs mainly depends on the value of $m_{\tilde{g}}$ which dictates the total $\tilde{g}\tilde{g}$ production cross section in the case of heavy squarks. One would thus expect a similar LHC13 reach for gluino pair production in the RNSw case as for RNSh and as for mSUGRA/CMSSM for comparable gluino masses and heavy squarks. Also, in the RNSw case, then charginos $\widetilde{W}_1$ will still be largely invisible due to their soft decay products.

The $\widetilde{W}_1 - \widetilde{Z}_1$ mass gap tends to lie in the 5-10 GeV range, since μ is 100-200 GeV as required by naturalness, and so charged winos will be short-lived with no discernable tracks or kinks. However, in the RNSw case, then the $\widetilde{Z}_2 - \widetilde{Z}_1$ mass gap does become large and the well-known dilepton mass edge at $m_{\widetilde{Z}_2} - m_{\widetilde{Z}_1}$ should

be observable for energetic enough $\widetilde{Z}_2 \to \widetilde{Z}_1 \ell^+ \ell^-$ decays if $m_{\widetilde{Z}_2} - m_{\widetilde{Z}_1} < M_Z$. In the case where the decay $\widetilde{Z}_2 \to \widetilde{Z}_1 Z$ opens up, then the gluino cascade decay events (which, depending on the spectrum, should mostly proceed via real or virtual stop decays because stops are much lighter than first/second generation squarks) should be rich in OS/SF dileptons which reconstruct M_Z. Note also that for modest values of M_2, then $\widetilde{Z}_3$ is also expected to be relatively light, and should also be accessible via gluino decays. For yet smaller values of M_2, $\widetilde{Z}_{2,3} \to \widetilde{Z}_1 h$ may also be allowed and should occur with a comparable branching fraction to the decay to real Zs.

In Fig. 4.11, I show NLO cross sections from Prospino [108] for electroweak -ino pair production at LHC13 for the RNS benchmark but for variable M_2. Chargino pair production – shown in the topmost frame – occurs via wino as well as via higgsino pair production. For large M_2 the latter dominates, but as M_2 is reduced, wino pair production increases in importance until it completely dominates for $M_2 \sim 100$ GeV. $\widetilde{W}_1\widetilde{W}_2$ production, for the most part occurs via small gaugino/higgsino content, and so has a smaller cross section than the kinematically disfavoured $\widetilde{W}_2\widetilde{W}_2$ production. The level crossing as the light chargino transitions from being higgsino-like to wino-like as M_2 reduces is also evident in the upper two curves.

Chargino-neutralino production, shown in the middle frame, also occurs via wino as well as higgsino-pair production processes. For large values of M_2, higgsino pair production dominates and $\widetilde{W}_1\widetilde{Z}_{1,2}$ production processes have the largest cross sections. For very small values of M_2, pair production of winos is dynamically

and kinematically favoured, and $\widetilde{W}_1\widetilde{Z}_1$ occurs at the highest rate. The higgsino-like states $\widetilde{W}_2, \widetilde{Z}_{2,3}$ have masses μ and are also produced with substantial cross sections. Notice that $\widetilde{W}_1\widetilde{Z}_2$ production remains significant even for small values of M_2, presumably because it is favoured by kinematics (and increased parton luminosity).

Neutralino pair production (shown in the bottom frame) can only occur via higgsino pair production since electroweak gauge invariance precludes a coupling of Z to neutral gauginos. As a result, $\widetilde{Z}_1\widetilde{Z}_2$ production dominates for large M_2. For small values of M_2 (where $\widetilde{Z}_1$ becomes wino-like) $\widetilde{Z}_2\widetilde{Z}_3$ production becomes important; however, $\widetilde{Z}_1\widetilde{Z}_2$ production remains large because of large parton densities.

One sees that for $M_2 \lesssim 300$ GeV, the cross sections for $\widetilde{W}_1\widetilde{Z}_1$ and $\widetilde{W}_1\widetilde{W}_1$ production processes increase rapidly with decreasing M_2 since $\widetilde{W}_1$ and $\widetilde{Z}_1$ become increasingly wino-like. However, since the $\widetilde{W}_1 - \widetilde{Z}_1$ mass gap reduces even below the higgsino-LSP case, these states remain difficult – perhaps impossible – to detect. Although the cross section for wino-like $\widetilde{W}_1\widetilde{Z}_1$ production becomes very large at low M_2, this process is difficult to detect. However, $\widetilde{W}_1\widetilde{Z}_2$ production remains at viable rates even for low M_2. In this case, one might look for relatively hard OS/SF dileptons from $\widetilde{Z}_2$ decay recoiling against only soft tracks and $E_T^{\rm miss}$. Other possibly more promising reactions at low M_2 include $\widetilde{W}_2\widetilde{Z}_3$, $\widetilde{W}_2\widetilde{Z}_2$, $\widetilde{Z}_2\widetilde{Z}_3$ and maybe also $\widetilde{Z}_2\widetilde{Z}_4$ production, since the decay products from both the chargino and neutralino should be relatively hard and can lead to $E_T^{\rm miss}$ events with three or more leptons, or real Z and Higgs bosons. LHC collaborations are already

searching for an excess of just such events [125, 126, 127]. Note also that $\widetilde{W}_1\widetilde{Z}_3$ and $\widetilde{Z}_1\widetilde{Z}_2$ production each has a cross section in excess of 100 fb at low M_2 but would be considerably more difficult to detect.

4.3.2 Implications for ILC

At ILC, the natural SUSY scenario with low M_2 becomes both more challenging and richer. The cross sections for chargino and neutralino pair production at ILC500 are shown in Fig. 4.12 for unpolarized beams. For $M_2 = 700$ GeV, we have the higgsino pair production reactions $e^+e^- \to \widetilde{W}_1^+\widetilde{W}_1^-$ and $\widetilde{Z}_1\widetilde{Z}_2$ dominating. As M_2 is lowered, then the $\widetilde{W}_1$ becomes more wino-like and lighter leading to a larger cross section. However, the mass gap $\widetilde{W}_1 - \widetilde{Z}_1$ drops below 10 GeV making chargino pairs more difficult but likely still possible to detect with specially designed cuts. Beam polarization would serve to ascertain the higgsino/wino content of the chargino. Also, the $\widetilde{Z}_1\widetilde{Z}_2$ reaction falls with decreasing M_2 as the $Z - \widetilde{Z}_1 - \widetilde{Z}_2$ coupling decreases (Z only couples to higgsino components). As M_2 falls below 300 GeV, then the $\widetilde{Z}_2\widetilde{Z}_3$ reaction turns on and grows in importance because the $\widetilde{Z}_3$ becomes increasingly higgsino-like. Here, we expect $\widetilde{Z}_3$ to decay via 2-body modes into Z-bosons or Higgs bosons and $\widetilde{Z}_2$ to decay either to 2- or 3-body modes depending on the mass gap. This reaction should be distinctive and easily visible.

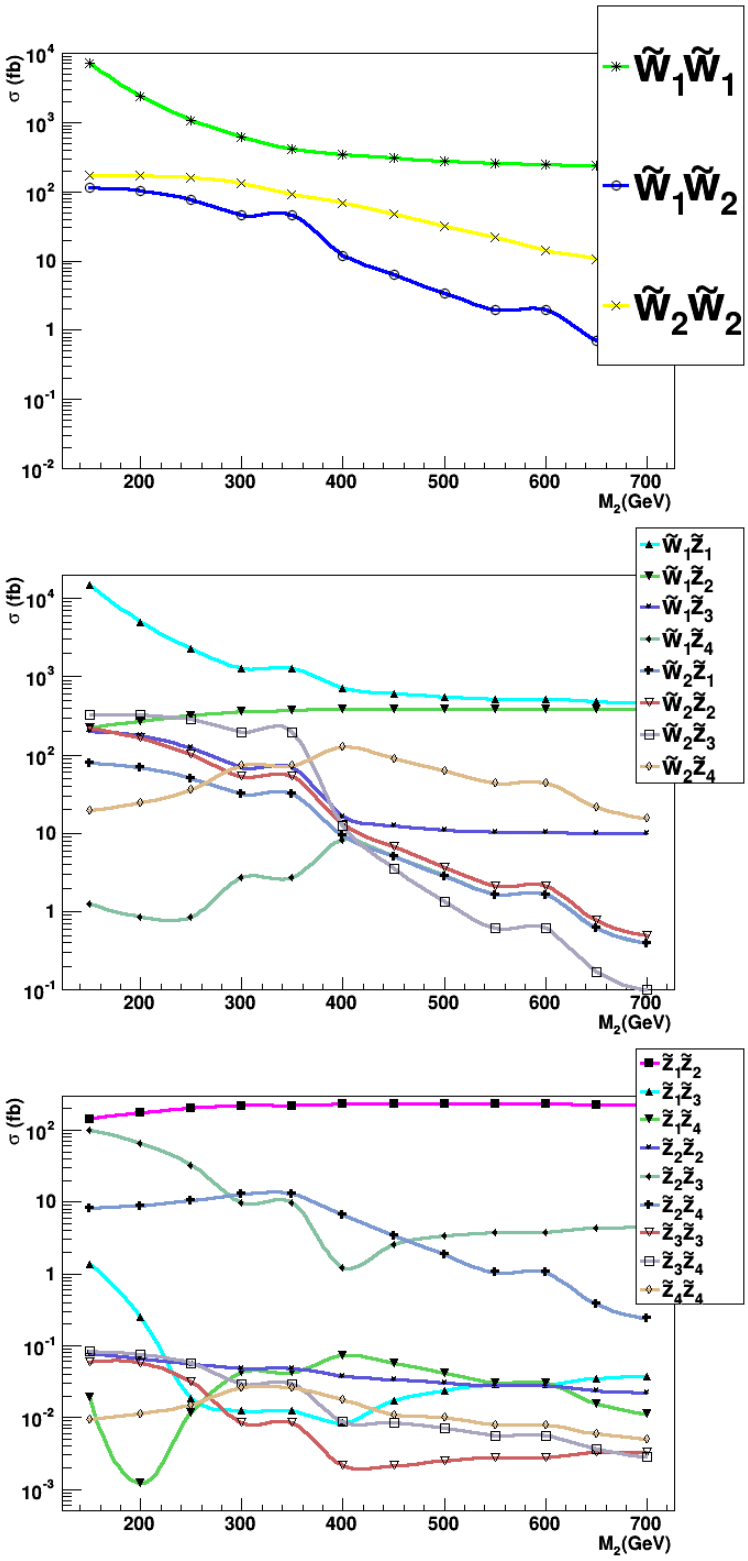

Figure 4.11: Electroweak-ino pair production cross sections versus M_2 for the RNS SUSY benchmark model with variable M_2 but with $M_1 = M_3$

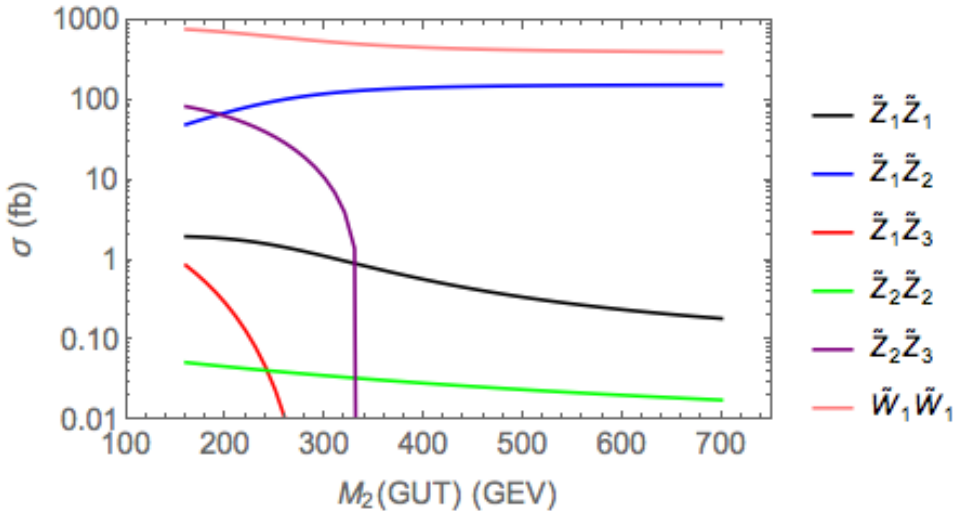

Figure 4.12: Chargino and neutralino production cross sections with unpolarized electron and positron beams at a linear e^+e^- collider with $\sqrt{s} = 500$ GeV for the RNS SUSY benchmark model with variable M_2 but with $M_1 = M_3$

4.3.3 Implications for WIMP detection

WIMP detection for models with radiatively-driven naturalness and a wino-like WIMP may be either more and less difficult than the case with gaugino mass unification since, though the nucleon neutralino scattering cross section is larger, the local abundance for a thermally produced wino-like LSP is below the already low value typical of a higgsino-like LSP. Of course, the thermal wino abundance can be augmented by non-thermal processes involving moduli decay [128] or axino/saxion decay [104] in the early universe.

In Fig. 4.6 the SI direct detection $\widetilde{Z}_1 p$ scattering cross section versus M_2 is shown as the curve with blue pluses. Starting off at large M_2, one sees that as M_2 is decreased, the $\sigma^{SI}(\widetilde{Z}_1 p)$ cross section increases, and the increase is substantially larger than the case of a bino-like LSP. This cross section proceeds mainly via

light h exchange which depends on a product of gaugino and higgsino components of the neutralino LSP [25]. In this case, the wino-component, which involves the larger $SU(2)$ gauge coupling g, becomes enhanced leading to the large cross section. For small enough $M_2 < 250$ GeV, the cross section turns around and decreases with decreasing M_2 since the $\widetilde{Z}_1$ becomes more purely wino-like and the higgsino components are diminished. Though the cross section in Fig. 4.6 exceeds the stated bounds ($1 - 2 \times 10^{-9}$ pb for $m_{\widetilde{Z}_1} = 100 - 200$ GeV) in Ref. [103], these bounds are not directly applicable because they were obtained assuming the neutralino constitutes the entire dark matter content of the Universe. For the natural SUSY scenario, the rates in direct detection experiments could be much smaller, as these scale by the neutralino fraction of the total local dark matter density. A wino-like neutralino that forms the bulk of the local dark matter would be excluded.

In Fig. 4.7 the spin-dependent direct detection cross section $\sigma^{SD}(\widetilde{Z}_1 p)$ versus M_2 is shown as the blue curve. Here, the SD scattering cross section which proceeds mainly by Z exchange becomes large since there is less cancellation in the $Z - higgsino - higgsino$ coupling. For small enough M_2, then again the cross section turns over and decreases due to the diminishing higgsino components. One sees that the cross section exceeds its 90% CL IceCube upper limit $\sim 1.5 \times 10^{-4}$ pb [105] obtained assuming that LSPs in the sun annihilate dominantly to W-pairs if $M_2 < 700$ GeV. As discussed earlier, the expected event rate must be re-scaled by ξ ($= 0.01 - 0.1$ for thermally produced wino LSPs), before comparing with IceCube limits. Then the IceCube limit on the cross section will be correspondingly

degraded, assuming that the neutralino density in the sun is determined by equilibrium between capture and annihilation rates. The RNSw scenario satisfies the IceCube bound assuming that the wino relic density is close to its thermally produced value and that the axion or some other particle makes up the remainder of the dark matter. Models where the dark matter is dominantly a wino-like neutralino are strongly excluded by IceCube.

In Fig. 4.8 $\langle \sigma v \rangle|_{v \to 0}$ versus M_2 is plotted as the blue shaded curve. In this case, as M_2 falls, then $\widetilde{Z}_1 \widetilde{Z}_1 \to WW$ becomes large and the annihilation rate increases. One might expect increased liklihood for indirect WIMP detection via gamma rays and antimatter detection. However, the increased annihilation rate is counter-balanced by a likely decreasing local WIMP abundance where the detection rate is proportional to the square of the reduced local abundance. One sees that although the predicted rate naively exceeds the upper limit from Fermi-LAT in Ref. [124], after the ξ^2 scaling discussed above exclusion is not possible.

Chapter 5

Naturalness implies intra-generational degeneracy for decoupled squarks and sleptons[129]

While realistic and natural SUSY models of particle physics can be constructed in accord with all experimental constraints, especially those arising from recent LHC searches, they are subject to a host of open questions[130]. Included amongst these are

- the SUSY flavor problem[57], wherein unfettered flavor-mixing soft terms lead to *e.g.* large $K - \bar{K}$ mass difference and anomalous contributions to flavor-changing decays such as $b \to s\gamma$ and $\mu \to e\gamma$,
- the SUSY CP problem[57], in which unfettered CP violating phases lead to large contributions to electron and various atomic electromagnetic dipole moments (EDMs),
- the SUSY gravitino problem[131], wherein thermally produced gravitinos in the early universe may decay after Big Bang nucleosynthesis (BBN), thus destoying the successful prediction of light element abundances created in the early universe, and
- the SUSY proton decay problem[132], wherein even in R-parity conserving GUT theories, the proton is expected to decay earlier than recent bounds from experimental searches.

While there exist particular solutions to each of these problems , there is one solution which potentially tames all four: decoupling of squarks and sleptons[137, 138, 139]. For the decoupling solution, squark and slepton masses $\stackrel{>}{\sim}$ a few TeV is sufficient for the SUSY CP problem while $m_{3/2} \stackrel{>}{\sim} 5$ TeV allows for gravitino decay before the onset of BBN. For the SUSY flavor problem, then first/second generation scalars ought to have mass $\stackrel{>}{\sim} 5 - 100$ TeV depending on which process is examined, how large of flavor-violating soft terms are allowed and possible GUT relations amongst GUT scale soft terms[140]. For proton decay, again multi-TeV matter scalars seem sufficient to suppress decay rates depending on other GUT scale parameters[75, 141].

Naively, the decoupling solution seems in conflict with notions of SUSY naturalness, wherein sparticles are expected at or around the weak scale[133] typified by the recently discovered Higgs mass $m_h = 125.09 \pm 0.24$ GeV[24]. To move beyond this, one may require the necessary condition for naturalnesss, quantified by the measure of electroweak fine-tuning (EWFT) which requires that there be *no large cancellations within the weak scale contributions to* m_Z *or to* m_h[18, 19, 142, 75, 69].

Recall that minimization of the one-loop effective potential $V_{tree} + V_{rad}$ leads to the well-known relation

$$\frac{M_Z^2}{2} = \frac{m_{H_d}^2 + \Sigma_d^d - (m_{H_u}^2 + \Sigma_u^u)\tan^2\beta}{\tan^2\beta - 1} - \mu^2 \ . \tag{5.1}$$

Typically, the dominant radiative corrections to Eq. (5.1) come from the top-squark contributions $\Sigma_u^u(\tilde{t}_{1,2})$. By adopting a large value of the weak scale trilinear soft term A_t, then each of $\Sigma_u^u(\tilde{t}_1)$ and $\Sigma_u^u(\tilde{t}_2)$ can be minimized whilst lifting up m_h into the 125 GeV regime[18].

For first/second generation sfermions, neglecting the small Yukawa couplings, we find the contributions

$$\Sigma_{u,d}^{u,d}(\tilde{f}_{L,R}) = \mp \frac{c_{col}}{16\pi^2} F(m^2_{\tilde{f}_{L,R}}) \left(-4g_Z^2(T_3 - Q_{em}x_W)\right), \tag{5.2}$$

where T_3 is the weak isospin, Q_{em} is the electric charge assignment (taking care to flip the sign of Q_{em} for R-sfermions), $c_{col} = 1(3)$ for color singlet (triplet) states, $x_W \equiv \sin^2\theta_W$ and where

$$F(m^2) = m^2\left(\log\frac{m^2}{Q^2} - 1\right). \tag{5.3}$$

Here an optimized scale choice $Q^2 = m^2_{\rm SUSY} \equiv m_{\tilde{t}_1} m_{\tilde{t}_2}$ is adopted. The explicit first generation squark contributions to Σ_u^u (neglecting the tiny Yukawa couplings) are given by

$$\begin{aligned}
\Sigma_u^u(\tilde{u}_L) &= \frac{3}{16\pi^2} F(m^2_{\tilde{u}_L}) \left(-4g_Z^2(\frac{1}{2} - \frac{2}{3}x_W)\right) \\
\Sigma_u^u(\tilde{u}_R) &= \frac{3}{16\pi^2} F(m^2_{\tilde{u}_R}) \left(-4g_Z^2(\frac{2}{3}x_W)\right) \\
\Sigma_u^u(\tilde{d}_L) &= \frac{3}{16\pi^2} F(m^2_{\tilde{d}_L}) \left(-4g_Z^2(-\frac{1}{2} + \frac{1}{3}x_W)\right) \\
\Sigma_u^u(\tilde{d}_R) &= \frac{3}{16\pi^2} F(m^2_{\tilde{d}_R}) \left(-4g_Z^2(-\frac{1}{3}x_W)\right).
\end{aligned} \tag{5.4}$$

These contributions, arising from electroweak D-term contributions to masses, are frequently neglected since the various contributions cancel amongst themselves in the limit of mass degeneracy due to the fact that weak isospins and electric charges (or weak hypercharges) sum to zero in each generation. However, if squark and slepton masses are in the multi-TeV regime but are *non-degenerate* within each generation, then the contributions may be large and non-cancelling. In this case, they may render a theory which is otherwise considered to be natural, in fact, unnatural.

The first generation slepton contributions to Σ_u^u are given by

$$\begin{aligned}
\Sigma_u^u(\tilde{e}_L) &= \frac{1}{16\pi^2}F(m^2_{\tilde{e}_L})\left(-4g_Z^2(-\frac{1}{2}+x_W)\right) \\
\Sigma_u^u(\tilde{e}_R) &= \frac{1}{16\pi^2}F(m^2_{\tilde{e}_R})\left(-4g_Z^2(-x_W)\right) \\
\Sigma_u^u(\tilde{\nu}_L) &= \frac{1}{16\pi^2}F(m^2_{\tilde{\nu}_{eL}})\left(-4g_Z^2(\frac{1}{2})\right).
\end{aligned} \tag{5.5}$$

These may also be large for large $m^2_{\tilde{\ell}}$ although again they cancel amongst themselves in the limit of slepton mass degeneracy.

This chapter examines the case where the scalar masses are large, as suggested by the decoupling solution, but where the masses are not necessarily degenerate. In models such as radiatively driven natural SUSY[19]– where $m^2_{H_u}$, μ^2 and $\Sigma_u^u(\tilde{t}_{1,2})$ are all $\sim 100-200$ GeV – then for non-degenerate first generation squarks and sleptons, the $\Sigma_u^u(\tilde{q}_i)$ and $\Sigma_u^u(\tilde{\ell}_i)$ may be the dominant radiative corrections: and if they are sufficiently large, then large cancellations will be needed amongst independent contributions to yield a value of m_Z of just ~ 91.2 GeV: *i.e.* the model

will become highly electroweak fine-tuned. Alternatively, requiring electroweak naturalness (low $\Delta_{EW} \lesssim 30$) will require a rather high degree of intra-generational degeneracy amongst decoupled matter scalars.

5.1 Results

To a very good approximation, the masses of first and second generation sfermions (whose Yukawa couplings can be neglected) are given by

$$m^2_{\tilde{f}_i} = m^2_{F_i} + m^2_{f_i} + M_Z^2 \cos 2\beta \left(T_3 - Q_{em} \sin^2 \theta_W\right) \simeq m^2_{F_i}, \tag{5.6}$$

where $m^2_{F_i}$ is the corresponding weak scale soft-SUSY breaking parameter, and the sign of Q_{em} is flipped for R-sfermions as described just below Eq. (5.2). The latter approximate equality holds in the limit of large soft masses (decoupling), where D-term contributions are negligible.

In the limit of negligible hypercharge D-terms and $m^2_{f_i}$, then the elements of each squark and slepton doublet are essentially mass degenerate; in this case, the weak isospin contributions to Eq. (5.2) cancel out, and one is only left with the possibility of non-cancelling terms which are proportional to electric charge. The summed charge contributions (multiplied by c_{col}) of each multiplet are then $Q(Q_1) = +1$, $Q(U_1) = -2$, $Q(D_1) = +1$, $Q(L_1) = -1$ and $Q(E_1) = +1$. To achieve further cancellation, one may then cancel the $Q(U_1)$ against any two of $Q(Q_1)$, $Q(D_1)$ and $Q(E_1)$. The remaining term may cancel against $Q(L_1)$. Thus, the possible cancellations break down into four possibilities:

1. separate squark and slepton degeneracy: $m_{U_1} = m_{Q_1} = m_{D_1}$ and $m_{L_1} = m_{E_1}$,

2. separate right- and left- degeneracy: $m_{U_1} = m_{D_1} = m_{E_1}$ and $m_{L_1} = m_{Q_1}$,

3. $SU(5)$ degeneracy: $m_{U_1} = m_{Q_1} = m_{E_1} \equiv m_{10_1}$ and $m_{L_1} = m_{D_1} \equiv m_{5_1}$ and

4. $SO(10)$ degeneracy: $m_{U_1} = m_{Q_1} = m_{E_1} = m_{L_1} = m_{E_1} \equiv m_{16_1}$.

Here, the gaugino masses are assumed to be small enough so that splittings caused by the renormalization of the mass parameters between the GUT scale and the SUSY scale is negligible so that these relations may equally be taken to be valid at the GUT scale. Any major deviation from the first three of these patterns (which implies a deviation to the fourth $SO(10)$ pattern) can lead to unnaturalness in models with decoupled scalars. In models such as the phenomenological MSSM, or pMSSM, where m_{U_1}, m_{Q_1}, m_{E_1}, m_{L_1} and m_{E_1} are all taken as independent, a decoupling solution to the SUSY flavor, CP, gravitino and proton-decay problems would likely be unnatural.

Fig. 5.1 illustrates the growth of Δ_{EW} for *ad hoc* sfermion masses. The green curve plots the summed contribution to Δ_{EW} from first generation matter scalars by taking all soft masses $m_{F_i} = 20$ TeV except m_{U_1} which varies from 5-30 TeV. The summed $\Sigma_u^u(\tilde{f}_1)$ contributions to Δ_{EW} for $m_{U_1} = 5$ TeV begin at ~ 250 and slowly decrease with increasing m_{U_1}. The summed contributions reach zero at $m_{U_1} = 20$ TeV where complete cancellation amongst the various squark/slepton contributions to Δ_{EW} is achieved. A nominal value of low EWFT adopted in Ref. [19] is 30: higher values of Δ_{EW} require worse than $\Delta_{EW}^{-1} = 3\%$ EWFT. We

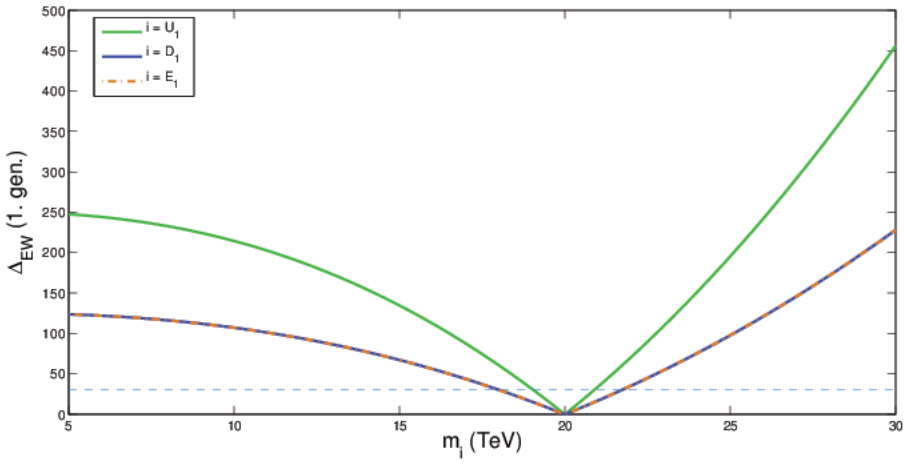

Figure 5.1: Contribution to Δ_{EW} from first generation squarks and sleptons where all scalar soft masses are set to 20 TeV except m_{U_1} (green) or m_{D_1} (blue) or m_{E_1} (orange-dashed) with $m_{\rm SUSY} = 2.5$ TeV and $\tan\beta = 10$.

see from the plot that for $\Delta_{EW} < 30$, then $m_{U_1} \sim 19 - 21$ TeV, *i.e.* a rather high degree of degeneracy of m_{U_1} in one of the above four patterns is required by naturalness.

In Fig. 5.1, plotted as the blue curve (with red dashes lying atop) is Δ_{EW} for all scalar soft masses = 20 TeV except now varying m_{D_1}. The contributions to Δ_{EW} are much reduced due to the lower d-squark charge, but are still significant: in this case, $m_{D_1} \sim 18 - 22$ TeV is required for $\Delta_{EW} < 30$. Also shown as the dashed red curve is the contribution to Δ_{EW} from first generation scalars where we take soft masses = 20 TeV but now vary m_{E_1}. The curve lies exactly atop the varying m_{D_1} curve since the color factor of 3 in Eq. (5.5) exactly compensates the increased electric charge by a factor three in Eq. (5.6). Thus, for $m_{F_1} = 20$ TeV, then $m_{E_1} \sim 18-22$ TeV is required to allow for electroweak naturalness. Requiring Δ_{EW} as low as 10, as can occur in radiatively-driven natural SUSY[19, 69], requires

even tighter degeneracy.

Adopting a variant on the degenerate $SO(10)$ case with all sfermions but the $\tilde{u}_R$ squark having the same mass, Fig. 5.2 shows the color-coded regions of first generation squark contributions to Δ_{EW} in the m_{U_1} vs. m_{F_1} plane, where m_{F_a} stands for the common sfermion mass other than m_{U_1}. The regions in between the lightest grey bands (which have $\Delta_{EW} \lesssim 30$) would mark the rough boundary of the natural region. This plot illustrates that if weak scale soft squark masses are below ~ 10 TeV, then the $\Sigma_u^u(\tilde{f}_i)$ are all relatively small, and there is hardly any naturalness constraint on non-degenerate sfermion masses. As one moves to much higher sfermion masses in the $\gtrsim 10 - 15$ TeV regime, then the sfermion soft masses within each generation are required to be increasingly degenerate in order to allow for EW naturalness.

Similarly, one can show contributions to Δ_{EW} from first generation sleptons in the m_{L_1} vs. m_{F_1} mass plane. The various regions have qualitatively similar shapes (but different widths, reflecting the different coefficient $Q(L_1)$ that enters in the calculation) to Fig. 5.2 with the replacements $m_{U_1} \to m_{L_1}$: a high degree of left-slepton mass degeneracy with another multiplet is required by naturalness once slepton masses reach above about $10 - 15$ TeV.

Such degeneracy is not necessarily expected in generic SUSY models such as the pMSSM unless there is a protective symmetry: for instance, $SU(5)$ or $SO(10)$ GUT symmetry provides the required degeneracy provided additional contributions (such as running gauge contributions) are not very large. These calculations seem to hint at the existence of an additional organizing principle

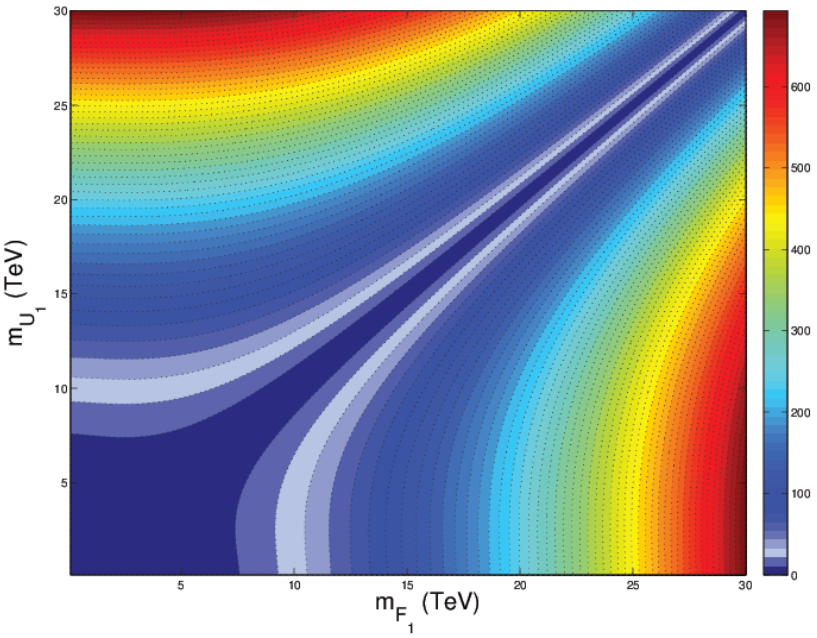

Figure 5.2: Plot of contours of $\Delta_{EW}(\tilde{f}_1)$ (summed over just first generation sfermions) in the m_{U_1} vs. m_{F_1} plane with $m_{\rm SUSY} = 2.5$ TeV and $\tan\beta = 10$.

if a decoupling solution (with sfermions heavier than ~ 10 TeV) to the SUSY flavor, CP, gravitino and proton-decay problems is invoked along with electroweak naturalness.

Chapter 6

Summary

Recent null results from LHC8 SUSY searches along with the discovery of a SM-like Higgs boson with mass $m_h \sim 125$ GeV indicate sparticle masses in the TeV range and set the limits $m_{\tilde{g}} \gtrsim 1.8$ TeV (for $m_{\tilde{g}} \simeq m_{\tilde{q}}$) and $m_{\tilde{g}} \gtrsim 1.3$ TeV (for $m_{\tilde{g}} \ll m_{\tilde{q}}$). This causes tension with conventional measures of electroweak fine-tuning such as the Higgs mass Δ_{HS} and traditional Δ_{BG} fine-tuning measures.

We propose a Rule of Fine-tuning which should be followed under any credible evaluation of fine-tuning.To accomodate the Fine-tuning Rule, dependent terms must be combined. Under recombination then both, Δ_{HS} and Δ_{BG} reduce to the model-independent electroweak fine-tuning measure Δ_{EW}. This occurs by combining dependent contributions to m_Z or m_h into independent units.

In order to generate low values of Δ_{EW}, one must generate 1. $\mu \sim 100 - 200$ GeV, 2. a weak scale value of $-m_{H_u}^2 \sim m_Z$ and 3. top-squarks in the few TeV range with large mixing. The large mixing reduces top-squark radiative corrections to Δ_{EW} while lifting m_h into the 125 GeV range. Following this, the radiatively-driven natural SUSY model has emerged as a way to reconcile low electroweak fine-tuning with lack of SUSY signals at the LHC8 and the 125 GeV light Higgs scalar. The RNS model cannot be realized within the restrictive mSUGRA/CMSSM framework, but can be realized within the context of NUHM2 models where μ can be a free input value.

A scan over the SUGRA19 model probes whether the additional freedom of 13

extra parameters allows for much lower Δ_{EW} than what can be achieved within the NUHM2 model. Here, no substantial reduction in the minimal Δ_{EW} value has been found. The parameter freedom of NUHM2 appears sufficient to minimize Δ_{EW} to its lowest values of $\sim 5-10$.

To put supersymmetry under seige, using Δ_{EW}, EW fine-tuning was evaluated for a variety of SUSY models including mSUGRA, NUHM1, NUHM2, mGMSB, mAMSB, hyper-charged AMSB, gaugino AMSB and nine cases of mixed moduli-anomaly (mirage) mediated SUSY breaking models (MMAMSB) whilst respecting LHC Higgs mass and B-decay constraints. While the NUHM1 model is moderately fine-tuned, mSUGRA, mGMSB and the AMSB models are all found to be highly fine-tuned. Only the NUHM2 model which allows for radiatively-driven naturalness (RNS) allows for fine-tuning at a meager 10% level in the case where the TeV-scale top squarks are well-mixed and $m(higgsinos) \sim 100-200$ GeV. .

In natural SUSY models higgsinos are always light because μ^2 cannot be much larger than m_Z^2, while squarks and gluinos may be very heavy: $\gtrsim 2$ TeV. Unless gluinos are discovered at LHC13, the commonly assumed unification of gaugino mass parameters will imply correspondingly heavy winos and binos, resulting in a higgsino-like LSP and small inter-higgsino mass splittings. The small visible energy release in higgsino decays makes their pair production difficult to detect at the LHC. Relaxing gaugino mass universality allows for relatively light winos and binos without violating LHC gluino mass bounds and without affecting naturalness. In the case where the bino mass $M_1 \lesssim \mu$, then one obtains a mixed bino-higgsino LSP with instead sizable $\widetilde{W}_1 - \widetilde{Z}_1$ and $\widetilde{Z}_2 - \widetilde{Z}_1$ mass gaps. The thermal neutralino

abundance can match the measured dark matter density in contrast to models with a higgsino-like LSP where WIMPs (weakly interacting massive particles) are underproduced by factors of 10-15. If instead $M_2 \lesssim \mu$, then one obtains a mixed wino-higgsino LSP with large $\widetilde{Z}_2 - \widetilde{Z}_1$ but small $\widetilde{W}_1 - \widetilde{Z}_1$ mass gaps with still an under-abundance of thermally-produced WIMPs. There are a number of other direct and indirect detection experiments for dark matter and bounds from these must be interpreted with care. LHC13 experiments should be able to probe these non-universal mass scenarios via a variety of channels including multi-lepton + $E_T^{\rm miss}$ events, $WZ + E_T^{\rm miss}$ events, $Wh + E_T^{\rm miss}$ events and $W^{\pm}W^{\pm} + E_T^{\rm miss}$ events from electroweak chargino and neutralino production.

Although realistic and natural SUSY models can be constructed in accord with experimental constraints, they leave a number of questions unanswered such as the SUSY flavor, CP, gravitino and proton-decay problem. These are all solved to varying degree by a decoupling of squarks and sleptons. Models within the RNS framework allow for a co-existence of naturalness with the decoupling solution wherein first/second generation matter scalars would exist in the multi-TeV regime. However, if sfermions are heavier than $\sim$ 10 TeV, then a small first/second generation contribution to electroweak fine-tuning (EWFT) requires a rather high degree of intra-generational degeneracy of either 1. (separately) squarks and sleptons, 2. (separately) left- and right-type sfermions, 3. members of $SU(5)$ multiplets, or 4. all members of a single generation as in $SO(10)$. These (partial) degeneracy patterns required by naturalness are not necessarily expected in generic SUSY models and hint at the existence of an organizing principle.

In conclusion, supersymmetric models within the RNS framework reconcile electroweak naturalness with lack of SUSY signals and the light Higgs scalar mass. The model-independent EW fine-tuning measure Δ_{EW} implies intra-generational degeneracy for decoupled sfermions and truely puts most SUSY models under siege. Only the NUHM2 model and its generalizations survive, and even thrive. Relaxing the gaugino mass universality of the NUHM2 model vastly increases SUSY discovery prospects at the LHC13 without impacting naturalness. One may hope for a future ILC, which could discover the predicted light higgsinos and open new doorways to probe the exciting world of supersymmetry.

References

[1] G. Aad *et al.* [ATLAS Collaboration], *Phys. Rev.* **D 87** (2013) 012008.

[2] S. Chatrchyan *et al.* [CMS Collaboration], *J. High Energy Phys.* **1210** (2012) 018 and *J. High Energy Phys.* **1406** (2014) 055.

[3] A. Chamseddine, R. Arnowitt and P. Nath, *Phys. Rev. Lett.* **49** (1982) 970; R. Barbieri, S. Ferrara and C. Savoy, *Phys. Lett.* **B 119** (1982) 343; N. Ohta, *Prog. Theor. Phys.* **70** (1983) 542; L. Hall, J. Lykken and S. Weinberg, *Phys. Rev.* **D 27** (1983) 2359; V. D. Barger, M. S. Berger and P. Ohmann, Phys. Rev. D **47** (1993) 1093; G. Kane, C. Kolda, L. Roszkowski and J. Wells, *Phys. Rev.* **D 49** (1994) 6173 H. Baer, C. H. Chen, R. Munroe, F. Paige and X. Tata, *Phys. Rev.* **D 51** (1995) 1046;.

[4] J. R. Ellis, K. Enqvist, D. V. Nanopoulos and F. Zwirner, Mod. Phys. Lett. A **1** (1986) 57.

[5] R. Barbieri and G. Giudice, *Nucl. Phys.* **B 306** (1988) 63.

[6] G. W. Anderson and D. J. Castano, *Phys. Lett.* **B 347** (1995) 300 and *Phys. Rev.* **D 52** (1995) 1693.

[7] S. Dimopoulos and G. F. Giudice, *Phys. Lett.* **B 357** (1995) 573.

[8] G. L. Kane, C. F. Kolda, L. Roszkowski and J. D. Wells, Phys. Rev. D **49** (1994) 6173;

[9] P. H. Chankowski, J. R. Ellis and S. Pokorski, *Phys. Lett.* **B 423** (1998) 327; P. H. Chankowski, J. R. Ellis, M. Olechowski and S. Pokorski, *Nucl. Phys.* **B 544** (1999) 39.

[10] G. L. Kane and S. F. King, *Phys. Lett.* **B 451** (1999) 113; M. Bastero-Gil, G. L. Kane and S. F. King, *Phys. Lett.* **B 474** (2000) 103.

[11] S. Cassel, D. M. Ghilencea and G. G. Ross, *Nucl. Phys.* **B 825** (2010) 203 and *Nucl. Phys.* **B 835** (2010) 110; S. Cassel, D. M. Ghilencea, S. Kraml, A. Lessa and G. G. Ross, *J. High Energy Phys.* **1105** (2011) 120;

[12] I. Gogoladze, F. Nasir and Q. Shafi, Int. J. Mod. Phys. A **28**, 1350046 (2013);

[13] H. Baer, V. Barger and M. Padeffke-Kirkland, Phys. Rev. D **88** (2013) 055026.

[14] R. Kitano and Y. Nomura, *Phys. Lett.* **B 631** (2005) 58 and *Phys. Rev.* **D 73** (2006) 095004.

[15] M. Papucci, J. T. Ruderman and A. Weiler, *J. High Energy Phys.* **1209** (2012) 035;

[16] C. Brust, A. Katz, S. Lawrence and R. Sundrum, *J. High Energy Phys.* **1203** (2012) 103; R. Essig, E. Izaguirre, J. Kaplan and J. G. Wacker, *J. High Energy Phys.* **1201** (2012) 074.

[17] C. Wymant, Phys. Rev. D **86** (2012) 115023.

[18] H. Baer, V. Barger, P. Huang, A. Mustafayev and X. Tata, Phys. Rev. Lett. **109** (2012) 161802.

[19] H. Baer, V. Barger, P. Huang, A. Mustafayev and X. Tata, Phys. Rev. Lett. **109** (2012) 161802; H. Baer, V. Barger, P. Huang, D. Mickelson, A. Mustafayev and X. Tata, Phys. Rev. D **87** (2013) 11, 115028.

[20] P. Higgs, Phys. Rev. Lett. **13** (1964) 508-509.

[21] F. Englert, R. Brout, Phys. Rev. Lett. **13** (1964) 321-323.

[22] G. Aad *et al.* [ATLAS Collaboration], *Phys. Lett.* **B 716** (2012) 1.

[23] S. Chatrchyan *et al.* [CMS Collaboration], *Phys. Lett.* **B 716** (2012) 30.

[24] G. Aad *et al.* [ATLAS and CMS Collaboration], arXiv:1503.07589 [hep-ex].

[25] H. Baer and X. Tata, *Weak Scale Supersymmetry: From Superfields to Scattering Events*, (Cambridge University Press, 2006).

[26] L. E. Ibañez and G. G. Ross, Phys. Lett. **B110**, 215 (1982); K. Inoue *et al.* Prog. Theor. Phys. **68**, 927 (1982) and **71**, 413 (1984); L. Ibañez, Phys. Lett. **B118**, 73 (1982); J. Ellis, J. Hagelin, D. Nanopoulos and M. Tamvakis, Phys. Lett. **B125**, 275 (1983); L. Alvarez-Gaumé. J. Polchinski and M. Wise, Nucl. Phys. **B221**, 495 (1983).

[27] H. Baer and J. List, Phys. Rev. D **88** (2013) 055004.

[28] H. Baer, A. Mustafayev, S. Profumo, A. Belyaev and X. Tata, Phys. Rev. D **71** (2005) 095008.

[29] D. Matalliotakis and H. P. Nilles, Nucl. Phys. B **435** (1995) 115; P. Nath and R. L. Arnowitt, Phys. Rev. D **56** (1997) 2820; J. Ellis, K. Olive and Y. Santoso, *Phys. Lett.* **B 539** (2002) 107; J. Ellis, T. Falk, K. Olive and Y. Santoso, *Nucl. Phys.* **B 652** (2003) 259; H. Baer, A. Mustafayev, S. Profumo, A. Belyaev and X. Tata, *J. High Energy Phys.* **0507** (2005) 065.

[30] M. Dine, W. Fischler and M. Srednicki, Nucl. Phys. B **189** (1981) 575; S. Dimopoulos and S. Raby, Nucl. Phys. B **192** (1981) 353; M. Dine and W. Fischler, Phys. Lett. B **110** (1982) 227; C. R. Nappi and B. A. Ovrut, Phys. Lett. B **113** (1982) 175; L. Alvarez-Gaume, M. Claudson and M. B. Wise, Nucl. Phys. B **207** (1982) 96; M. Dine and A. E. Nelson, Phys. Rev. D **48** (1993) 1277; M. Dine, A. E. Nelson and Y. Shirman, Phys. Rev. D **51** (1995) 1362; M. Dine, A. E. Nelson, Y. Nir and Y. Shirman, Phys. Rev. D **53** (1996) 2658; for a review, see G. F. Giudice and R. Rattazzi, Phys. Rept. **322** (1999) 419.

[31] Y. Kats, P. Meade, M. Reece and D. Shih, JHEP **1202** (2012) 115.

[32] P. Draper, P. Meade, M. Reece and D. Shih, Phys. Rev. D **85** (2012) 095007.

[33] L. Randall and R. Sundrum, Nucl. Phys. B **557** (1999) 79; G. F. Giudice, M. A. Luty, H. Murayama and R. Rattazzi, JHEP **9812** (1998) 027

[34] R. Dermisek, H. Verlinde and L. -T. Wang, Phys. Rev. Lett. **100** (2008) 131804; H. Baer, R. Dermisek, S. Rajagopalan and H. Summy, JHEP **0910** (2009) 078.

[35] S. P. de Alwis, JHEP **1003** (2010) 078.

[36] H. Baer, S. de Alwis, K. Givens, S. Rajagopalan and H. Summy, JHEP **1005** (2010) 069; H. Baer, S. P. de Alwis, K. Givens, S. Rajagopalan and W. Sreethawong, JHEP **1101** (2011) 005.

[37] H. Baer, V. Barger, D. Mickelson and M. Padeffke-Kirkland, Phys. Rev. D **89** (2014) 115019.

[38] E. Gildner and S. Weinberg, Phys. Rev. D **13** (1976) 333; E. Gildner, Phys. Rev. D **14** (1976) 117; See also L. Susskind, Phys. Rev. D **20** (1979) 2619.

[39] H. Baer, V. Barger, P. Huang, D. Mickelson, A. Mustafayev, W. Sreethawong and X. Tata, Phys. Rev. Lett. **110** (2013) 15, 151801.

[40] A. G. Delannoy, B. Dutta, A. Gurrola, W. Johns, T. Kamon, E. Luiggi, A. Melo and P. Sheldon *et al.*, Phys. Rev. Lett. **111** (2013) 061801.

[41] H. Baer, V. Barger and D. Mickelson, Phys. Lett. B **726** (2013) 330.

[42] See *e.g.* H. Baer, In *Kane, G. (ed.); Perspectives on supersymmetry II* 446-468 [arXiv:0912.3270 [hep-ph]].

[43] A. Djouadi, J. -L. Kneur and G. Moultaka, Comput. Phys. Commun. **176** (2007) 426; J. Conley, S. Gainer, J. Hewett, M. Le and T. Rizzo, *Eur. Phys. J.* **C 71** (2011) 1697; S. Sekmen, S. Kraml, J. Lykken, F. Moortgat, S. Padhi, L. Pape, M. Pierini and H. B. Prosper *et al.*, *J. High Energy Phys.* **1202** (2012) 075; M. W. Cahill-Rowley, J. L. Hewett, A. Ismail and T. G. Rizzo, Phys. Rev. D **86** (2012) 075015 and Phys. Rev. D **88** (2013) 3, 035002; C. Boehm, P. S. B. Dev, A. Mazumdar and E. Pukartas, JHEP **1306** (2013) 113.

[44] V. D. Barger, M. S. Berger and P. Ohmann, Phys. Rev. D **49** (1994) 4908.

[45] J. A. Evans, Y. Kats, D. Shih and M. J. Strassler, arXiv:1310.5758 [hep-ph].

[46] J. L. Feng, Ann. Rev. Nucl. Part. Sci. **63** (2013) 351.

[47] L. E. Ibanez, C. Lopez and C. Munoz, *Nucl. Phys.* **B 256** (1985) 218; A. Lleyda and C. Munoz, *Phys. Lett.* **B 317** (1993) 82.

[48] H. Abe, T. Kobayashi and Y. Omura, *Phys. Rev.* **D 76** (2007) 015002.

[49] S. P. Martin, *Phys. Rev.* **D 75** (2007) 115005.

[50] ISAJET, by H. Baer, F. Paige, S. Protopopescu and X. Tata, hep-ph/0312045.

[51] H. Baer, C. H. Chen, R. Munroe, F. Paige and X. Tata, *Phys. Rev.* **D 51** (1995) 1046; H. Baer, J. Ferrandis, S. Kraml and W. Porod, *Phys. Rev.* **D 73** (2006) 015010.

[52] J. Hisano, H. Murayama, and T. Yanagida, *Nucl. Phys.* **B 402** (1993) 46; Y. Yamada, *Z. Physik* **C 60** (1993) 83 ; J. L. Chkareuli and I. G. Gogoladze, *Phys. Rev.* **D 58** (1998) 055011.

[53] S. Martin and M. Vaughn, *Phys. Rev.* **D 50** (1994) 2282.

[54] Y. Yamada, *Phys. Lett.* **B 316** (1993) 109; *Phys. Rev. Lett.* **72** (1994) 25; *Phys. Rev.* **D 50** (1994) 3537.

[55] H. Haber and R. Hempfling, *Phys. Rev.* **D 48** (1993) 4280.

[56] D. Pierce, J. Bagger, K. Matchev and R. Zhang, *Nucl. Phys.* **B 491** (1997) 3.

[57] F. Gabbiani, E. Gabrielli, A. Masiero and L. Silvestrini, *Nucl. Phys.* **B 477** (1996) 321.

[58] Joint LEP 2 Supersymmetry Working Group, *Combined LEP Chargino Results up to 208 GeV*,
`http://lepsusy.web.cern.ch/lepsusy/www/inos_moriond01/charginos_pub.html`.

[59] V. Barger, M. Berger and R.J.N. Phillips, *Phys. Rev. Lett.* **70** (1993) 1368; J. Hewett, *Phys. Rev. Lett.* **70** (1993) 1045.

[60] H. Baer and M. Brhlik, *Phys. Rev.* **D 55** (1997) 3201; H. Baer, M. Brhlik, D. Castano and X. Tata, Phys. Rev. D **58** (1998) 015007.

[61] S. Rai Choudhury and N. Gaur, *Phys. Lett.* **B 451** (1998) 86; K. S. Babu and C. F. Kolda, *Phys. Rev.* **D 84** (2000) 28; our calculation uses the formulae in J. Mizukoshi, X. Tata and Y. Wang, *Phys. Rev.* **D 66** (2002) 115003.

[62] D. Asner *et al.* [Heavy Flavor Averaging Group], arXiv:1010.1589.

[63] M. Misiak *et al.*, *Phys. Rev. Lett.* **98** (2007) 022002.

[64] R. Aaij *et al.* (LHCb Collaboration), arXiv:1211.2674.

[65] R. Aaij *et al.* [LHCb Collaboration], Phys. Rev. Lett. **111** (2013) 101805.

[66] S. Chatrchyan *et al.* [CMS Collaboration], Phys. Rev. Lett. **111** (2013) 101804.

[67] H. Baer, V. Barger and P. Huang, JHEP **1111** (2011) 031.

[68] H. Baer, V. Barger, P. Huang, D. Mickelson, A. Mustafayev and X. Tata, Phys. Rev. **D87** (2013) 035017.

[69] H. Baer, V. Barger and D. Mickelson, Phys. Rev. D **88** (2013) 095013.

[70] V. S. Kaplunovsky and J. Louis, Phys. Lett. B **306** (1993) 269.

[71] A. Brignole, L. E. Ibanez and C. Munoz, Nucl. Phys. B **422** (1994) 125 [Erratum-ibid. B **436** (1995) 747].

[72] S. K. Soni and H. A. Weldon, Phys. Lett. B **126** (1983) 215.

[73] H. Baer, K. Y. Choi, J. E. Kim and L. Roszkowski, review on non-thermal dark matter to appear.

[74] H. Baer, V. Barger, P. Huang, D. Mickelson, A. Mustafayev and X. Tata, Phys. Rev. D **87** (2013) 3, 035017.

[75] K. L. Chan, U. Chattopadhyay and P. Nath, Phys. Rev. D **58** (1998) 096004 [hep-ph/9710473]; S. Akula, M. Liu, P. Nath and G. Peim, Phys. Lett. B **709** (2012) 192; M. Liu and P. Nath, arXiv:1303.7472 [hep-ph].

[76] J. L. Feng, K. T. Matchev and T. Moroi, Phys. Rev. D **61** (2000) 075005; J. L. Feng and K. T. Matchev, Phys. Rev. D **63** (2001) 095003; J. L. Feng, K. T. Matchev and D. Sanford, Phys. Rev. D **85** (2012) 075007; J. L. Feng and D. Sanford, Phys. Rev. D **86** (2012) 055015.

[77] M. Dine, A. Kagan and S. Samuel, *Phys. Lett.* **B 243** (1990) 250; A. Cohen, D. B. Kaplan and A. Nelson, *Phys. Lett.* **B 388** (1996) 588; N. Arkani-Hamed and H. Murayama, *Phys. Rev.* **D 56** (1997) R6733; T. Moroi and M. Nagai, Phys. Lett. B **723** (2013) 107.

[78] M. Y. Khlopov and A. D. Linde, Phys. Lett. B **138** (1984) 265.

[79] D. E. Kaplan, G. D. Kribs and M. Schmaltz, *Phys. Rev.* **D 62** (2000) 035010; Z. Chacko, M. A. Luty, A. E. Nelson and E. Ponton, *J. High Energy Phys.* **01** (2000) 003; for phenomenology, see M. Schmaltz and W. Skiba, *Phys. Rev.* **D 62** (2000) 095005 and *Phys. Rev.* **D 62** (2000) 095004; H. Baer, A. Belyaev, T. Krupovnickas and X. Tata, *Phys. Rev.* **D 65** (2002) 075024; A. De Simone, J. J. Fan, M. Schmaltz and W. Skiba, *Phys. Rev.* **D 78** (2008) 095010.

[80] J. R. Ellis, C. Kounnas and D. V. Nanopoulos, Nucl. Phys. B **247** (1984) 373; J. R. Ellis, A. B. Lahanas, D. V. Nanopoulos and K. Tamvakis, Phys. Lett. B **134** (1984) 429; G. A. Diamandis, J. R. Ellis, A. B. Lahanas and D. V. Nanopoulos, Phys. Lett. B **173** (1986) 303; For a review, see A. Lahanas and D. V. Nanopoulos, *Phys. Rept.* **145** (1987) 1.

[81] S. Kachru, R. Kallosh, A. D. Linde and S. P. Trivedi, Phys. Rev. D **68** (2003) 046005.

[82] K. Choi, A. Falkowski, H. P. Nilles, M. Olechowski and S. Pokorski, *J. High Energy Phys.* **0411** (2004) 076; K. Choi, A. Falkowski, H. P. Nilles and M. Olechowski, *Nucl. Phys.* **B 718** (2005) 113; K. Choi, K-S. Jeong and K. Okumura, *J. High Energy Phys.* **0509** (2005) 039; A. Falkowski, O. Lebedev and Y. Mambrini, *J. High Energy Phys.* **0511** (2005) 034; M. Endo, M. Yamaguchi and K. Yoshioka, *Phys. Rev.* **D 72** (2005) 015004; H. Baer, E. -K. Park, X. Tata and T. T. Wang, JHEP **0608** (2006) 041; L. L. Everett, I. -W. Kim, P. Ouyang and K. M. Zurek, JHEP **0808** (2008) 102.

[83] K. Choi, K. S. Jeong, T. Kobayashi and K. -i. Okumura, Phys. Lett. B **633** (2006) 355; K. Choi, K. S. Jeong, T. Kobayashi and K. -i. Okumura, Phys. Rev. D **75** (2007) 095012.

[84] O. Lebedev, H. P. Nilles and M. Ratz, hep-ph/0511320.

[85] H. Baer, E. -K. Park, X. Tata and T. T. Wang, JHEP **0706** (2007) 033.

[86] H. Baer, V. Barger, P. Huang, D. Mickelson, A. Mustafayev, W. Sreethawong and X. Tata, JHEP **1312** (2013) 013.

[87] M. Koratzinos, A. P. Blondel, R. Aleksan, O. Brunner, A. Butterworth, P. Janot, E. Jensen and J. Osborne *et al.*, arXiv:1305.6498 [physics.acc-ph].

[88] H. Baer, V. Barger, P. Huang, D. Mickelson, A. Mustafayev, W. Sreethawong and X. Tata, arXiv:1306.3148 [hep-ph].

[89] H. Baer, V. Barger, P. Huang, D. Mickelson, M. Padeffke-Kirkland and X. Tata, *Phys. Rev.* **D 91** (2015) blank.

[90] H. Baer, V. Barger, P. Huang, D. Mickelson, A. Mustafayev, W. Sreethawong and X. Tata, JHEP **1312** (2013) 013.

[91] C. Han, A. Kobakhidze, N. Liu, A. Saavedra, L. Wu and J. M. Yang, *J. High Energy Phys.* **1402** (2014) 049 [arXiv:1310.4274 [hep-ph]].

[92] H. Baer, A. Mustafayev and X. Tata, *Phys. Rev.* **D 89** (2014) 055007.

[93] R. D. Peccei and H. R. Quinn, *Phys. Rev. Lett.* **38** (,) 19771440; S. Weinberg, *Phys. Rev. Lett.* **40** (1978) 223; F. Wilczek, *Phys. Rev. Lett.* **40** (1978) 279.

[94] K. -Y. Choi, J. E. Kim, H. M. Lee and O. Seto, **77** (2008) 123501; H. Baer, A. Lessa, S. Rajagopalan and W. Sreethawong, JCAP **1106** (2011) 031.

[95] J. Ellis *et al.* Phys. Lett. **B155** (1985) 381; M. Drees, Phys. Lett. **B158** (1985) 409.

[96] G. Anderson, H. Baer, C. h. Chen and X. Tata, *Phys. Rev.* **D 61** (2000) 095005.

[97] K. Choi, A. Falkowski, H. P. Nilles, M. Olechowski and S. Pokorski, *J. High Energy Phys.* **0411** (2004) 076.

[98] I. Gogoladze, F. Nasir and Q. Shafi, Int. J. Mod. Phys. A **28** (2013) 1350046; I. Gogoladze, F. Nasir and Q. Shafi, JHEP **1311** (2013) 173.

[99] S. Martin, *Phys. Rev.* **D 89** (2014) 035011.

[100] H. Baer, C. Balazs and A. Belyaev, JHEP **0203** (2002) 042.

[101] M. Misiak *et al. Phys. Rev. Lett.* **98** (2007) 022002.

[102] J. P. Lees *et al.* (BaBar Collaboration) *Phys. Rev.* **D 86** (2012) 052012; T. Saito *et al.* (Belle Collaboration) arXiv:1411.7198.

[103] D. Akerib *et al.* (LUX Collaboration) *Phys. Rev. Lett.* **112** (2014) 091303; see also E. Aprile et al. (XENON100 Collaboration) *Phys. Rev. Lett.* **109** (2012) 181301, for results from an earlier, independent search.

[104] H. Baer, K. Y. Choi, J. E. Kim and L. Roszkowski, arXiv:1407.0017 [hep-ph].

[105] M. Aartsen *et. al.* (IceCube Collaboration) *Phys. Rev. Lett.* **110** (2013) 131302.

[106] Z. Han, G. D. Kribs, A. Martin and A. Menon, *Phys. Rev.* **D 89** (2014) 075007.

[107] H. Baer, A. Mustafayev and X. Tata, Phys. Rev. D **90** (2014) 11, 115007.

[108] W. Bennakker, R. Hopker and M. Spira, hep-ph/9611232.

[109] A. Chamseddine, P. Nath and R. Arnowitt, *Phys. Lett.* **B 129** (1983) 445; D. Dicus, S. Nandi and X. Tata, *Phys. Lett.* **B 129** (1983) 451. H. Baer and X. Tata, Phys. Lett. B **155** (1985) 278; H. Baer, K. Hagiwara and X. Tata, Phys. Rev. D **35** (1987) 1598; P. Nath and R. L. Arnowitt, Mod. Phys. Lett. A **2** (1987) 331; R. Barbieri, F. Caravaglios, M. Frigeni and M. L. Mangano, Nucl. Phys. B **367** (1991) 28; H. Baer and X. Tata, *Phys. Rev.* **D 47** (1993) 2739; H. Baer, C. Kao and X. Tata, Phys. Rev. D **48** (1993) 5175; J. L. Lopez, D. V. Nanopoulos, X. Wang and A. Zichichi, Phys. Rev. D **52** (1995) 142; V. Barger, C. Kao and T. Li, Phys. Lett. B **433**, 328 (1998); V. Barger and C. Kao, Phys. Rev. D **60**, 115015 (1999); H. Baer, M. Drees, F. Paige, P. Quintana and X. Tata, Phys. Rev. D **61**, 095007 (2000); K. Matchev and D. Pierce, *Phys. Lett.* **B 467** (1999) 225; E. Accomando, R. L. Arnowitt and B. Dutta, Phys. Lett. B **475** (2000) 176; S. Dube, J. Glatzer, S. Somalwar, A. Sood and S. Thomas, J. Phys. G **39** (2012) 085004.

[110] H. Baer, C. H. Chen, F. Paige and X. Tata, *Phys. Rev.* **D 50** (1994) 4508 and *Phys. Rev.* **D 53** (1996) 6241; H. Baer, T. Krupovnickas, S. Profumo and P. Ullio, JHEP **0510** (2005) 020; S. Bhattacharya, A. Datta and B. Mukhopadhyaya, Phys. Rev. D **78** (2008) 115018.

[111] H. Baer, V. Barger, S. Kraml, A. Lessa, W. Sreethawong and X. Tata, JHEP **1203** (2012) 092.

[112] T. Han, S. Padhi and S. Su, *Phys. Rev.* **D 88** (2013) 115010.

[113] T. A. W. Martin and D. Morrissey, JHEP **1412** (2014) 168.

[114] H. Baer, V. Barger, A. Lessa, W. Sreethawong and X. Tata, *Phys. Rev.* **D 85** (2012) 055022.

[115] H. Baer, V. Barger, D. Mickelson, A. Mustafayev and X. Tata, JHEP **1406** (2014) 172.

[116] T. Tsukamoto, K. Fujii, H. Murayama, M. Yamaguchi and Y. Okada, Phys. Rev. D **51** (1995) 3153.

[117] H. Baer, R. B. Munroe and X. Tata, Phys. Rev. D **54** (1996) 6735.

[118] M. Dine, W. Fischler and M. Srednicki, Phys. Lett. **B104** (1981) 199; A. P. Zhitnitskii, Sov. J. Phys. **31** (1980) 260.

[119] K. J. Bae, H. Baer and H. Serce, Phys. Rev. D **91** (2015) 015003.

[120] K. J. Bae, H. Baer and E. J. Chun, Phys. Rev. D **89** (2014) 031701 and JCAP **1312** (2013) 028.

[121] H. Baer, C. Balazs, A. Belyaev and J. O'Farrill, JCAP **0309** (2003) 007.

[122] C. Cheung, L. J. Hall, D. Pinner and J. T. Ruderman, JHEP **1305**, 100 (2013).

[123] P. Huang and C. E. M. Wagner, Phys. Rev. D **90**, 015018 (2014).

[124] M. Ackermann *et al.*, *Phys. Rev.* **D 89** (2014) 042001.

[125] V. Khatchatryan *et al.* (CMS Collaboration) *Eur. Phys. J.* **C 74** (2012) 3036.

[126] G. Aad *et al.* (ATLAS Collaboration) *J. High Energy Phys.* **1405** (2014) 071.

[127] ATLAS Collaboration, ATLAS-CONF-2014-062.

[128] T. Moroi and L. Randall, *Nucl. Phys.* **B 570** (2000) 455; B. S. Acharya, G. Kane, S. Watson and P. Kumar, Phys. Rev. D **80** (2009) 083529; R. Allahverdi, B. Dutta and K. Sinha, Phys. Rev. D **87** (2013) 075024.

[129] H. Baer, V. Barger, M. Padeffke-Kirkland and X. Tata, Phys. Rev. D **89** (2014) 037701.

[130] K. R. Dienes and C. F. Kolda, hep-ph/9712322.

[131] S. Weinberg, Phys. Rev. Lett. **48** (1982) 1303.

[132] H. Murayama and A. Pierce, Phys. Rev. D **65** (2002) 055009.

[133] S. Dimopoulos and H. Georgi, Nucl. Phys. B **193** (1981) 150.

[134] Y. Nir and N. Seiberg, Phys. Lett. B **309** (1993) 337.

[135] M. Y. Khlopov and A. D. Linde, Phys. Lett. B **138** (1984) 265; see also M. Kawasaki, K. Kohri, T. Moroi and A. Yotsuyanagi, Phys. Rev. D **78** (2008) 065011.

[136] P. Nath and R. M. Syed, Phys. Rev. D **77** (2008) 015015.

[137] M. Dine, A. Kagan and S. Samuel, Phys. Lett. B **243** (1990) 250.

[138] A. G. Cohen, D. B. Kaplan and A. E. Nelson, Phys. Lett. B **388** (1996) 588.

[139] J. Bagger, J. L. Feng and N. Polonsky, Nucl. Phys. B **563** (1999) 3.

[140] T. Moroi and M. Nagai, Phys. Lett. B **723** (2013) 107.

[141] J. Hisano, D. Kobayashi, T. Kuwahara and N. Nagata, JHEP **1307** (2013) 038.

[142] M. Perelstein and C. Spethmann, JHEP **0704** (2007) 070.

[143] M. Drees, Phys. Lett. B**181**, 279 (1986); J.S. Hagelin and S. Kelley, Nucl. Phys. B**342**, 95 (1990); A.E. Faraggi, *et al.*, Phys. Rev. D**45**, 3272 (1992); Y. Kawamura and M. Tanaka, Prog. Theor. Phys. **91**, 949 (1994); Y. Kawamura, *et al.*, Phys. Lett. B**324**, 52 (1994); Phys. Rev. D**51**, 1337 (1995); N. Polonsky and A. Pomarol, Phys. Rev. D**51**, 6532 (1994); H.-C. Cheng and L.J. Hall, Phys. Rev. D**51**, 5289 (1995); C. Kolda and S.P. Martin, Phys. Rev. D**53**, 3871 (1996).